INTERNATIONAL STUDIES AND EVALUATIONS IN THE FIELD OF

ELECTRICAL, ELECTRONICS AND COMMUNICATION ENGINEERING

December 2024

EDITOR

ASSOC. PROF. DR. MEHMET CİHAT ÖZGENEL

SERÜVEN YAYINEVİ

Genel Yayın Yönetmeni / Editor in Chief • C. Cansın Selin Temana

Kapak & İç Tasarım / Cover & Interior Design • Serüven Yayınevi

Birinci Basım / First Edition • © Aralık 2024

ISBN • 978-625-5955-71-5

Serüven Yayınevi / Serüven Publishing
Türkiye Adres / Turkey Address: Kızılay Mah. Fevzi Çakmak 1. Sokak
Ümit Apt No: 22/A Çankaya/ANKARA
Telefon / Phone: 05437675765
web: www.seruvenyayinevi.com
e-mail: seruvenyayinevi@gmail.com

Baskı & Cilt / Printing & Volume
Sertifika / Certificate No: 47083

INTERNATIONAL STUDIES AND EVALUATIONS IN THE FIELD OF

ELECTRICAL, ELECTRONICS AND COMMUNICATION ENGINEERING

DECEMBER 2024

EDITOR

ASSOC. PROF. DR. MEHMET CİHAT ÖZGENEL

CONTENTS

CHAPTER 1

AN OVERVIEW OF THE HARMFUL EFFECTS OF ELECTROMAGNETIC INTERFERENCE AND THE USE OF TEXTILES AS SHIELDING MATERIALS

Ali Recai ÇELİK[1]

1 Dr., Dicle University, Electrical and Electronics Engineering Department
ORCID ID: 0000-0002-6917-5170

1. INTRODUCTION

Electromagnetic (EM) waves occur when an electric field comes into contact with a magnetic field. They can move in any medium, such as air, water, solid material, etc. EM spectrum showing different types of EM energy according to their frequencies or wavelengths is given in the Figure 1 (Sajjadi et al., 2014). Since electricity is an indispensable part of our lives and the use of electronic devices (especially compact ones operating with high energy capacities), wireless communications, 4G/5G systems, Bluetooth devices, and TV/Radio transmissions has increased intensively, the problem of EM radiation pollution has begun to occur worldwide. This pollution and 'EM interference (EMI)' above certain limit values cause undesirable damages by harming humans and living things (Willson et al., 2020; Singh et al., 2020).

According to many studies on the biological effects of EM radiation, constant exposure to radiation causes the neurological disorders, cognitive diseases, tissue damages, blood disorders, heart diseases, stress, fatigue, disturbed sleep patterns, decreased learning potential, and lack of attention (Kovacic and Somanathan, 2010; Kamiya and Sasatani, 2012: Diab, 2020). Furthermore, EM radiations can enter cells and have the possibility of disrupting DNA strands. Changing the DNA structure harms the proper functioning of cells and cause cancer (Demers et al. 1991; Caplan et al. 2000). EMI is also known to cause electronic devices to malfunction and signals to become distorted. To eliminate or minimize such negative effects, materials that protect from the bad effects of EM waves are needed. Therefore, the demand for materials with high EMI shielding performance has begun to increase.

EMI shielding and protection methods that can be applied to eliminate or minimize the harms of radiation have been one of the important research topics in recent years. For this purpose, some initiatives regarding radiation and EMI protection have been initiated by researchers (Wu et al., 2017; Wilson et al., 2020; Khan et al., 2020). These methods based on EM wave reflection or absorbtion by charge carriers which means high electrical conductivity is required for EMI shielding materials. While they can be used to protect from the effects of an external radiation source, they can also be used to prevent unnecessary emission of EM energy radiated through internal sources (Periyasamy et al., 2020). Maity et. al. defined EMI shielding as "a

process in which the penetration of EM radiation into space is limited or prevented by a barrier composed of conductive material" (Maity et al. 2013).

Thanks to shielding applications, human health is protected from non-ionizing radiation, and on the other hand, the protection of electronic equipment is ensured by the proper functioning of EM compatibility principles. To summarize, the radiation pollution can be reduced by EMI shielding materials with a dominant microwave absorption and reflection mechanism.

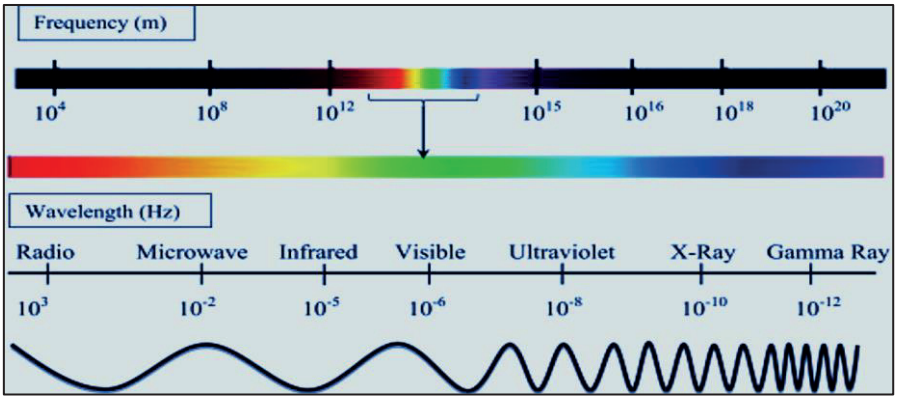

Figure 1. Electromagnetic radiation spectrum

The use of textile-substrate materials and clothings as personal protection materials has come to the fore as one of the shielding methods. Since natural textile fabrics are not conductive, they must be made conductive against electric current before being used as shields for EMI purposes. Fortunately, by changing their structures, insulating fabrics can be converted into conductive fabrics and, thus, EMI shielding materials. Various advanced materials or conductive inks can be employed for this aim. The fabrics are required to be flexible, stretchable, light, durable, and comfortable. Recently, various EM protective clothings and fabrics providing these features have been produced and are in great demand (Ghosh et al., 2018). The process of protecting humans and other living things from harmful radiation with advanced materials and organisms is summarized in (Akram et al., 2023) and given in Figure 2.

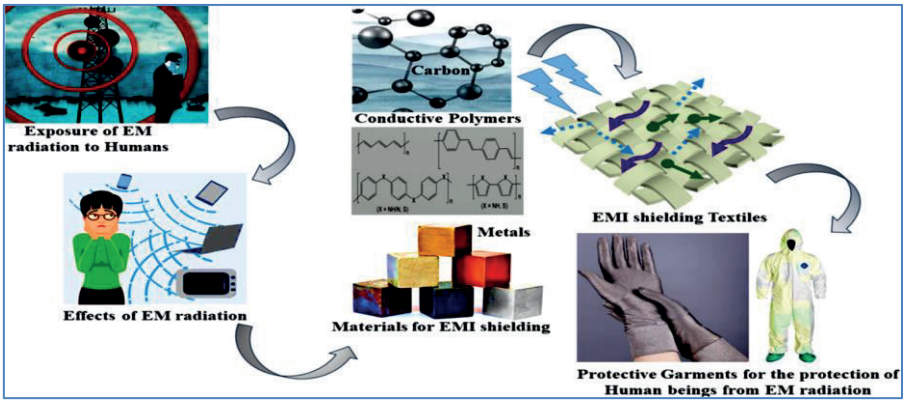

Figure 2. Scheme of EMI shielding process prepared by (Akram et al. 2023)

In this Chapter, first of all, EM waves are defined, EM theory is briefly discussed, and the EM spectrum containing waves of different frequencies is shown. The causes of EM pollution are mentioned and the harmful effects of EMI on humans, living things, and electronic devices are given in detail. Then, it is mentioned that EMI shielding and protection methods have been developed to reduce and, if possible, eliminate these negative effects, and the working principles of these methods are explained. The effects of absorption, reflection, and multiple internal reflections losses on the Shielding Effectiveness (SE) are mentioned and the necessary equations are given. In the continuation of the study, it is emphasized that the use of textiles as protection materials is one of the most important EMI shielding methods, and it is explained that natural textile fabrics need structural changes to make them conductive against electric current. The properties of additives that can be used for this purpose are examined in detail. The merits and drawbacks of metal-based materials, conductive polymers, and carbon-based composites, which are effective for EMI protection, are examined and some studies using these materials in the literature are reviewed.

2. HOW EMI SHIELDING WORKS?

When EM rays pass through an object or environment, they can interact with molecules in two ways: 'absorption-based' and 'reflection-based' attenuations. The attenuation due to absorbtion mode occurs in the form of heat, which is a form of energy loss from the charge due to the oscillation of forces in a medium. On the other hand, when waves hit a conductive layer, the charges of the wave and the object oscillate at the same frequency values. These oscillating charges can be thought of as an antenna that causes reflection from

the surface. Due to this scattering, the signal decreases and disappears. Reflection-based attenuation is the name given to this mode of signal loss (Chandra et al. 2019). Specifically, researchers are trying to develop an EMI shielding material with an absorption mechanism, or microwave absorber, that would reduce secondary radiation pollution.

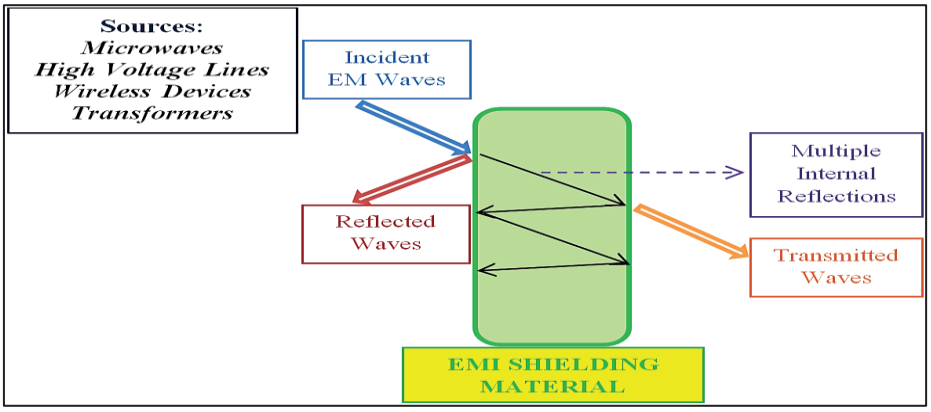

Figure 3. Schematic representation of the EMI shielding mechanism

As a result, the operation of EMI shields is based on the mechanisms of absorption within a conductive object or reflected signals from the surface of this material as given in Figure 3. Thus, blocking or reducing potentially harmful radiation energy can be provided by the protective material. The 'Total Shielding Effectiveness (SE_T)', which is the EMI shielding capability of a material, can be determined by the combined effect of effectiveness of the absorption (SE_A) and reflection (SE_R) losses. As can be seen from the Figure 3, apart from these losses, there are also multiple internal reflections (M) in the system. Therefore, they are also taken into account as SE_M in the general formula given in Equation 1. However, it is a parameter that is generally important only at low frequencies and when the protective material is very thin. It can be neglected when the SE_A value is greater than 15 decibels (dB) (Shacklette and Colaneri, 1991; Tong, 2016; Jiang et al., 2019). As additional information, since EM waves reflected by protective materials can cause EM pollution again, researches are generally carried out to increase the SE_A factor of the materials. Another method to define SE_T is to calculate the ratio between the incoming power (P_1) and outgoing power (P_2) of the wave as given in Equation 2 (Yang and Gupta, 2005).

$$SE_T = SE_A + SE_R + SE_M \qquad (1)$$

$$SE_T = 10 \log \frac{P1}{P2} \quad dB \qquad (2)$$

SE_T can be calculated in practice using vector or scalar network analyzers, as well as in a simulation environment. The extent to which attenuation is prevented according to the obtained SE value is shown in the Table 1 (Zhang et al. 2020). Accordingly, a SE_T value of ≥ 20 dB provides attenuation by absorbing/reflecting approximately 99% of EM energy. Hence, it is assumed that at least 20 dB SE_T is required to implement excellent EMI shielding (King et al., 2016; Sankaran et al. 2018).

Table 1. Attenuations according to the SE Values

SE (dB)	20	30	40	50	60	70
Attenuation (%)	99	99.9	99.99	99.999	99.9999	99.9999

3. MATERIALS USED FOR EMI SHIELDING IN TEXTILE

In general, when examining the shielding performance, the conductivity, permittivity, permeability, thickness, pore amounts, and shapes of the materials are taken into consideration. Related to this, some important properties that materials must have for EMI protection are summarized below (Ali et al., 2018; Rybicki, 2019; Rubežienė and Varnaitė-Žuravliova, 2020):

- Superior electrical conductivity,
- High permittivity (dielectric constant),
- Low magnetic permeability,
- Ease of design and manufacturing,
- Solid and reliable structure,
- Low coefficient of expansion,
- Effective shielding against radiation,
- High strength-to-weight ratio,
- Light and flexible structure,
- High surface area,
- Low density,
- Good chemical and mechanical stability,
- Environmentally friendly structure.

It is not easy to find a substance/material that provides all the superior features listed above. For this reason, metals, conductive polymers, and carbon-based materials are widely preferred for EMI shielding applications in

textiles, even though they provide only some of these properties (Esen et al., 2020).

3.1. Metal-based materials for EMI shielding

Since metals are excellent electrical conductors, they are one of the most suitable materials with high efficiency in EMI shielding applications as mentioned above. Silver (Ag), Copper (Cu), Nickel (Ni), Zinc (Zn), and Zinc Oxide (ZnO) are widely used metals to make conductive textiles. For example, in a study by (Moazzenchi and Montazer, 2019), the shielding performance of Ni was examined. Accordingly, Ni nanoparticles were synthesized on the polyester fabric surface and the results were shared that the treated fabric exhibited 100% shielding in the frequency range of 8.4-12.4 GHz. It was emphasized that the electrical resistance of the nickel-treated polyester fabric is lower than 2 Ω and that its magnetic and antibacterial properties are high. The EMI shielding performance of these fabrics is given in Figure 4.

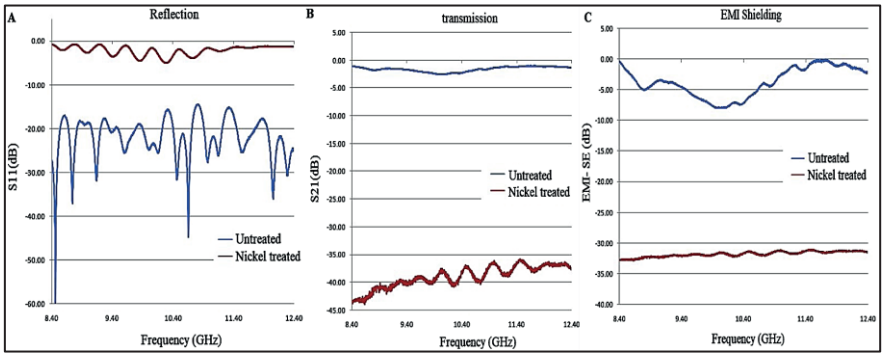

Figure 4. EMI shielding performance of untreated and nickel-treated polyester fabric
(Moazzenchi and Montazer, 2019)

In another study where five different woven fabric samples were created, experimental results for EMI SE were given clearly (Radulescu et al., 2020). The contribution of the copper plasma coating on the fabric with inserted silver yarns obtained in that study is given in Figure 5 as an example.

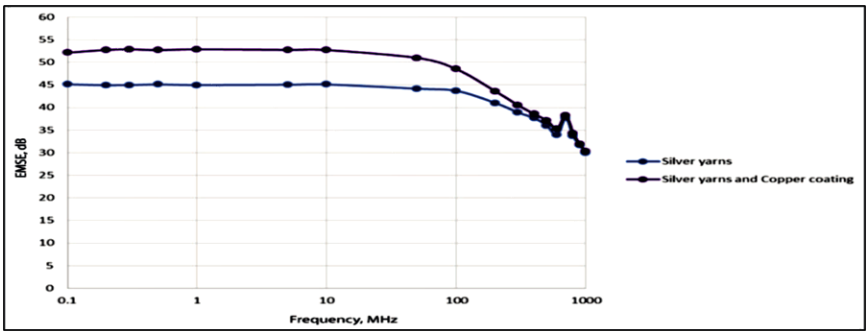

Figure 5. Contribution to EMI SE of copper plasma coating on fabrics with inserted silver yarns given in (Radulescu et al., 2020)

3.2. Conductive polymers for EMI shielding

Although metals are widely used as traditional protective materials as mentioned above, they have some disadvantages such as corrosion, low flexibility, and complex processing. Moreover, since EM signals are highly reflected from the metal surfaces, it is not possible to completely eliminate or reduce EM pollution in environment (Thomassin et al., 2013). Hence, researchers have focused on developing new materials with lightness, flexibility, high corrosion resistance, and easy machinability. For example, conductive coating polymer has been proposed as a new material for EMI shielding. They are suitable for use in insulation fabrics and that's why polymers and their composites have begun to replace metal-based materials due to their superior electrical and physical properties.

Although conductive polymer-based composites can both absorb and reflect the radiations, it is known that they generally exhibit higher levels of absorption than reflection (Kaynak and Håkansson, 2009). On the other hand, they present some challenges in terms of EMI shielding performance, such as complex processing, uniform distribution, and high loading of fillers. Despite these disadvantages, they stand out as smart textiles and are widely used for shielding purposes, thanks to their features such as being flexible, lightweight, cheap, resistant to corrosion, and easy to manufacture. Polymer coatings replace the non-conductive surfaces of the fabric into a highly electrically conductive material. One of the interesting polymers used for conductive textiles is polyaniline (PANI) due to its exceptional properties such as easy synthesis, biocompatibility, low-cost, redox-free doping, environmental stability, and in situ polymerization. Another conductive polymer commonly

used for EMI shielding is polypyrrole (PPy) (Zou et al, 2020). The EMI SE of some conductive textile materials are summarized in Table 2.

Table 2. SE values of various conductive textiles

Material	Testing Frequency (GHz)	EMI SE (dB)	Reference
Polyaniline-coated polyester	101	21.48	Dhaean et al., 2002
Polyaniline-coated silica	101	35.61	Dhaean et al., 2002
PPy-coated polyester	1.5	36.6	Kim et al., 2002
PPy-coated glass	2.4	21.16	Abbasi and Militky, 2013
PPy-coated cotton	2.5	01	Yildiz et al., 2013

3.3. Carbon-based composite for EMI shielding

Another material of interest for EMI shielding is carbon-based (CB) composites. Different materials such as graphene, carbon nanotube, carbon fiber, and carbon black have become popular components in shielding due to their superior properties such as high electrical conductivity, good mechanical performance, high specific strength, large aspect ratio, heat resistance, vibration attenuation, various molecular structures, lightweight, and flexibility (Mei et al., 2019; Li et al., 2020; Jia et al., 2020; Dai et al., 2020). Search results of CB EMI shielding materials archived in Web of Science for the last five years (2019-2023) are given in the Figure 6 (WoS CB Results, 2024). For example; research on CB shielding materials was the subject of more than 800 articles in 2023. This amount is much higher compared to studies examining metals and conductive polymers as protective materials as shown in the same figure (WoS Metal Results, 2024; WoS Conductive Polymers Results, 2024).

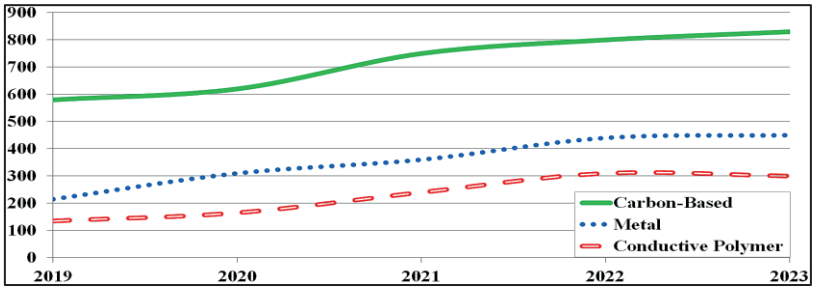

Figure 6. Development trend of carbon-based EMI shielding materials in the last five years

CB EMI shielding materials generally include film, composites, foam, and textiles with particular attention paid to frequency selectivity attributed to the periodic structure (Zhong et al., 2021). The film has an ultra-thin planar structure, lightness, flexibility, and an easy preparation process. Therefore, it can be said that it is a good choice for EMI protection. The prominent features of composites are their high strength modulus and corrosion resistance. The reason why foams are widely preferred in shielding is to provide a large surface area. On the other hand, textiles have become an important material for EMI shielding due to their merits such as softness, flexibility, breathability, reusability, recyclability, and low cost. Figure 7 shows the search results of these materials based on the Web of Science in the past five years (2019-2023) (WoS CB Composite Results, 2024; WoS CB Film Results, 2024; WoS CB Foam Results, 2024; WoS CB Textile Results, 2024)

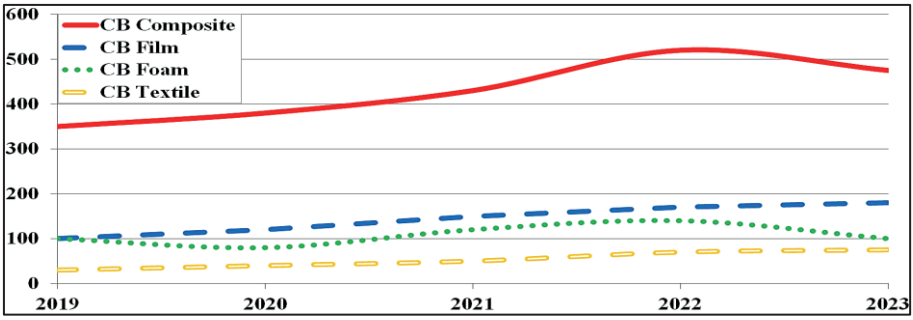

Figure 7. Development trend of different types of carbon-based EMI shielding materials in the past five years.

4. CONCLUSIONS

With the advancement of industry and the widespread use of electronic devices, EM radiations that have the potential to have negative effects on the human body, other living things, and sensitive electronic equipment have increased. For this reason, the development of EMI shielding materials and obtaining high efficiency from these materials has become an inevitable need. For this purpose, efforts to convert clothing fabrics into EMI shielding materials have increased. In this study, where EM wave are defined, its theory is explained, its spectrum is shown, its pollution is mentioned, the harmful effects of EMI are given, and shielding and protection methods are mentioned, the use of textile materials as protection materials is examined in detail. It has been emphasized that EMI protection materials should have features such as

lightness, flexibility, durability, and comfort in addition to their high SE. Regarding this, the importance and place of 'Metal-Based Materials', 'Conductive Polymers', and 'Carbon Based Composites', which provide some, but not all, of the given properties, in EMI SE applications have been examined. Then, a brief review of these three materials has been made using important studies in the literature. In conclusion, it is of great importance to develop textiles with EMI shielding properties that can be used in many places. Therefore, the focus should be on developing textile materials with the necessary properties for EMI shielding applications.

REFERENCES

Abbasi, A.R. and Militky, J. (2013). "EMI shielding effectiveness of polypyrrole coated glass fabric", *Journal of Chemistry and Chemical Engineering,* 7, pp. 256–259.

Akram, S., Ashraf, M., Javid, A., Abid, H. A., Ahmad, S., Nawab, Y., et al. (2023). "Recent advances in electromagnetic interference (EMI) shielding textiles: A comprehensive review", *Synthetic Metals,* 294, 117305.

Ali, A., Nguyen, N.H., Baheti, V., Ashraf, M., Militky, J., Mansoor, T., Noman, M.T., Ahmad, S. (2018). "Electrical conductivity and physiological comfort of silver coated cotton fabrics", *The Journal of The Textile Institute*, 109, pp. 620–628, https://doi.org/10.1080/00405000.2017.1362148.

Caplan, L.S., Schoenfeld, E.R., O'Leary, E.S., Leske, M.C. (2000). "Breast cancer and electromagnetic fields-a review", *Annals of Epidemiology,* 10, pp. 31–44.

Chandra, R.J., Shivamurthy, B., Kulkarni, S.D., Kumar, M.S. (2019). "Hybrid polymer composites for EMI shielding application-a review", *Materials Research Express – IOPscience,* 6, 082008, https://doi.org/10.1088/2053-1591/aaff00

Dai, M., Zhai, Y., Zhang, Y. (2020). "A green approach to preparing hydrophobic, electrically conductive textiles based on waterborne polyurethane for electromagnetic interference shielding with low reflectivity", Chemical Engineering Journal, 127749, https://doi.org/10.1016/j.cej.2020.127749

Demers P.A., Thomas D.B., Rosenblatt K.A., Jimenez L.M., McTiernan A., Stalsberg H., et al. (1991). "Occupational exposure to electromagnetic fields and breast cancer in men". *American Journal of Epidemiology,* 134(4), pp. 340–347.

Dhaean, S.K., Singh, N. and Venkatachalam, S. (2002). "Shielding effectiveness of conducting polyaniline coated fabrics at 101 GHz", *Synthetic Metals,* 125, pp. 389–393.

Diab, K. A. (2020). "The impact of the low frequency of the electromagnetic field on human", *Cell Biology and Translational Medicine,* Volume 7: Stem Cells and Therapy: Emerging Approaches, pp. 135–149.

Esen, M., İlhan, İ., Karaaslan, M. et al. (2020). "Investigation of electromagnetic and ultraviolet properties of nano-metal-coated textile surfaces", *Applied Nanoscience,* 10, pp. 551–561. https://doi.org/10.1007/s13204-019-01122-1

Ghosh, S., Mondal, S., Ganguly, S., Remanan, S., Singha, N., Das, N.C. (2018). "Carbon nanostructures based mechanically robust conducting cotton fabric for improved electromagnetic interference shielding", *Fibers and Polymers,* 19, pp. 1064–1073, https://doi.org/10.1007/s12221-018-7995-4.

Jia, Z., Zhang, M., Liu, B., Wang, F., Wei, G., Su, Z. (2020). "Graphene foams for electromagnetic interference shielding: a review", ACS Applied Nano Materials Journal, 3, pp. 6140–6155, https://doi.org/10.1021/acsanm.0c00835

Jiang, D., Murugadoss, V., Wang, Y., Lin, J., Ding, T., Wang, Z., et al. (2019). "Electromagnetic interference shielding polymers and nanocomposites-a review", *Polymers,* https://doi.org/10.1080/15583724.2018.1546737

Kamiya, K. and Sasatani, M. (2012). "Effects of radiation exposure on human body", *Nihon Rinsho,* 70(3), pp. 367–74. Japanese. PMID: 22514910.

Kaynak, A. and Håkansson, E. (2009). "Characterization of conducting polymer coated fabrics at microwave frequencies. International journal of clothing science and technology", 21(2/3), pp.117-126.

Khan, A., Nazir, A., Rehman, A., Naveed, M., Ashraf, M., Iqbal, K., Basit, A., Maqsood, H.S. (2020). "A review of UV radiation protection on humans by textiles and clothing", *International Journal of Clothing Science and Technology,* 32, pp. 869–890, https://doi.org/10.1108/IJCST-10-2019-0153.

Kim, M.S., Kim H.K., Byun S.W., et al. (2002). "PET fabric/polypyrrole composite with high electrical conductivity for EMI shielding", *Synthetic Metals,* 126, pp. 233–239.

King, J.A., Pisani, W.A., Klimek-McDonald, D.R., Perger, W.F., Odegard, G.M., Turpeinen, D.G. (2016). "Shielding effectiveness of carbon-filled polypropylene composites", *Journal of Composite Materials,* 50, pp.2177–2189, https://doi.org/10.1177/0021998315602326

Kovacic, P. And Somanathan, R. (2010). "Electromagnetic fields: mechanism, cell signaling, other bioprocesses, toxicity, radicals, antioxidants and beneficial effects", *Journal of Receptors and Signal Transduction,* 30, pp. 214–226, https://doi.org/10.3109/10799893.2010.488650

Li, Y., Lan, X., Wu, F., Liu, J., Huang, P., Chong, Y., Luo, H., Shen, B., Zheng, W. (2020). "Steam-chest molding of polypropylene/carbon black composite foams

as broadband EMI shields with high absorptivity", *Composites Communications,* 22, 100508, https://doi.org/10.1016/j.coco.2020.100508

Maity, S., Singha, K., Debnath, P., Singha, M. (2013). "Textiles in electromagnetic radiation protection", Journal of Safety Engineering 2, pp. 11–19.

Mei, X., Lu, L, Xie, Y., Wang, W., Tang, Y., Teh, K.S. (2019). "An ultra-thin carbon-fabric/ graphene/poly (vinylidene fluoride) film for enhanced electromagnetic interference shielding", *Nanoscale,* 11, pp. 13587–13599, https://doi.org/10.1039/C9NR03603B

Moazzenchi, B. and Montazer, M. (2019). "Click electroless plating of nickel nanoparticles on polyester fabric: electrical conductivity, magnetic and EMI shielding properties", *Colloids and Surfaces A: Physicochemical and Engineering Aspects*, 571, pp. 110–124, https://doi.org/10.1016/j.colsurfa.2019.03.065

Periyasamy, A.P., Yang, K., Xiong, X., Venkataraman, V., Militky, J., Mishra, R., Kremenakova, D. (2020). "Effect of silanization on copper coated milife fabric with improved EMI shielding effectivenessMaterials Chemistry and Physics, 239, 122008, https://doi.org/10.1016/j.matchemphys.2019.122008

Radulescu, I. R., Surdu, L., Mitu, B., Morari, C., Costea, M., Golovanov, N. (2020). "Conductive textile structures and their contribution to electromagnetic shielding effectiveness", *Industria Textila,* 71(5), pp. 432–437.

Rubežienė, V. and Varnaitė-Žuravliova, S. (2020). "EMI shielding textile materials", in *Materials for Potential EMI Shielding Applications*, Elsevier, pp. 357–378. https://doi.org/10.1016/B978-0-12-817590-3.00022-1.

Rybicki, T. (2019). "EMI Shielding and reflection from textile mesh grids compared with analytic models", *IEEE Transactions on Electromagnetic Compatibility,* 61, pp. 372–380, https://doi.org/10.1109/TEMC.2018.2830968

Sajjadi, B., Aziz, A. A., Ibrahim, S. (2014). "Investigation, modelling and reviewing the effective parameters in microwave-assisted transesterification", Renewable and Sustainable Energy Reviews, 37, pp. 762–777.

Sankaran, S., Deshmukh, K., Ahamed, M.B., Khadheer Pasha, S.K. (2018). "Recent advances in electromagnetic interference shielding properties of metal and carbon filler reinforced flexible polymer composites: a review", *Composites Part A: Applied Science and Manufacturing,* 114, pp. 49–71.

Shacklette, L.W. and Colaneri, N.F. (1991). "EMI shielding measurements of conductive polymer blends", *IEEE Instrumentation and Measurement Technology Conference,* https://doi.org/10.1109/IMTC.1991.161543

Singh, A.K., Shishkin, A., Koppel, T., Gupta, N. (2020). "Porous materials for EMI shielding", in: *Materials for Potential EMI Shielding Applications,* Elsevier, pp. 287–314, https://doi.org/10.1016/B978-0-12-817590-3.00018-X.

Thomassin, J. M., Jérôme, C., Pardoen, T., Bailly, C., Huynen, I., & Detrembleur, C. (2013). "Polymer/carbon based composites as electromagnetic interference (EMI) shielding materials", *Materials Science and Engineering: R: Reports,* 74(7), pp.211–232.

Tong, X.C. (2016). "Advanced materials and design for electromagnetic interference shielding", *CRC Press,* pp. 11–16, https://doi.org/10.1201/9781420073591

Web of Science (WoS), Search results of Carbon Based electromagnetic shielding materials in recent five years (2019–2023), (accessed 20 November 2024)

Web of Science (WoS), Search results of Metal electromagnetic shielding materials in recent five years (2019–2023), (accessed 20 November 2024)

Web of Science (WoS), Search results of Conductive Polymer electromagnetic shielding materials in recent five years (2019–2023), (accessed 20 November 2024)

Web of Science (WoS), Search results of electromagnetic shielding Carbon Based Foam in recent five years, (2019–2023), (accessed 20 November 2024)

Web of Science (WoS), Search results of electromagnetic shielding Carbon Based Composite in recent five years, (2019–2023), (accessed 20 November 2024)

Web of Science (WoS), Search results of electromagnetic shielding Carbon Based Film in recent five years, (2019–2023), (accessed 20 November 2024)

Web of Science (WoS), Search results of electromagnetic shielding Carbon Based Textile in recent five years, (2019–2023), (accessed 20 November 2024)

Wilson, R., George, G., Joseph, K. (2020). "An introduction to materials for potential EMI shielding applications: status and future", in: *Materials for Potential EMI Shielding Applications,* Elsevier, pp. 1–8, https://doi.org/10.1016/B978-0-12-817590-3.00001-4

Wu, Y., Wang, Z., Liu, X., Shen, X., Zheng, Q., Xue, Q., Kim, J.-K. (2017). "Ultralight graphene foam/conductive polymer composites for exceptional electromagnetic interference shielding", *ACS Applied Materials & Interfaces,* (9), pp. 9059–9069, https://doi.org/10.1021/acsami.7b01017.

Yang, Y.L. and Gupta, M.C. (2005). "Novel carbon nanotube-polystyrene foam composites for electromagnetic interference shielding", *Nano Letters,*5, pp. 2131–2134.

Yildiz, Z., Usta, I. and Gungor, A. (2013). "Investigation of the electrical properties and electromagnetic shielding effectiveness of polypyrrole coated cotton yarns", *Fibres & Textiles in Eastern Europe,* 98, pp. 32–37.

Zhang, L., Bi, S., Liu, M. (2020). "Lightweight electromagnetic interference shielding materials and their mechanisms", *IntechOpen,* doi: 10.5772/intechopen.82270

Zhong, L., Yu, R., Hong, X. (2021). "Review of carbon-based electromagnetic shielding materials: film, composite, foam, textile", *Textile Research Journal,* 91(9-10), pp. 1167–1183.

Zou, L., Lan, C., Yang, L., Xu, Z., Chu, C., Liu, Y., Qiu, Y. (2020). "The optimization of nanocomposite coating with polyaniline coated carbon nanotubes on fabrics for exceptional electromagnetic interference shielding", *Diamond and Related Materials,* 104, 107757. https://doi.org/10.1016/j.diamond.2020.107757

CHAPTER 2

FIBER OPTIC SENSING

İremnur Duru[1]
Timuçin Emre Tabaru[2]

1 Res. Asst., Sivas University of Science and Technology, Faculty Of Engineering And Natural Sciences, iremduru@sivas.edu.tr, ORCID ID: 0000-0001-5492-803X
2 Assoc. Prof. Dr., Sivas University of Science and Technology, Faculty Of Engineering And Natural Sciences, etabaru@sivas.edu.tr, ORCID ID: 0000-0002-1373-3620

1.INTRODUCTION

With the invention of the laser in the late 1960s, there has been a significant shift towards optical systems for telecommunications applications. As lasers entered our lives, researchers began exploring the potential of fiber optics for communication and sensing applications (Hocker, 1979). With lasers capable of transmitting large amounts of data, research was conducted across various wavelengths. The first fibers used had very high losses, so they were not preferred for communication applications (Fields, Asawa, Ramer, & Barnoski, 1980).

Fiber optic sensor technology enables detection by measuring parameters such as strain, temperature, and pressure in harsh conditions (Grattan & Sun, 2000). It is a measurement technique that facilitates the detection of physical, chemical, biological, and environmental parameters through the transmission of light waves along an optical fiber. These sensors modulate properties of the light wave, such as phase and intensity, within the optical fiber. The measurement data is transmitted using the optical fiber medium. Fiber optic sensors have become preferred over traditional sensors due to their sensitivity, durability, lightweight, small size, immunity to electromagnetic interference (EMI), high-temperature performance, bandwidth, and environmental resilience. These sensors have found applications in improving industrial processes, quality control systems, diagnostic systems, and process control (Grattan & Sun, 2000). Recently, with advancements in optoelectronics and fiber optic communication technology, new research directions have emerged. Noteworthy studies have explored various approaches for optimal fiber design (Grattan & Sun, 2000). The pursuit of designing fiber-based sensing systems and components has led to a focus on reducing the costs of fiber materials, driven by the increasing demand for fiber materials in the communication sector. Furthermore, the increasing preference for fibers has shown excellent performance results. As the use of fiber optic sensors grows, they have replaced traditional sensors in applications such as measuring acceleration, electrical and magnetic fields, chemical measurements, and many other sensor applications. Fiber optics used in sensing applications establish communication with the sensor or continuously monitor changes.

Fiber optic sensing applications have become increasingly popular in recent years. However, optical fibers are subject to disruptive effects in the environments they are placed in. These disruptive effects lead to changes in the fiber's properties, such as size, shape, refractive index, and mode conversion. In order to ensure continuous signal transmission and reception for communication applications, these disruptive effects must be minimized. In fiber optic sensing, the external responses caused by disturbances serve as indicators of disruptive effects. Since the signal passing through the fiber is modulated, the fiber itself, acting as a modulator, is responsible for the detection.

The fiber acts as a converter, transforming various signals into changes in optical radiation. Changes occur as properties such as phase, frequency, and polarization are characterized. The accuracy of the optical sensor depends on the characterization and the sensitivity of the fiber optic sensor. Fiber optic sensors have been preferred in medical, energy, environmental, and security applications. This study will first discuss the structure of optical fibers, classification of fiber optics, types of fiber optic sensing, components of fiber optic systems, and applications, followed by innovations in fiber optic sensing technology, future trends, and will conclude with results and future work.

Fiber optic sensors are preferred in healthcare systems due to their unique capabilities, such as small size, resistance to electromagnetic radiation, and sensitivity. This study examines types of optical fiber sensors and their latest applications in healthcare. The goal of this study is to provide an in-depth perspective on optical sensor technology, while also finding solutions to challenges encountered in healthcare through fiber optic sensors. The use of fiber optic sensors in healthcare is one of the topics that requires in-depth research.

This study reviews the recent achievements of fiber optic sensors and the use of new technologies in healthcare applications. The first section of this study will discuss the structure and working principles of optical fibers, while later sections will compare different types of optical sensors, and the final section will cover fiber optic sensors and their applications.

2. STRUCTURE OF OPTICAL FIBER

In fiber optic sensors, information is transmitted by the optical sensor through changes in phase, polarization, frequency, intensity, or combinations of these properties. Light on the detector surface is detected by a photodetector, which is a semiconductor device (Sabri, Aljunid, Salim, & Fouad, 2015). For detection through polarization, phase, or frequency modulation, the signal is transmitted to locations outside the sensor via an interferometric or grating-based signal transmission system. The advantages of fiber optic sensors include immunity to electromagnetic interference, wide bandwidth, and high sensitivity (Lee et al., 2012). Due to their dielectric structure, optical fibers, which are passive by nature, can maintain their structure even at high temperatures without degradation (Schena, Tosi, Saccomandi, Lewis, & Kim, 2016).

The core of fiber optic sensors enables long-distance transmission due to light propagation through total internal reflection with low loss. Since the introduction of the first fiber optic system in 1965, its use has expanded across various applications. Fiber optic sensor technologies have a wide range of applications, from advancements in machine learning (Venketeswaran et al., 2022) to strain/temperature detection in composite materials (Ramakrishnan

et al., 2016), industrial applications (Berthold III, 2024), environmental monitoring techniques (Shanafield et al., 2018), and general sensor applications (Annamdas & Annamdas, 2010). One of the popular applications is long-distance high-speed communication, which can reduce transmission losses to as low as 0.2 dB/km (Huang et al., 2019). As shown in Figure 1, the single-mode optical fiber used for fiber optic applications consists of three concentric layers. The silica core, which is typically 2-10 μm in diameter and doped with materials like germanium to increase the refractive index, the silica cladding with a diameter of 125 μm, and the buffer coating that protects the fiber from external factors form the outermost layer (Leung, Shankar, & Mutharasan, 2007). The buffer coating in the outermost layer does not direct the light. This structure provides protection and mechanical support from external factors. Due to total internal reflection conditions, it is necessary that n_1 > n_2. Optical fibers are made from combinations of materials, including plastic, chalcogenide glasses, or different components in the core and cladding (Schuster et al., 2014). Fiber optic sensors with silica cores and plastic coatings can be found. Fiber optic sensors are classified as single-mode and multi-mode, with their classification depending on the core size, operating wavelength, and the wavelength difference between the core and cladding. In a single-mode fiber, the distribution of light energy along the core of the optical fiber is Gaussian, while in multi-mode fibers, a more complex distribution occurs. Optical sensors detect changes in optical parameters depending on the physicochemical parameters of the surrounding environment. Optical fibers are useful tools for optical sensing applications, either as external or internal sensors, by directing light to the measurement area or collecting light from the measurement area.

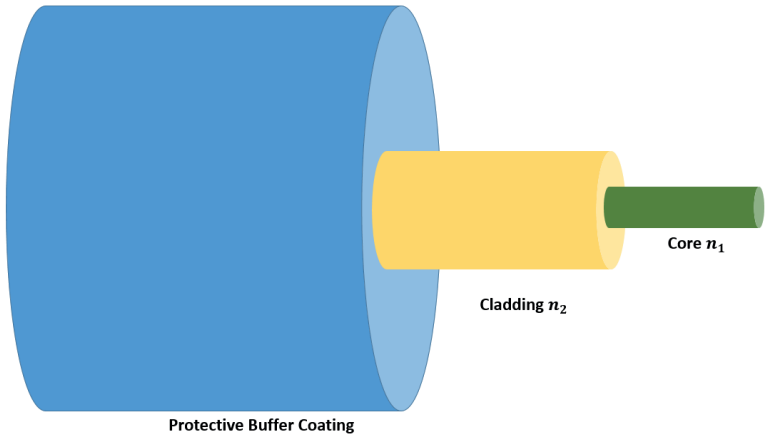

Figure 1. *Schematic representation of single-mode optical fiber including core, cladding and protective buffer coating.*

Fiber optics operate by measuring changes in light propagation caused by external factors, ranging from physical parameters such as strain, pressure, and temperature to analytical chemical parameters. Fiber optic sensors have several advantages over traditional sensor technologies. Some of the key advantages include immunity to electromagnetic interference, durability in harsh conditions, and tolerance to high temperatures. Additionally, thanks to biocompatible and easily replicable sensors, multiple measurements can be taken simultaneously.

3. FIBER OPTIC CLASSIFICATION

Fiber optic sensors are classified based on their intended use, modulation and demodulation types, structural properties, and application areas. They can be divided into two categories based on modulation and demodulation types. Amplitude (density) sensors detect changes in light intensity to identify external effects. Light intensity is influenced by changes such as bending and refraction in the light medium. Amplitude sensors are among the simpler and more cost-effective fiber optic sensors. Phase sensors detect changes in the phase of light (Miller, 2012). External factors encountered while light travels through the medium cause phase shifts. Phase sensors are preferred for applications requiring high precision. Frequency sensors detect changes in light frequency. Frequency sensors, which perform high-frequency measurements, contain piezoelectric crystals and resonance structures. Polarization describes the direction of oscillations in the plane perpendicular to the direction of the wave's motion. By examining the change in light properties, such as polarization, the variations in characteristics like magnetic fields and temperature can be detected. The measurement is performed by detecting the change of two light waves within an interferometric structure. These sensors, which detect changes in phase, frequency, and polarization, are useful but quite costly. Sensors are also categorized based on their application areas (Fang, Chin, Qu, & Cai, 2012).

Physical sensors are the first category. They are used for measuring physical quantities such as temperature and pressure. High-temperature resistant sensors are used for temperature measurements, while pressure sensors are insensitive to pressure changes. Chemical sensors are used in applications where chemical changes are measured. The changes in light signals inside the optical sensor are detected due to chemical changes. Biological sensors measure biological parameters, such as blood levels and glucose amounts, and detect changes (Hui & O'Sullivan, 2022).

Based on their structural properties, sensors are divided into external and internal categories. In external sensors, detection occurs outside the fiber, where the light is carried and reflected only from the detection region of the fiber. In internal sensors, detection occurs directly inside the fiber. The optical

properties of the fiber change due to external factors, and by detecting these changes, measurements are made.

3.1. FIBER OPTIC DETECTION TYPES

Fiber optic detection types are examined in 3 main groups. Distributed detection is a type of detection that makes measurements continuously or at certain intervals at every point of the fiber. There is a separate detection point at every point of the fiber. Signal processing in these systems, which have the ability to monitor in real time at long distances, is quite complex and time-consuming. Point detection is known as detection at a certain point. Only the parameters at that point are measured with a sensor at any specified point of the fiber. Simple and reliable measurements are made with point detection. Separate fibers should be considered for each measurement point. Although this situation increases the cost, it is quite effective for single-point measurements that require high precision. Spectroscopic detection is performed by measuring the reflection and absorption status of light by interacting with the substance. This type of detection, where spectral properties are measured, is based on the interaction at different wavelengths. Fiber optic sensors are used to transmit and detect light (Gholamzadeh & Nabovati, 2008).

3.2. COMPONENTS OF FIBER OPTIC DETECTION SYSTEMS

Fiber optic sensing systems are used to measure physical and chemical parameters. They are high-precision detection systems that measure changes in the properties of light. In fiber optic sensing systems, components such as the light source, optical fiber cable, sensor head, detector, modulator, signal processing, and data transmission systems are included. The light within the optical system is transmitted by the light source. The light source is designed to produce monochromatic or coherent light. Lasers or LEDs are used as light sources. The choice of light source is determined based on the sensor's sensitivity and application area (Fidanboylu & Efendioglu, 2009). Although LEDs are lower in cost, they have a lower bandwidth. Lasers enable high-intensity and long-distance transmission. With optical fiber cables, light first travels to the detection point and then to the detection device. Optical fiber cables are very thin, hair-like structures made of dielectric materials like glass. Depending on the type of fiber used, single-mode or multi-mode fibers are chosen. Single-mode fibers are preferred for long distances and applications requiring high sensitivity, while multi-mode fibers are used for shorter distances. The measurement of the optical sensor system is carried out with the sensor head. The sensor head at the end of the fiber interacts with physical, chemical, or biological parameters, causing changes in the light properties. The modulated light is detected and converted into an electrical signal by the photodetector. Photodiodes or, depending on the application,

photomultiplier tubes are used as photodetectors. Photodiodes are commonly preferred due to cost-effectiveness, while photomultiplier tubes, which have a more complex structure and higher sensitivity, are required for applications demanding high precision. An optical modulator is used to modulate the optical properties of light. Signal processing is used to process and analyze the signals coming from the detector (Pierce, Yu, & Richards-Kortum, 2011). Raw data is filtered and amplified. The data transmission system transmits the collected data through optical fibers or wireless communication.

4. APPLICATIONS OF FIBER OPTIC SENSOR

Fiber optic sensor technology initially emerged for data transmission and telecommunications applications, but over time, it has become the preferred choice due to its excellent detection capabilities and ability to perform in harsh environments. Its greatest advantages include cost-effectiveness, miniaturized size, lightness, portability, and immunity to electromagnetic interference. Due to these advantages, optical fibers have achieved numerous successes and have become the preferred choice in many applications. Some of the most important applications include disease detection (Nejati-Koshki et al., 2023), drug delivery (Zhang et al., 2024), environmental monitoring (García, Monzón-Hernández, & Bustos, 2017), gas detection (Wolfbeis, 2006), and many others. Unlike traditional sensor types, fiber optic sensors are an indispensable detection method for explosive detection. Fabry-Perot interferometric sensors are commonly preferred for high-precision acoustic detection and pressure applications (Yoshino, Kurosawa, Itoh, & Ose, 1982). They play roles in underwater acoustic detection, pressure monitoring in oil and gas drilling, and medical events such as blood pressure and glucose measurement. Fiber Bragg Grating sensors (Othonos, 1997) are preferred for temperature, deformation detection, strain changes, structural health monitoring of aircraft wings, analysis of wind turbines, construction security checks, and applications in the aerospace sector. With their multi-point measurement capabilities, these sensors enable detection over large surfaces.

Micro-bending sensors work based on the bending of optical fiber cables. They are preferred for detecting mechanical loads and deformations. They are also used in structural health monitoring, earthquake detection, and vibration sensing in industrial machines (Sun, Zhang, Zeng, Hu, & Duan, 2022).

Michelson interferometer-based sensors are preferred for sound source detection, vibration sensing, and acoustic imaging applications (Dandridge, 2024). They are frequently used in underwater target detection, security, and monitoring applications.

Chemical fiber optic sensors used for chemical and biological detection are highly valuable in environmental monitoring, medical applications, and food safety (Pospíšilová, Kuncová, & Trögl, 2015). Gas detection sensors are

used for detecting harmful gases, biosensors monitor biological activities, and they are even used to detect bacterial contamination.

Thermal sensors, as the name suggests, are designed to detect temperature changes (Ramakrishnan, Rajan, Semenova, & Farrell, 2016). They are used in industrial process control systems, energy plants, space research, and other fields.

Raman and Brillouin scattering-based fiber optic sensors are preferred for long-distance applications (Muanenda, Oton, & Di Pasquale, 2019). These sensors are used in temperature and strain measurement applications, as well as for monitoring high-voltage power lines, large infrastructure projects, and oil and gas pipelines.

Thanks to these different sensor types, fiber optic technology has been applied to a wide range of fields. Through its innovative solutions, fiber optic sensors have remained a cornerstone of modern technology.

5. CONCLUSION

Fiber optic sensors provide a strong solution for applications requiring high precision, and due to their immunity to electromagnetic interference, they offer significant advantages for long-distance applications. These sensors are widely used in various sectors, including the energy sector, structural monitoring, biotechnology, and space industry applications. This study discusses various works conducted with fiber optic sensors, examining their impact on mechanical and optical performance in different environments. A better understanding of material properties has contributed to the development of solutions that enhance the efficiency and durability of these sensors. Future research could focus on integrating new materials and manufacturing techniques to further improve sensor performance, potentially expanding their range of applications. This study has provided crucial data for the design of high-precision measurement systems and has contributed to the development of advanced fiber optic sensors that can be used in industries such as energy, automotive, space, and biotechnology.

REFERENCES

Annamdas, K. K. K., & Annamdas, V. G. M. (2010, April). Review on developments in fiber optical sensors and applications. In Fiber optic sensors and applications VII (Vol. 7677, pp. 205-216). SPIE.

Berthold III, J. W. (2024). Industrial applications of fiber optic sensors. In Fiber optic sensors: An introduction for engineers and scientists (pp. 573-591).

Dandridge, A. (2024). Fiber optic sensors based on the Mach–Zehnder and Michelson interferometers. In Fiber optic sensors: an introduction for engineers and scientists (pp. 213-248).

Fang, Z., Chin, K., Qu, R., & Cai, H. (2012). Fundamentals of optical fiber sensors. John Wiley & Sons.

Fields, J. N., Asawa, C. K., Ramer, O. G., & Barnoski, M. K. (1980). Fiber optic pressure sensor. The Journal of the Acoustical Society of America, 67(3), 816-818.

Fidanboylu, K., & Efendioglu, H. S. (2009, May). Fiber optic sensors and their applications. In 5th International Advanced Technologies Symposium (IATS'09) (Vol. 6, pp. 2-3).

García, J. A., Monzón-Hernández, D., & Bustos, E. (2017). Fiber-optic sensor networks: environmental applications. In Undergr Sens Monit Hazard Detect Environ Infrastruct (pp. 322).

Gholamzadeh, B., & Nabovati, H. (2008). Fiber optic sensors. International Journal of Electronics and Communication Engineering, 2(6), 1107-1117.

Grattan, K. T., & Sun, T. (2000). Fiber optic sensor technology: an overview. Sensors and Actuators A: Physical, 82(1-3), 40-61.

Hocker, G. B. (1979). Fiber-optic sensing of pressure and temperature. Applied Optics, 18(9), 1445–1448.

Huang, M. F., Salemi, M., Chen, Y., Zhao, J., Xia, T. J., Wellbrock, G. A., ... & Aono, Y. (2019). First field trial of distributed fiber optical sensing and high-speed communication over an operational telecom network. Journal of Lightwave Technology, 38(1), 75-81.

Hui, R., & O'Sullivan, M. (2022). Fiber-Optic Measurement Techniques. Academic Press.

Krohn, D. A., MacDougall, T., & Mendez, A. (2014). Fiber optic sensors: fundamentals and applications (Vol. 4). Bellingham, Washington: Spie Press.

Lee, B. H., Kim, Y. H., Park, K. S., Eom, J. B., Kim, M. J., Rho, B. S., & Choi, H. Y. (2012). Interferometric fiber optic sensors. Sensors, 12(3), 2467-2486.

Leung, A., Shankar, P. M., & Mutharasan, R. (2007). A review of fiber-optic biosensors. Sensors and Actuators B: Chemical, 125(2), 688-703.

Miller, S. (Ed.). (2012). Optical fiber telecommunications. Elsevier.

Muanenda, Y., Oton, C. J., & Di Pasquale, F. (2019). Application of Raman and Bril-

louin scattering phenomena in distributed optical fiber sensing. Frontiers in Physics, 7, 155.

Nejati-Koshki, K., Fathi, F., Arabzadeh, A., & Mohammadzadeh, A. (2023). Biomarkers and optical based biosensors in cardiac disease detection: early and accurate diagnosis. Analytical Methods, 15(41), 5441-5458.

Othonos, A. (1997). Fiber bragg gratings. Review of scientific instruments, 68(12), 4309-4341.

Pierce, M., Yu, D., & Richards-Kortum, R. (2011). High-resolution fiber-optic microendoscopy for in situ cellular imaging. Journal of Visualized Experiments: JoVE, (47), 2306.

Pospíšilová, M., Kuncová, G., & Trögl, J. (2015). Fiber-optic chemical sensors and fiber-optic bio-sensors. Sensors, 15(10), 25208-25259.

Ramakrishnan, M., Rajan, G., Semenova, Y., & Farrell, G. (2016). Overview of fiber optic sensor technologies for strain/temperature sensing applications in composite materials. Sensors, 16(1), 99.

Sabri, N., Aljunid, S. A., Salim, M. S., & Fouad, S. (2015). Fiber optic sensors: short review and applications. Recent trends in physics of material science and technology, 299-311.

Schena, E., Tosi, D., Saccomandi, P., Lewis, E., & Kim, T. (2016). Fiber optic sensors for temperature monitoring during thermal treatments: An overview. Sensors, 16(7), 1144.

Schuster, K., Unger, S., Aichele, C., Lindner, F., Grimm, S., Litzkendorf, D., ... & Bartelt, H. (2014). Material and technology trends in fiber optics. Advanced Optical Technologies, 3(4), 447-468.

Shanafield, M., Banks, E. W., Arkwright, J. W., & Hausner, M. B. (2018). Fiber-optic sensing for environmental applications: Where we have come from and what is possible. Water Resources Research, 54(11), 8552-8557.

Sun, X., Zhang, L., Zeng, L., Hu, Y., & Duan, J. A. (2022). Micro-bending sensing based on single-mode fiber spliced multimode fiber Bragg grating structure. Optics Communications, 505, 127513.

Venketeswaran, A., Lalam, N., Wuenschell, J., Ohodnicki Jr, P. R., Badar, M., Chen, K. P., ... & Buric, M. (2022). Recent advances in machine learning for fiber optic sensor applications. Advanced Intelligent Systems, 4(1), 2100067.

Wolfbeis, O. S. (2006). Fiber-optic chemical sensors and biosensors. Analytical Chemistry, 78(12), 3859-3874.

Yoshino, T., Kurosawa, K., Itoh, K., & Ose, T. (1982). Fiber-optic Fabry-Perot interferometer and its sensor applications. IEEE Transactions on Microwave Theory and Techniques, 30(10), 1612-1621.

Zhang, Y., Zheng, J., Jin, F., Xiao, J., Lan, N., Xu, Z., ... & Guan, B. O. (2024). Fiber-optic drug delivery strategy for synergistic cancer photothermal-chemotherapy. Light: Science & Applications, 13(1), 228.

CHAPTER 3

PERMANENT MAGNET SYNCHRONOUS MOTORS AND THEİR FUTURE PERSPECTİVES

Arda Ahmet ATEŞ[1]

Mehmet GÜÇYETMEZ[2]

1 Arş. Gör., Mühendislik ve Doğa Bilimleri Fakültesi, Elektrik-Elektronik Mühendisliği Bölümü, Elektrik Tesisleri Anabilim Dalı) Sivas Bilim Ve Teknoloji Üniversitesi, ardaates@sivas.edu.tr,
ORCID ID: 0009-0009-3845-6840
2 Dr. Öğr. Üyesi, Mühendislik ve Doğa Bilimleri Fakültesi, Elektrik-Elektronik Mühendisliği Bölümü, Elektrik Tesisleri Anabilim Dalı) Sivas Bilim Ve Teknoloji Üniversitesi, mehmetgcy@sivas.edu.tr,
ORCID ID: 0000-0003-2191-8665

1. Introduction

Electric motors are rotary electric machines that have been used for many years to obtain mechanical motion from electrical energy, especially in many machines used in industrial production. Later, the use of electric motors in electrical home appliances at various power levels has also become widespread. Electric transportation, which has developed and spread especially since the 2020s, and especially the use of electric motors in electric vehicles, is still in rapid development. It is estimated that there will be an increasing use of electric motors in both ground and aerial electric transportation in the next decade (Cai, W. et. al, 2021).

The earth needs mechanical motion, and therefore electric motors, due to the increasing world population and the various needs of this population. Currently, energy production and conversions in many sectors are carried out using traditional sources such as gasoline, diesel, natural gas, and coal. Developing technology and increasing needs also create environmental problems such as global warming. Electric motors, on the other hand, stand before us as an important option for many such traditional and environmentally harmful situations (Husain, I. et al, 2021).

There are many types of electric motors that are energized by direct and alternating current or by using both types together. The selection of electric motor is determined according to the area of use and power requirement, however, in order to reduce mechanical maintenance and costs, it is generally preferred to use magnets instead of windings. Studies are ongoing to obtain lighter weight and higher torque per unit area.

There are some parameters that limit electric motors. These can be given as torque vibrations, weight, and increased acoustic noise. The further development of the electrical and mechanical parameters of electric motors, especially in electric transportation, will lead to the device or chassis on which the motor will be used to be lighter and thus more efficient (Sudha, B. et al, 2020).

Permanent magnet synchronous motors (PMSM) stand out among electric motors due to their advantages such as using magnets instead of windings, being suitable for electric vehicles and having adjustable power or torque values in a wide area (Ullah, K. et al, 2022). The features of these motors and comparisons with other motor types from various perspectives and various suggestions to be made in the future regarding PMSMs are presented below.

2. Classification of Electric Motors

As the structures of electric motors are developed, their classifications also change. For example, linear types have been developed for many motors in recent years. However, it is still possible to make a classification based on

alternating and direct current for electric motors. Special purpose electric motors are generally classified as types outside the basic classification (Mikail, R 2006.).

2.1 DC Motors

DC motors are motors that operate with direct current and are generally used in applications requiring high torque.

• **Structure:**

DC motors consist of basic components such as stator (the part that creates a fixed magnetic field), rotor (the rotating part), commutator and brushes. Permanent magnets or electromagnets in the stator create a magnetic field on the rotor. Brushes and commutator change the direction of direct current, allowing the rotor to rotate continuously (Rambabu, S. 2007).

- **Avantages:**

o Speed control is easy and can operate in a wide speed range.

o It produces high starting torque, which provides superior performance in the early stages of movement.

o It requires a simple control system.

- **Disadvantages:**

o Requires regular maintenance as mechanical parts such as brushes and commutators wear out.

o Its efficiency is low compared to modern AC motors.

o Its use is limited in large-scale applications.

- **Area of use:**

o Electric vehicles, cranes, elevators and small portable devices (Dursun, E. H. 2016, Manohar, V. J. 2023).

2.2 AC Motorlar

AC motors are motors that run electrical energy using alternating current and are divided into two main subtypes: induction motors and synchronous motors.

2.2.1 Induction Motors (Asynchronous Motors)

• **Structure:**

The stator creates a magnetic field when alternating current is applied. This magnetic field induces current in the rotor, causing it to rotate. The rotor is usually made of aluminum or copper in the form of a cage.

- **Avantages:**

o Speed control is easy and can operate in a wide speed range.

o It produces high starting torque, which provides superior performance in the early stages of movement.

o It requires a simple control system.

- **Disadvantages:**

o Starting torque is low.

o Speed control is more difficult compared to synchronous motors.

- **Area of use:**

o Industrial machinery, HVAC systems and pumps (Marino, R. et al, 2010).

2.2.2 Synchronous Motors

• Structure:

The rotor rotates at the same speed as the magnetic field of the stator (synchronous speed). It is usually equipped with permanent magnets or field windings.

- **Avantages:**

o Provides high energy efficiency.

o Ideal for applications operating at constant speed.

- **Disadvantages:**

o Requires a more complex startup mechanism (Spargo, C. D. 2016).

o Has a high startup cost.

- **Area of use:**

o Power generation facilities and industrial applications requiring high precision**.**

2.3 Stepper Motors

Stepper motors have a step-by-step operating principle and are generally preferred in applications requiring position control (Marino, R. et al, 2010).

• Structure:

The rotor moves at certain angles by directing the magnetic fields in a controlled manner. No brushes are used during operation.

- **Avantages:**

o Provides precise motion control.

- Has a long life thanks to its brushless structure.
- Provides high accuracy in repetitive movements.

- **Disadvantages:**

- Efficiency is lower than other motors.
- Torque loss may occur under load.

- **Area of use:**

- CNC machines, 3D printers and robotic arms (Hasan, M. et al, 2018).

2.4 General Classification of Electric Motors

The table 1 summarizes the general classification of electric motors and their basic characteristics:

Motor Type	Working Principle	Advantages	Disadvantages	Areas of Use
DC Motors	Direct current	Easy speed control, high torque	Requires regular maintenance	Electric vehicles, portable devices
AC Induction Motors	Alternating current	Durable, low cost	Complex speed control	Industrial machinery, pumps
AC Synchronous Motors	Alternating current	High efficiency at constant speed	The initial mechanism is complex	Power plants, sensitive applications
Stepper Motors	Control with magnetic fields	Provides precise positioning	Low productivity	CNC machines, robotic systems

Table 1. *General Classification of Electric Motors*

3. Permanent Magnet Synchronous Motor (PMSM)

PMSMs are a type of synchronous motor that uses permanent magnets to convert electrical energy into mechanical energy. Their high energy efficiency and compact design make PMSMs an important component in modern industrial and technological applications. The defining feature of PMSMs is the use of permanent magnets in the rotor, enabling synchronous operation and maximizing energy transfer efficiency through the interaction of magnetic fields between the rotor and stator (Yang, Y. et al, 2020, Ren, J. et al, 2021).

3.1 PMSM's Structure

PMSM consists of two primary components:

- **Stator:** Generates a rotating magnetic field when alternating current is applied.

- **Rotor:** includes permanent magnets, which are often composed of materials with a high energy density, including neodymium-iron-boron (NdFeB). These magnets reduce losses and stabilize the magnetic field. High power density is another benefit they offer (Shen, Q. et al, 2022).

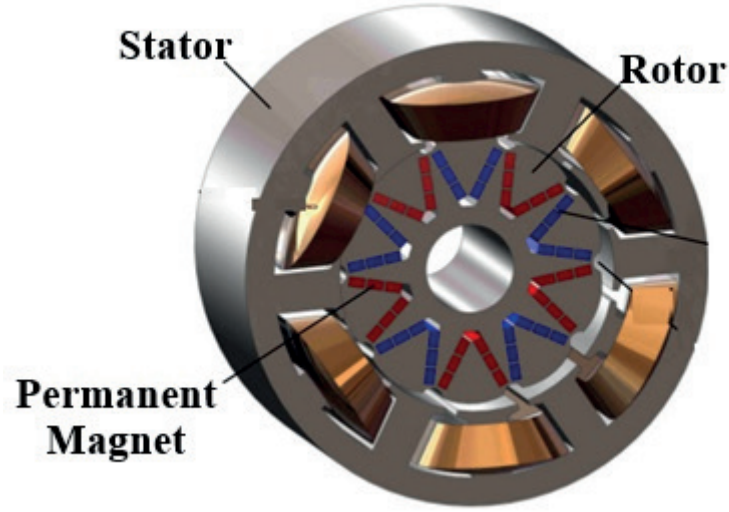

Fig 1. *Permanent Magnet Synchronous Motor Structure (Zhao, X. et al, 2022)*

3.2 Working Principle

The revolving magnetic field produced by the stator windings and the permanent magnets in the rotor interact to power PMSM. The rotor does not slip and revolves at the same speed as the stator's magnetic field. Accurate and steady speed control is made possible by this synchronization. The motor functions synchronously when the rotor's speed and the stator's rotating magnetic field coincide (Mohd Zaihidee, F. et al, 2019, Ma, D., & Jiang, J., 2023).

3.3 Technical Details

1. **Use of Permanent Magnets:**

o The permanent magnets with rotor mean that the motor is light in weight also allows the magnetic flux to circulate more efficient. These magnets minimize energy losses, as well as maintenance requirements.

2. **High Efficiency and Power Density:**

o So the efficiency of PMSM can get more than 90% (Mĭnaz, M. R., 2020). The design ensures high power output from a small and light-weight

permanent magnet and synchronous system, ideal for portable and compact applications including electrical vehicles, wind turbines and industrial machinery.

3. **Quiet Operation:**

o PMSMs are brushless and commutator-less so they give low vibration and low noise working. This contributes to longer life and quieter operation, so PMSMs are preferred for home appliances and devices (ex: medical or robots) where low noise is very important.

3.4 Advantages of PMSM

PMSM offers several benefits over other motor types, including:

- High energy efficiency, leading to energy savings.
- Compact and lightweight design.
- Precise speed and torque control.
- Lack of components requiring maintenance (e.g., brushes).
- High power density, suitable for small yet powerful applications.

4. **Advantages of PMSM Over Other Motor Types**

It can be said that PMSMs have many visible advantages over other motor types for them to be preferred in applications (Gündoğan, A., 2018). The most important of these advantages are their high energy efficiency, usability even in narrow spaces due to their small size, and high dynamic performance (Rehman, A. U. et al, 2022) The advantages of PMSMs over alternative motor types will be examined in detail in this section.

4.1 Energy Efficiency

It is accepted that PMSMs can reach higher efficiency values compared to other motor structures (Huang, J. et al, 2023). In order to achieve high efficiency, the formation of a more regular and in most cases optimum magnetic field in the permanent magnets in the rotor of PMSM compared to the magnetic field formed in wound motors is an important factor. In this way, energy loss is also reduced. For most rotating electrical machines, except transformers, efficiency values are below 90%. However, PMSM motors typically exceed 90% in efficiency, making them suitable for almost all applications, especially where energy efficiency and low operating costs are needed (Minaz, M. R., 2020).

Comparison:

- **DC Motors:** Energy losses occur due to the brush and commutator.
- **Induction Motors:** Higher losses result from rotor currents.
- **Stepper Motors:** Lower efficiency and increased energy loss.

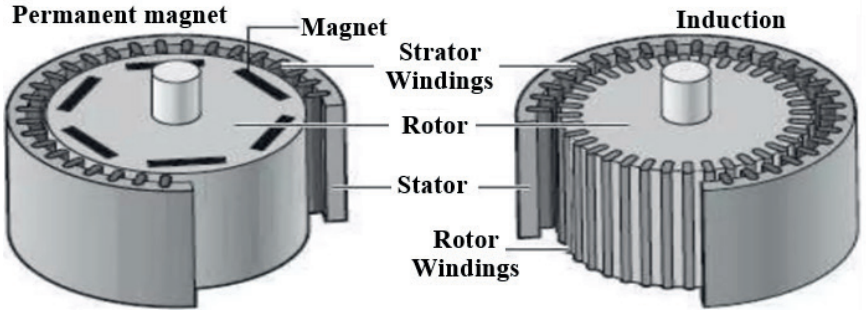

Fig 2. *Architectural comparison of induction motor and permanent magnet motor (newenergyandfuel.com)*

4.2 Compact Design

Compact design is one of the most important parameters targeted for electric motors. It is possible to obtain higher torque per unit area by reducing the motor size with a compact design. PMSMs offer a structure suitable for these goals. In this case, the most effective is the use of permanent magnets instead of windings. This reduces the motor's weight and volume while providing high power density (Chasiotis, I. D., & Karnavas, Y. L., 2018).

- For instance, a PMSM is significantly lighter than an induction motor for the same power output.
- Its compact structure is highly advantageous for applications with limited space, such as electric vehicles, drones, and portable devices (Jian, L., 2018, Motlagh, N. H. et al, 2016).

4.3 Dynamic Performance

PMSM excels in speed control and stability thanks to its superior dynamic performance (Ullah, K. et al, 2022). Leveraging the principle of synchronous operation:

- Precise torque control is achievable.
- Rapid response to load variations is ensured.
- It delivers maximum performance in applications requiring constant speed.

Comparison with Other Motors:

- Induction Motors: Speed control is more complex, and dynamic performance is limited.
- Stepper Motors: Struggles to maintain steady speed due to torque ripples.

4.4 Comparative Table

In table 2 compares PMSM with other types of motors in terms of some critical parameters:

Parameter	PMSM	DC Motors	Induction Motors	Stepper Motor
Energy Efficiency	%90+	%70-85	%80-90	%60-75
Compact Design	+++++	+++	+++	++++
Dynamic Performance	+++++	++++	+++	+
maintenance	Low	High	Low	Very Low
Quiet Operation	+++++	+++	+++	++++
Cost	++++	+++	++	+++
+ Very Low	++ Low	+++ Average	++++ Good	+++++ Very Good

Table 2. *Comparison of Motor Types*

4.5 Areas Where PMSM Is Preferred

The features described above make PMSM stand out particularly in the following areas:

• Systems Requiring Energy Efficiency: Electric vehicles, renewable energy systems (e.g. wind turbines).

• Applications Requiring Compactness and Lightness: Drones, portable devices, medical equipment.

• Systems Requiring Precision and Stability: Robotic arms, CNC machines, aviation applications.

5. Applications of PMSM

PMSM has become a widely used motor in many applications for which a high level of efficiency, compact construction, and high level of control precision are required. These motors find their application primarily in industrial and commercial uses, but most importantly in uses which lie in the area of renewable energy, attributed mainly to the silent operation, long life, and high performance of these motors (Zheng, J. et al, 2017).

5.1 Robotic Systems

PMSM, particularly because of the torque and speed control it provides with high precision, is widely used in robotic applications, especially in industrial robot arms and automation systems. Its quiet operation is another feature that makes it desirable, especially for medical robots working closely with humans (Jieqiong, W., 2024).

5.2 HVAC Systems

In HVAC systems, PMSM motors are employed to reduce energy consumption and improve overall system efficiency. Their ability to provide variable speed control optimizes performance and lowers energy costs, making them attractive for both commercial and residential HVAC applications (Ashok Kumar, L., & Indragandhi, V., 2020).

5.3 Renewable Energy Applications

PMSM motors are central to sustainable energy systems:

- **Wind Turbines**: PMSMs enhance energy conversion efficiency in wind turbines due to their ability to operate at variable speeds and are compatible with lighter turbine designs (Yan, J. et al, 2016).
- **Solar Energy Systems**: By minimizing losses, PMSM motors increase the efficiency of motorized equipment used in energy storage and transfer (Dubey, M. et al, 2014).

5.4 Transportation and Industrial Applications

PMSMs are also prominent in transportation and industrial processes:

- **Electric Trains and Metro Systems**: Preferred for their high torque, low maintenance requirements, and long service life (Shikata, K. et al, 2012).
- **Industrial Machines**: Utilized in CNC machines, compressors, and pumps requiring precise control (Lin, F. J. et al, 2006).
- **Electric Vehicles (EVs)**: With high energy efficiency and power density, PMSMs play a crucial role in EVs, extending range and enabling compact designs, making them indispensable in this field (Murali, N., & Ushakumari, S., 2020).

6. Conclusion

The diversity of electric motors comes from the unique advantages that each type of motor offers for a different application. In this context, Permanent Magnet Synchronous Motor (PMSM) shows far-reaching advancements in energy efficiency, compact size, and precise control features compared to the other types of motors. PMSM has a clear superiority in industrial and internal applications. It is such areas as sustainability, such as renewable energy, electric

transportation, and intelligent automation systems, and innovation that the effectiveness of PMSMs will be increased. Consequently, the increase and improvement of performance are the two basic objectives that require more research in the field of motor design, materials science, and control algorithms for PMSM. These efforts further optimize energy consumption of PMSM and widen its application all over the globe. PMSM is, and will remain, one of the cornerstones of modern engineering.

References:

Cai, W., Wu, X., Zhou, M., Liang, Y., & Wang, Y. (2021). Review and development of electric motor systems and electric powertrains for new energy vehicles. *Automotive Innovation*, *4*, 3-22.

Husain, I., Ozpineci, B., Islam, M. S., Gurpinar, E., Su, G. J., Yu, W., ... & Sahu, R. (2021). Electric drive technology trends, challenges, and opportunities for future electric vehicles. *Proceedings of the IEEE*, *109*(6), 1039-1059.

Sudha, B., Vadde, A., & Sachin, S. (2020, December). A review: High power density motors for electric vehicles. In *Journal of Physics: Conference Series* (Vol. 1706, No. 1, p. 012057). IOP Publishing.

Ullah, K., Guzinski, J., & Mirza, A. F. Critical Review on Robust Speed Control Techniques for Permanent Magnet Synchronous Motor (PMSM) Speed Regulation. Energies, 15(3), 1235. 2022.

Mikail, R. Fundamentals of Electric Motors and Transformers. Short Course on Energy Efficiency.

Rambabu, S. Modeling and Control of A Brushless DC Motors. 2007.

Dursun, E. H. Değişken Yüklü Dc Motorun Kayan Kipli Kontrolü. Selçuk Üniversitesi Fen Bilimleri Enstitüsü, Elektrik-Elektronik Mühendisliği Ana Bilim Dalı, Yüksek Lisans Tezi. Ağustos 2016.

Manohar, V. J. Advantages And Dısadvantages Of Brushless Dc Motor. Electrical Devices & Systems. March 2023

Marino, R., Tomei, P., Verrelli, C. M. Induction Motor Control Design.

Spargo, C. D. Synchronous Reluctance Motor Technology: İndustrial Opportunities, Challenges And Future Direction. Engineering & Technology Reference. Volume 2016.

Hasan, M., Refath, N. H., Ferdus, R. Design and Development of a Stepper Motor Position Control System in Micro-stepping Mode Using Atmega32 Microcontroller. Department of Electrical and Electronics Engineering, BRAC University. April, 2018.

Yang, Y., He, Q., Fu, C., Liao, S., & Tan, P. (2020). Efficiency improvement of permanent magnet synchronous motor for electric vehicles. *Energy*, *213*, 118859.

Ren, J., Wang, X., & Zhao, W. (2021). Magnetic field prediction of the saturated surface-mounted permanent magnet synchronous machine with rotor

Shen, Q., Zhou, Z., Li, S., Liao, X., Wang, T., He, X., & Zhang, J. (2022). Design and analysis of the high-speed permanent magnet motors: A review on the state of the art. *Machines*, *10*(7), 549.

X. Zhao, B. Kou, C. Huang, and L. Zhang, "Optimization Design and Performance Analysis of a Reverse-Salient Permanent Magnet Synchronous Motor," *Machines*, vol. 10, no. 3, Mar. 2022, doi: 10.3390/machines10030204.

Mohd Zaihidee, F., Mekhilef, S., & Mubin, M. (2019). Robust speed control of PMSM using sliding mode control (SMC)—A review. *Energies*, *12*(9), 1669.

Ma, D., & Jiang, J. (2023). A current source inverter with zero-voltage-switching for low-input voltage PMSM drive application. *Electrical Engineering*, *105*(5), 3161-3173.

Minaz, M. R. (2020). An effective method for detection of stator fault in PMSM with 1D-LBP. *ISA transactions*, *106*, 283-292.

Gündoğan, A. *Sabit mıknatıslı senkron makinelerin model tabanlı akım referansı kontrolü ile moment dalgalanmalarının azaltılması* (Master's thesis, Fen Bilimleri Enstitüsü).

Rehman, A. U., Basit, B. A., Choi, H. H., & Jung, J. W. (2022). Computationally efficient deadbeat direct torque control considering speed dynamics for a surface-mounted PMSM drive. *IEEE/ASME Transactions on Mechatronics*, *27*(5), 3407-3418.

Huang, J., Cao, G., & Zhang, L. (2023, July). Design and Optimization of PMSM for Injection Molding Machine. In *Journal of Physics: Conference Series* (Vol. 2557, No. 1, p. 012015). IOP Publishing.

"The Best Electric Vehicle Motor." Accessed: Dec. 14, 2023. [Online]. Available: https://newenergyandfuel.com/http:/newenergyandfuel/com/2010/02/09/the-best-electric-vehicle-motor/

Chasiotis, I. D., & Karnavas, Y. L. (2018, September). A study on design and optimization of high power density pmsm for pod propulsion system. In *2018 XIII International Conference on Electrical Machines (ICEM)* (pp. 534-540). IEEE.

Jian, L. (2018, September). Research status and development prospect of electric vehicles based on hub motor. In *2018 China International Conference on Electricity Distribution (CICED)* (pp. 126-129). IEEE.

Motlagh, N. H., Taleb, T., & Arouk, O. (2016). Low-altitude unmanned aerial vehicles-based internet of things services: Comprehensive survey and future perspectives. *IEEE Internet of Things Journal*, *3*(6), 899-922.

Ullah, K., Guzinski, J., & Mirza, A. F. (2022). Critical review on robust speed control techniques for permanent magnet synchronous motor (PMSM) speed regulation. *Energies*, *15*(3), 1235.

Zheng, J., Wang, Z., Wang, D., Li, Y., & Li, M. (2017, July). Review of fault diagnosis of PMSM drive system in electric vehicles. In *2017 36th Chinese Control Conference (CCC)* (pp. 7426-7432). IEEE.

Jieqiong, W. (2024). Real-time torque ripple compensationfor PMSMs in robotics applications.

Ashok Kumar, L., & Indragandhi, V. (2020). PMSM drive using predictive current control technique for HVAC applications. In *Proceedings of International Conference on Artificial Intelligence, Smart Grid and Smart City Applications: AISGSC 2019* (pp. 31-41). Springer International Publishing.

Yan, J., Feng, Y., & Dong, J. (2016). Study on dynamic characteristic of wind turbine emulator based on PMSM. *Renewable Energy*, *97*, 731-736.

Dubey, M., Sharma, S., & Saxena, R. (2014, March). Solar PV stand-alone water pumping system employing PMSM drive. In *2014 IEEE Students' Conference on Electrical, Electronics and Computer Science* (pp. 1-6). IEEE.

Shikata, K., Kawai, H., Nomura, H., Aoki, H., Fukasawa, S., & Tasaka, Y. (2012, October). PMSM propulsion system for Tokyo Metro. In *2012 Electrical Systems for Aircraft, Railway and Ship Propulsion* (pp. 1-6). IEEE.

Lin, F. J., Shieh, H. J., Shieh, P. H., & Shen, P. H. (2006). An adaptive recurrent-neural-network motion controller for XY table in CNC machine. *IEEE Transactions on Systems, Man, and Cybernetics, Part B (Cybernetics)*, *36*(2), 286-299.

Murali, N., & Ushakumari, S. (2020, November). Performance comparison between different rotor configurations of PMSM for EV application. In *2020 IEEE REGION 10 CONFERENCE (TENCON)* (pp. 1334-1339). IEEE.

CHAPTER 4

BLDC MOTORS AND DESIGN OF THEIR DRIVERS

Mehmet Cihat Özgenel[1]

1 Electric and Electronics Engineering Department, Engineering Faculty, Erzincan Binali Yıldırım University, mcozgenel@erzincan.edu.tr,
ORCID: 0000-0001-5304-1488

1. BRUSHED AND BRUSHLESS DIRECT CURRENT MOTORS

Electric motors are electrical machines that convert electrical energy into mechanical energy. Some electric motors, such as asynchronous motors and brushed direct current motors work when connected directly to a voltage source. However, some motors, such as stepper motors, brushless direct current motors, reluctance motors, and permanent magnet synchronous motors, cannot work directly from a voltage source. These motors need a driver to work. In addition, each driver is different from each other. In addition, if it is desired to control the speed and to reduce the initial starting current of these motors running directly from a voltage source, it is also necessary to use a driver for these motors. In addition to all this, using a driver saves energy. Before examining the drivers of brushless direct current motors, it is necessary to briefly look at the operation of conventional brushed direct current motors.

1.1 Commutation Process in Direct Current Motor

In order for an electric motor to work, the direction of the current passing through the windings of the motor must change. In an asynchronous motor, the current direction changes as the source voltage changes. In a conventional brushed DC motor, the direction of the armature windings changes with the help of the commutator on the armature and the brushes on the stator. Let's examine the operation and commutation of a 12-slot 2-pole brushed DC motor shown in Fig. 1.

The armature is illustrated in Fig. 1(a), and the armature opened in the middle is seen in (b). When the armature is connected to the direct current source via the brushes in Fig. 1, current flows through the armature windings in the direction depicted by the arrows. In the slots from slot 1 to slot 6, the current flows upwards, and in the slots from slot 7 to slot 12, the current flows downwards. The magnetic field created by the current passing through the armature conductors interacts with the magnetic fields of the permanent magnet in the stator, and the armature rotates to the left as shown in the Fig. 1. Let's assume that the armature rotates one slot to the left, in this case, the current directions passing through the conductors in the slots are as depicted in Fig. 2. As the armature rotates one slot to the left, the commutator

segments also shift one segment to the left. Thus, commutator segment 2 is connected to the voltage source positive terminal via the brush, and commutator segment 8 is connected to the voltage source negative terminal via the brush. When the commutator segments that the brushes contact changed, the current direction of the coils in the armature slots 1 and 7 changed in the opposite direction compared to the previous situation. However, note that in the previous and next cases, the number of coil edges under the stator N and S poles remains constant and the current directions remain the same. The event of changing the current directions of the coils in slots 1 and 7 with one slot rotation of the armature is called **commutation** (Ozgenel, 2017). When the armature is rotated one more slot to the left, this time the brushes will contact the commutator segments 3 and 9. Thus, as seen in Fig. 3, the current direction of the armature coils in the slots 2 and 8 will change. In other words, commutation (changing current direction) occurs in coils 2 and 8.

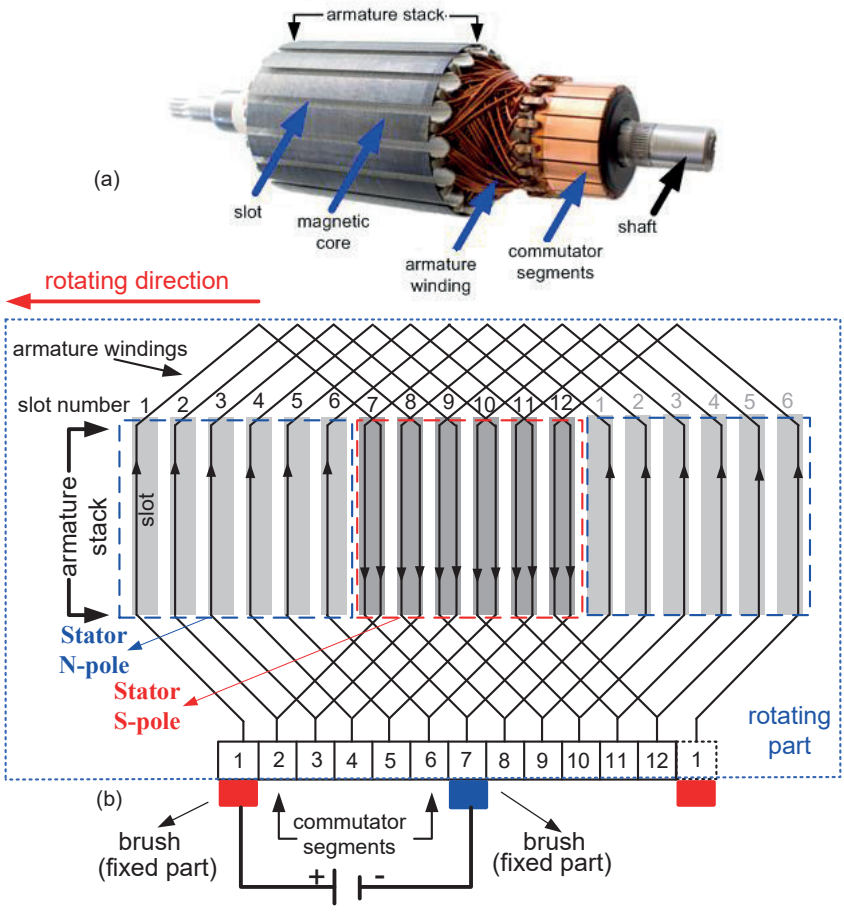

Fig. 1. *12-slot, 2-pole brushed dc motor armature.*

Thus, as the armature rotates, the commutator segments that the brushes touch will change, and the coils current directions will also change in sequence. Commutation will occur in each coil in its turn. The commutation process is done with the collector rotating with the armature and the fixed brushes. There are 6 coils under each pole of the stator in each position of the armature. The directions of the currents passing through these coils under one pole must be the same for the motor to produce maximum torque. In the armature position in Fig. 1, the current is upward in the slots from 1 to 6, while the current is downward in the slots from 7 to 12. The slots from 1 to 6 are under the N pole of the stator, and the slots from 7 to 12 are under the S pole of the stator. In Fig. 2, the armature is turned to the left by

one slot. The current direction of the coils under the N pole of the stator is upwards, the current direction of the coils under the S pole is downwards, and the magnetic field created by the coils interacts with the magnetic fields of the stator poles and rotates the armature to the left, and the armature reaches the position in Fig. 2.

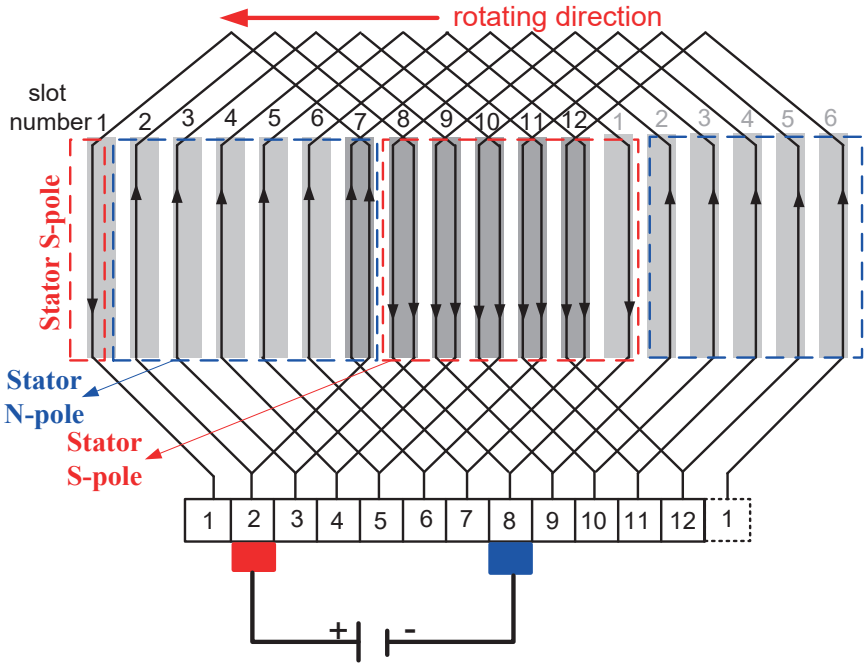

Fig. 2. *Current directions in the armature coils rotating one slot to the left.*

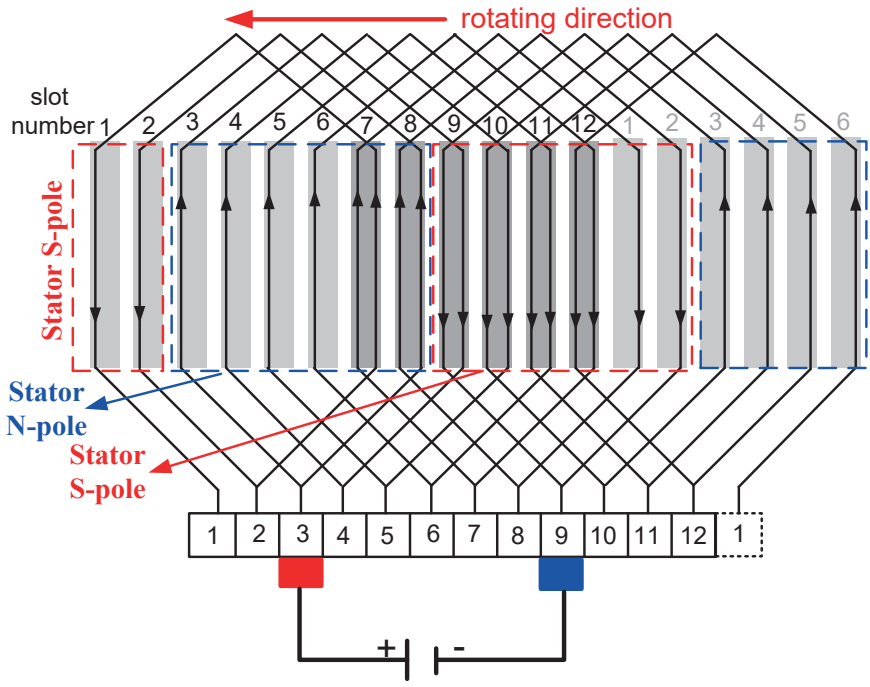

Fig. 3. *Current directions in the armature coils rotating one more slot to the left.*

If we look at Fig. 2, the current directions of coils 1 and 7 have changed. If the current directions of coils 1 and 7 had not changed, the current direction of one coil under the N pole would have been different from the current directions of the other 5 coils. The same situation would have happened in the coils under the S pole. Thus, the torque produced by the armature would have decreased. Again, if the current directions of the coils in Figure 3 had not changed, the current directions of the two coils under the N pole would have been different from the current directions of the other 3 coils. The same situation would have happened in the coils under the S pole. Thus, the torque producing capacity of the armature would have decreased significantly. In that case, the current direction of each coil that leaves from one pole and enters under the opposite pole must be changed. In brushed direct current motors, the process of changing the current direction (commutation) is done mechanically and automatically by commutator and brushes (Özgenel, 2011).

In brushed direct current motors, maintenance is necessary because the brushes and copper commutator wear out very frequently. In addition, the commutator and brushes increase the volume and cost of the motor. Replacing the brush and commutator assembly with an electronic assembly that performs its function electronically will eliminate these drawbacks. Thus, a direct current motor without brushes and commutator is obtained. This motor is a brushless direct current motor (BLDC). In the brushless DC motor, the permanent magnet stator of the conventional brushed DC motor is transferred to the rotor, and the rotating armature is transferred to the stator. Thus, the rotor and stator of the conventional brushed DC motor are replaced (Bal, 2004).

1.2 Brushless Direct Current Motor (BLDC Motor)

Brushless DC motor is a brushed motor in which the stator and rotor are replaced and the commutation is done by an electronic mechanism (Bal, 2004). However, for the BLDC motors to work, they need using an electronic BLDC motor driver. In the BLDC motor, the phase windings commutation is done by the driver according to the rotor position. As with the brushed DC motor, the currents passing through the coils in front of the permanent magnet rotor in the brushless DC motor must also be in the same direction. For example, the current directions of the phase coils in front of the N pole of the rotor must be upwards, and the current directions of the coils in front of the S pole must be downwards. Figure 4 illustrates the structure of brushless DC motors with distributed type stator windings and conventional brushed dc motors (Bodine-Electric nd).

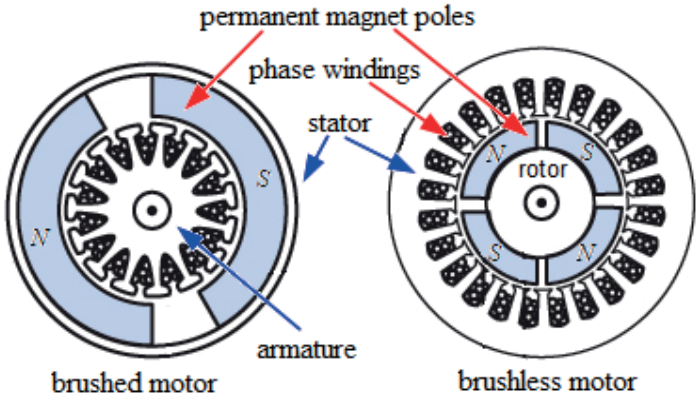

Fig. 4. *Brushed and brushless DC motors (Bodine-Electric).*

In the BLDC motor, as the permanent magnet rotor rotates, the current directions of the phase coils in front of the rotor poles are changed by the inverter according to the rotor position information received from the three-bit rotor position sensors.

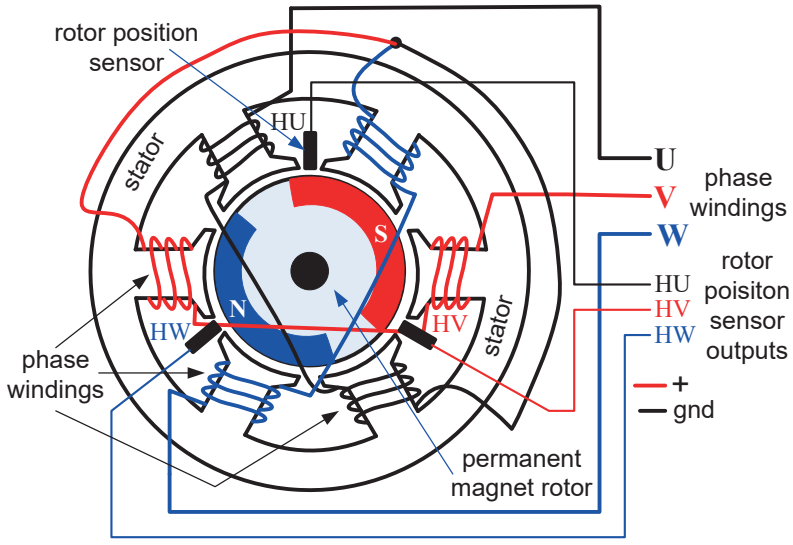

Fig. 5. *Centered type stator phase-windings BLDC motor.*

In brushless direct current motors, commutation is done according to the rotor position, which is a permanent magnet. In a brushless DC motor, one

phase winding is de-energized at any time. Because the rotor changes its position every 60 electrical degrees commutation occurs every 60 electrical degrees. Each phase winding has a current of 120 electrical degrees. Rotor position sensors are usually Hall-effect magnetic effect sensors. Hall-effect sensors are installed on the stator 120 electrical degrees apart from each other (NEC, 2006).

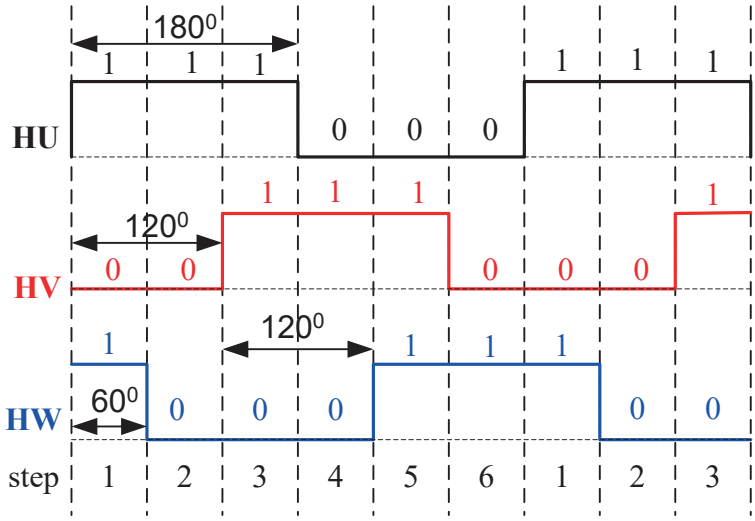

Fig. 6. *Rotor position signals and logic levels.*

Therefore, as seen in Fig. 6, there is a 120-electrical degree difference between their signals. In brushless DC motors, two types of stator windings are used: distributed and centered. Distributed winding types are shown in Fig. 4 and centered winding types are shown in Fig. 5. Permanent magnet rotor motors are classified with respect to the shape of the back electromotive force they produce. If the back emf is sinusoidal, this motor is a permanent magnet synchronous motor. If the back emf is trapezoidal, this motor is a brushless direct current motor. BLDC motors are generally produced in three phases and there is 120-degree phase difference between the each phase back emf.

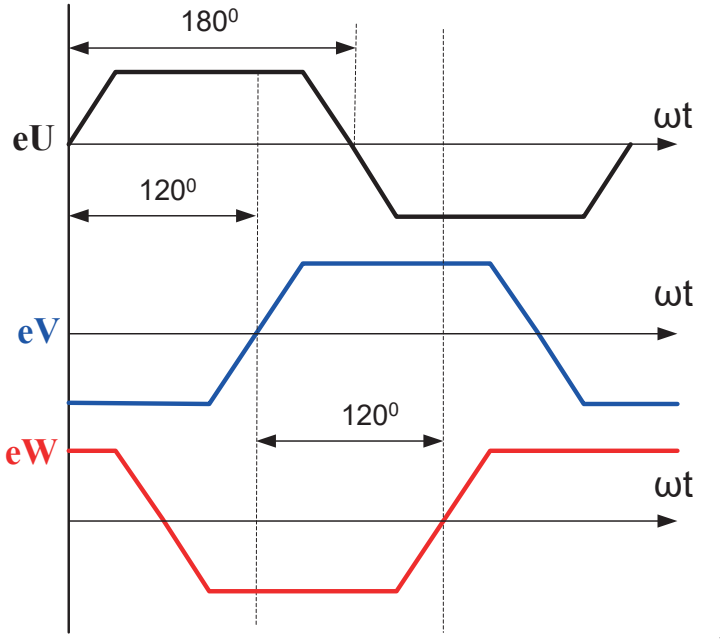

Fig. 7. *Three-phase BLDC motor back emfs.*

The waveforms of the back electromotive forces of the phases are given in Fig. 7. The back emfs produced by the phase windings as illustrated in Fig. 7 are in the form of trapezoidal waves (NEC, 2006).

1.2.1 Working of Brushless Direct Current Motor (BLDC Motor)

BLDC motors operate on the principle of Lorentz force. In a BLDC motor, mechanical power is produced by the interaction of the magnetic field created by the stator phase windings and the magnetic fields of the rotor permanent magnet poles. Two-phase windings are energized at any time and current passes through each phase winding for 120 degrees in BLDC motors. The two-phase windings work together for 60 degrees and a commutation occurs every 60 degrees. At any moment, current passes through two phase windings, the third phase is de-energized. After the current passes through each phase winding for 120 degrees, the phase winding current is cut off by the inverter transistor and this phase winding remains de-energized for 60 degrees. After 60 degrees, the phase winding current direction changes. This situation is shown in Table 1. In Table 1, the rotor position signals and the

switching states of the inverter transistors in the BLDC motor driver according to the rotor position are seen.

Table 1. *Conduction states of inverter transistors according to rotor position signals.*

Step	Angular position	Position signals			Inverter switch-states					
					U-phase		V-phase		W-phase	
		HU	HV	HW	S1	S4	S3	S2	S5	S6
1	0^0-60^0	0	0	1			1			1
2	60^0-120^0	0	1	1	1					1
3	120^0-180^0	0	1	0	1			1		
4	180^0-240^0	1	1	0				1	1	
5	240^0-300^0	1	0	0		1			1	
6	300^0-360^0 (0^0)	1	0	1		1	1			

Step 1 (0^0-60^0)

As seen in Table 1, step 1, the rotor position sensors are 0-0-1. The BLDC motor driver commutation circuit decodes the rotor position signals and conducts the inverter's S3 and S6 transistors. Thus, the V-phase winding becomes positively polarized, and the W-phase winding becomes negatively polarized. As seen in Figure 8, step 1, the V and W-phase windings work together in this step. The magnetic field created by the V and W-phase windings interacts with the fields of the rotor permanent magnet and rotates the rotor to the left and in this step the U-phase winding is float as shown in Figure 8, step 1. As seen in Table 1, each step is 60 degrees and commutation occurs every 60 degrees.

Step 2 (60^0-120^0)

After 60 degrees in the 2nd step, the rotor position signals become 0-1-1. The commutation circuit decodes these position signals and opens the S3 switch and makes the S1 switch is in conduction. Meanwhile the S6 switch remains conductive. Thus, the current of the V-phase winding is cut off, the U-phase winding becomes positively polarized with the closing of the S1 switch and the current starts to flow through U-phase winding, as illustrated in Figure 8,

step 2. In step 2, U and W-phase windings are connected together. In this step the V-phase winding is float. U and W-phase windings magnetic fields interact with the rotor poles, forcing the rotor to rotate to the left.

Step 3 (120^0-180^0)

As the rotor continues to rotate, the rotor position sensors produce 0-1-0. Thus, the rotor rotates another 60 electrical degrees and step 3 in Table 1 occurs. In step 3, switch S6 is opened, and the negative current of W- phase is cut off and switch S1 remains in conduction. In this step, the S2 switch closes and negative current starts to flow through the V-phase winding. At the same time, in this step, the U and V-phase windings start to work together and W-phase winding is float. From the 1st step to the 3rd step, the current passing in the positive direction of the V-phase was cut off, in the second step the V-phase winding remained 60 degrees de-energized and in the 3rd step the direction of the phase winding current changed.

Step 4 (180^0-240^0)

As the rotor continues to rotate, the rotor position sensors come to a position where they will produce 1-1-0. In other words, rotor has rotated another 60 degrees. Switch S1 opens and the current passing through the U-phase in the positive direction is cut off. Thus the U-phase winding becomes float state. Switch S5 closes and the current begins to pass through the W-phase in the positive direction. Switch S2 remains closed. Thus, the V and W-phase windings work together. The magnetic field created by these two windings rotates the rotor to the left.

Step 5 (240^0-300^0)

When the rotor rotates another 60 degrees, the sensors receive the 1-0-0 information. The commutation circuit decodes this code and generates the transistor control signals that will open the S2 switch and close the S4 switch in response to this code. The S5 switch remains closed. When the S4 switch closes, current begins to flow through the U-phase winding in the opposite direction to the current direction in steps 2 and 3. Thus, U-phase winding current direction has changed. In this step, the V-phase winding is de-

energized. The magnetic fields of the U and W-phase windings interact with the rotor magnetic field, causing the rotor to rotate to the left.

Step 6 (300^0-360^0) (300^0-0^0)

When the rotor rotates another 60 degrees, the sensors produce the 1-0-1 information. The commutation circuit decodes this code and generates the transistor control signals that opens the S5 switch and closes the S3 switch in response to this code. The S4 switch remains closed. In this step, positive current flows through the V-phase winding and negative current flows through the U-phase winding. In this step the W-phase winding is float state. The magnetic field produced by the V and U-phase windings interacts with the rotor magnetic field and causes the rotor to rotate to the left. When the rotor continues to rotate to the left, when the rotor position sensors produce the 0-0-1 information, the rotor reaches the position in step 1. After this, step 1 is repeated and the other steps are repeated in order and the rotor continues to rotate.

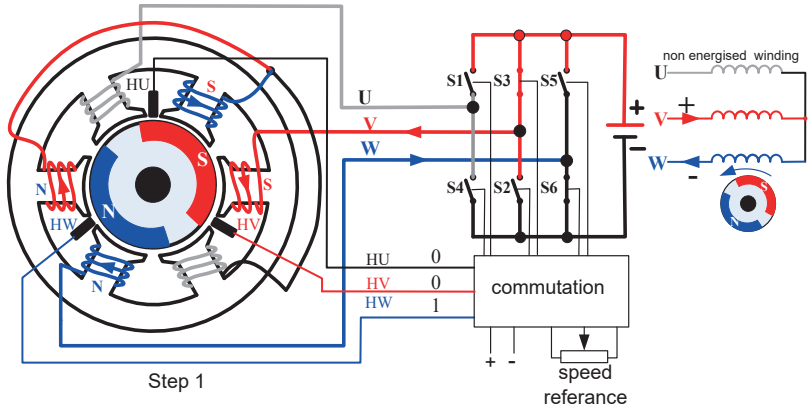

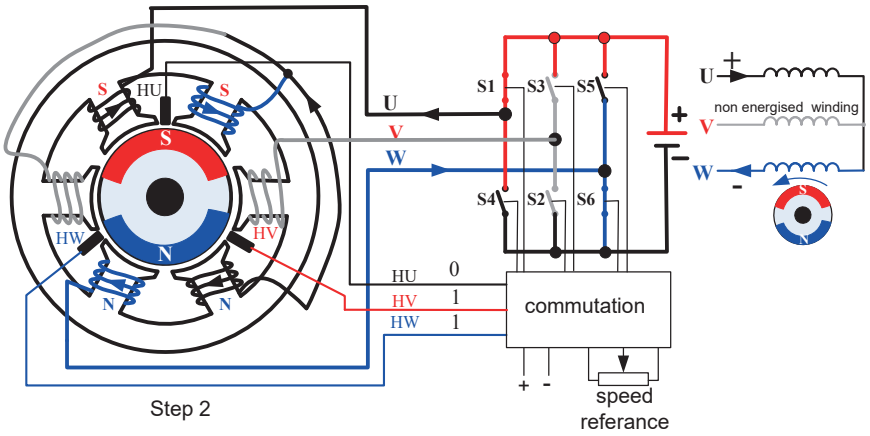

Step 2

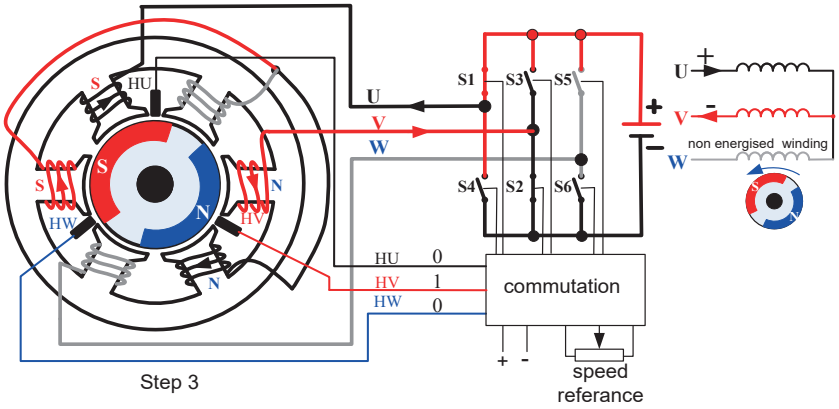

Step 3

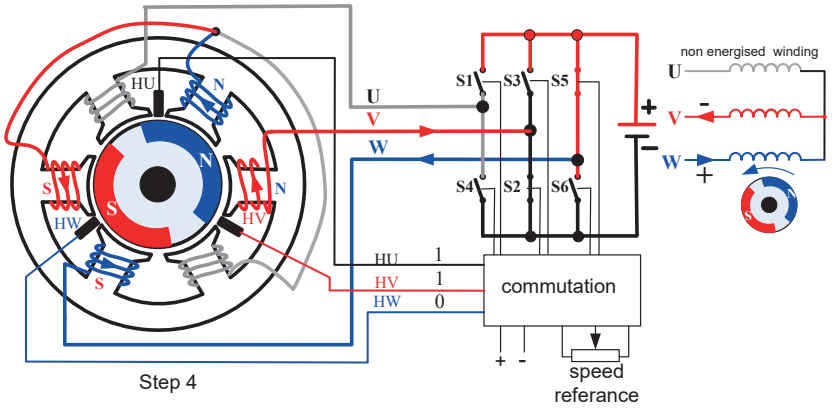

Step 4

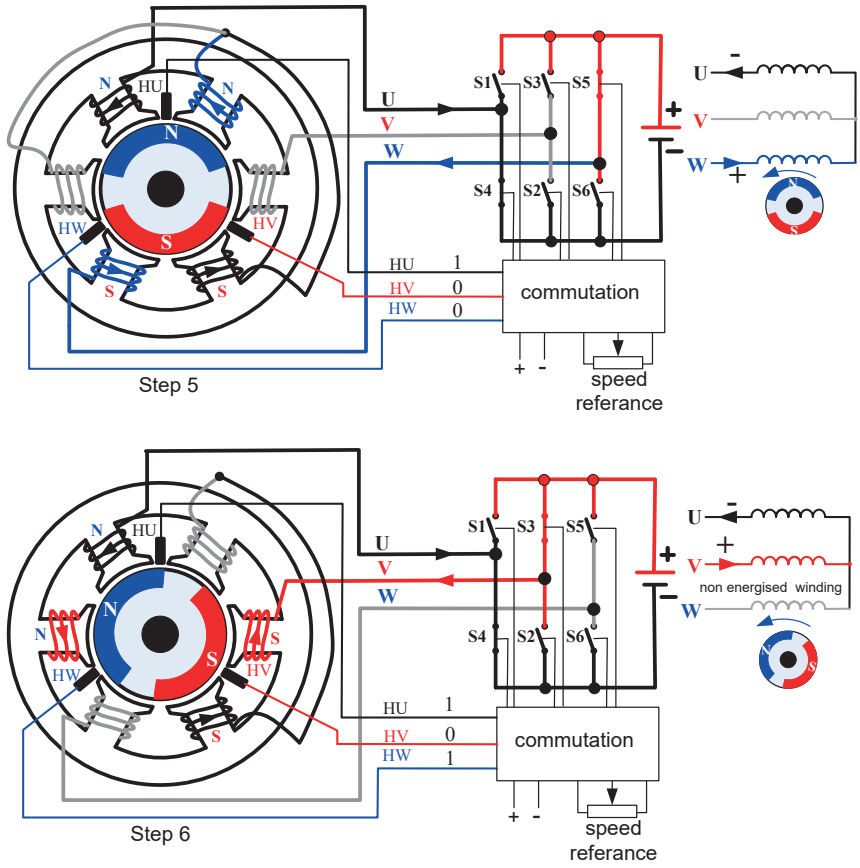

Fig. 8. *Commutation and operation of the BLDC motor with respect to rotor position signals.*

As seen in Figures 8 and 9, the current of the phase winding to be commuted is first cut off, then the current direction changes after the winding remains 60 degrees float (Özgenel, 2020).

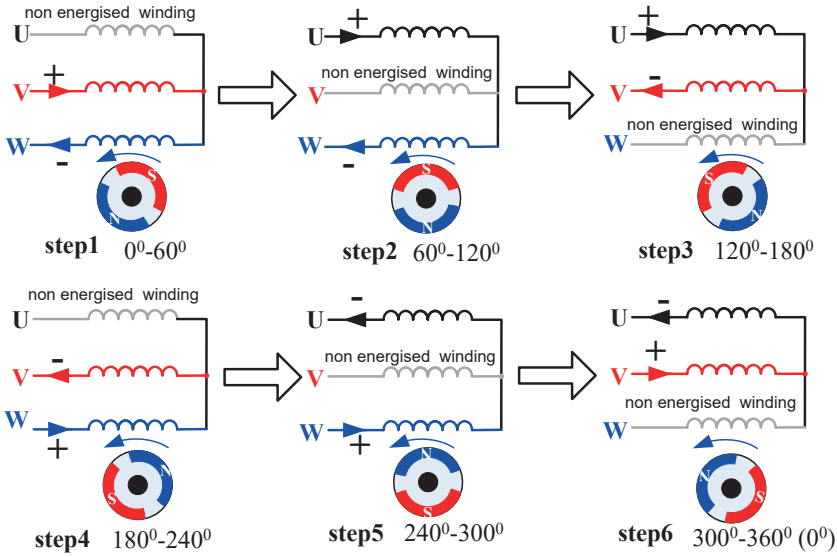

Fig. 9. *Order of change of current directions (commutation) of phase windings.*

2. BLDC MOTOR DRIVER DESIGN

In previous sections, it was mentioned that a BLDC motor needs a driver to work. As illustrated in Fig. 8, a BLDC motor driver consists of an inverter and a commutation circuit. The commutation circuit contains a rotor position decoder and a Pulse Width Modulation (PWM) generator. The motor speed is varied by changing the current passing through the motor phase windings employing the PWM technique. In the commutation circuit, the control signals of the switches are obtained by decoding the 3-bit rotor position sensors signals employing simple digital expressions. The transistor control signal is easily obtained using a truth table.

Table 2. *Obtaining control signals of inverter transistors.*

Step	Rotor position signals			Inverter switch-states						Transistor gate signal expressions
				U Phase		V Phase		W Phase		
	HU	HV	HW	S1	S4	S3	S2	S5	S6	
1	0	0	1			1			1	$S1=\overline{HU}.HV.HW+\overline{HU}.HV.\overline{HW}$
2	0	1	1	1					1	$S4=HU.\overline{HV}.\overline{HW}+HU.\overline{HV}.HW$
3	0	1	0	1			1			$S3=\overline{HU}.\overline{HV}.HW+HU.\overline{HV}.HW$
4	1	1	0				1	1		$S2=\overline{HU}.HV.\overline{HW}+HU.HV.\overline{HW}$
5	1	0	0		1			1		$S5=HU.HV.\overline{HW}+HU.\overline{HV}.\overline{HW}$
6	1	0	1		1	1				$S6=\overline{HU}.\overline{HV}.HW+\overline{HU}.HV.HW$

In Table 2, the logic expressions of the transistor control signals (commutation circuit) in the inverter were obtained by decoding the rotor position signals. By simplifying the logic expressions, a simpler commutation circuit is obtained. By simple simplification of the key control signals;

With respect to these logic expressions, the commutation circuit is drawn using basic gates.

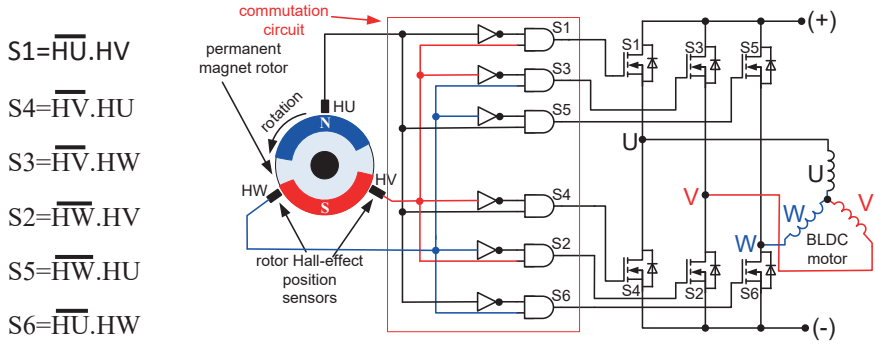

Fig. 10. *Commutation circuit according to logic expressions, and inverter.*

2.1. Speed Control of BLDC Motor

The BLDC motor operates with the driver circuit given in Fig. 10, but the speed and rotation direction of the motor cannot be changed. As it is known, in conventional brushed direct current motors, it is necessary to change the armature winding current in order to vary the speed of the motor. Similarly,

to change the speed of the BLDC motor, the motor phase winding currents are varied. To vary motor phase windings current, it is necessary to employ the PWM technique to the transistors in the inverter. There are many integrated circuits that generate the PWM in the market. The most common of these and requiring few external components are the TL494 and SG3524 integrated circuits.

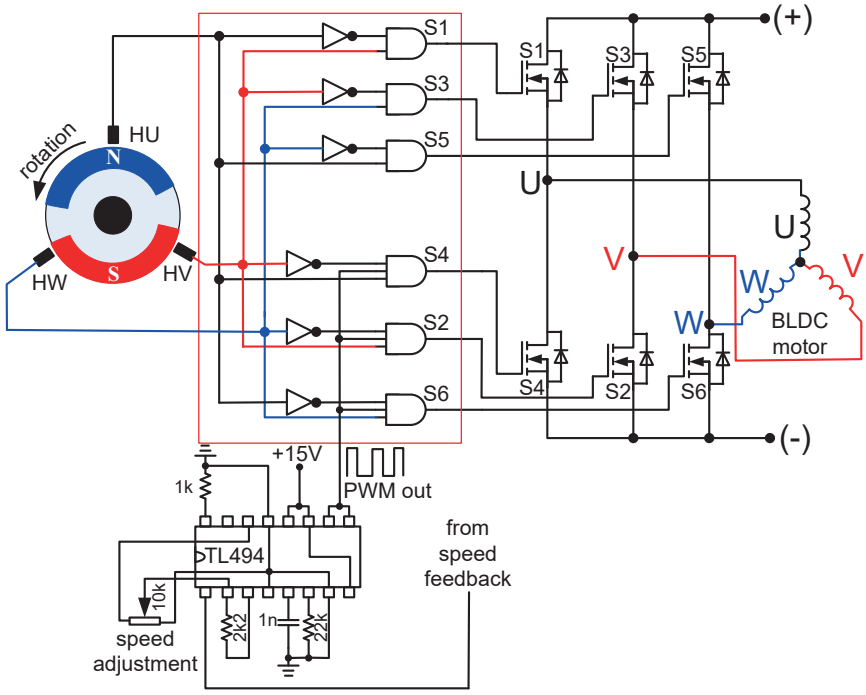

Fig. 11. *Speed adjustable BLDC motor driver.*

The driver circuit in Fig. 10 only enables the BLDC motor to operate and speed control cannot be performed. In order to perform speed control on the driver, a circuit that generates PWM via the TL494 integrated circuit has been added to the driver. It is sufficient for the S4, S2, S6 transistors in the driver to work in PWM mode. Therefore, a 3-input AND gate is used to inject PWM mode to transistors S4, S2, S6. The S1, S3, S5 transistors on the inverter do not need to work in PWM mode to avoid switching losses. When a transistor at the top is turned on, it is connected in series with a transistor of another phase at the bottom for 60 degrees.

In PWM mode, the load voltage is varied by changing the time the transistors are on and off. In this mode, the source voltage is not changed, only the periods during which the source voltage is applied to the load are changed. Thus, the average value of the load voltage is varied. When the load voltage varies, the current passing through the load changes depending on the voltage. As it is known, in order to vary the speed of direct current motors, the voltage applied to the armature terminals is changed. Because the speed of direct current motors is directly proportional to the voltage applied to the armature terminals.

When the PWM operating mode is applied to the BLDC motor phase windings, the phase winding voltage and the current passing through the phase winding are changed. Thus, the speed of the BLDC motor is varied. BLDC motor speed;

$$n = \frac{E - I_a . R_a}{K . \emptyset} \qquad (rpm) \qquad (1)$$

is explained with the (1) expression. Here E, is the voltage applied to the motor phase windings in volts, I_a is the current passing through the phase winding in amperes, R_a is the resistance of the phase winding in ohms, K is the motor constant, and Φ is the magnetic flux of one pole in Weber. As it can easily be seen from expression (1), the BLDC motor speed is directly proportional to the voltage applied to the phase windings and inversely proportional to the magnetic flux of the poles. Since the magnetic flux of the poles is constant, BLDC motor speed changing is achieved only by varying the voltage applied to the phase windings. Fig. 12 shows the change in current passing through the load by applying the PWM method (Ozgenel et al., 2017).

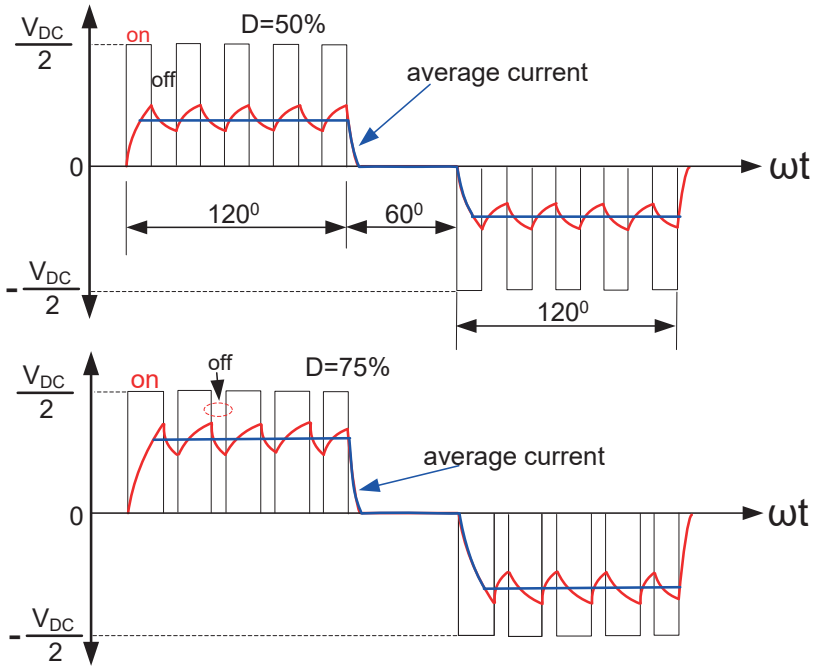

Fig.12. *Changing the current passing through the BLDC motor phase winding by employing the PWM method (NEC, 2006).*

Expression of average voltage in PWM method;

$$V_{avg} = V_{DC}.\frac{t_{on}}{T} \quad (V) \tag{2}$$

(2) is found with the expression. Where t_{on} is the time the transistor remains in conduction in second, T is the duration of one period in second, V_{DC} is the source voltage.

However, as it seen in Fig's 8 and 9, BLDC motors are generally star connected and two different phase windings work in series at any time. Therefore, one phase winding voltage is half of the source voltage. For this reason, the expression given by (2) must be adjusted for the star connected BLDC motor. Thus, the BLDC motor phase voltage expression becomes (3).

$$V_{avg} = \left(\frac{V_{DC}}{2}\right).\frac{t_{on}}{T} \quad (V) \tag{3}$$

2.2. Changing the Rotation Direction of BLDC Motor

In practice, the rotation direction of electric motors may need to be shifted, and in most applications, rotation direction of motors is changed. However, the method of changing the direction of rotation of each motor is different. For example, in order to change the direction of rotation in an induction motor, the place of any two phases is changed, while in the stepper motors, the order of the voltage applied to the phase windings is changed. In a permanent magnet pole direct current motor, the voltage direction applied to the armature is varied. BLDC motors are mostly manufactured with three-phase windings. In fact, the main principle is to change the direction of the current passing through the windings. In fact, the main principle is to change the direction of the current passing through the windings. However, since the structure of each motor is different, this implementation is applied in different ways. While the place of any two phases in motors such as asynchronous motors and synchronous motors is changed, the direction of the current in the phase windings in the BLDC motor is changed by controlling the inverter. Namely, as it illustrated in Fig. 13, the gate signal of the upper transistor of one phase leg in the inverter is imposed on the lower transistor, and the gate signal of the lower transistor is imposed on the upper transistor, thus, the current direction of each phase winding is changed. In short, the gate signals of the S1, S3, S5 transistors at the top of the inverter and the gate signals of the S4, S2, S6 transistors at the bottom of the inverter are swapped, respectively.

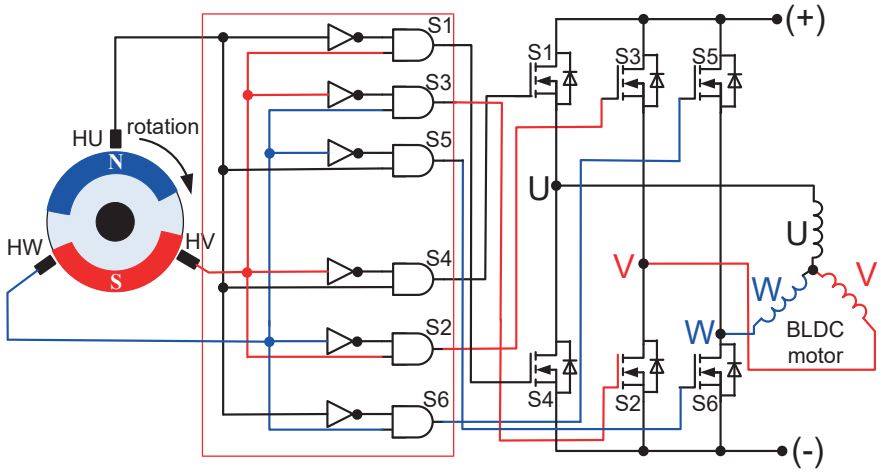

Fig. 13. *Changing the rotation direction of BLDC Motor.*

In Figs 10 and 11, while the rotor rotates counterclockwise, in Fig. 13 the transistors gate connections have been changed, thus changing the direction of the phase winding currents and the motor rotates clockwise. In the circuit illustrated in Fig. 11, the speed of the BLDC motor can be adjusted, but it is not possible to change the direction of rotation. In order for the driver to change the motor rotation direction, a commutation circuit must be added to the driver.

Using a 2x1 data selector integrated circuit for the commutation circuit is a practical solution. In Fig. 14, the rotation direction of the BLDC motor is changed using the 6-part 2x1 data selector. When the rotation direction switch is zero, the 6 data selector's inputs becomes zero. Accordingly, the 6 data selectors transfer the data at the I0-input to its output. In the first step in Table 2, the HU, HV and HW rotor position sensors produce the rotor position information 0, 0, 1, respectively.

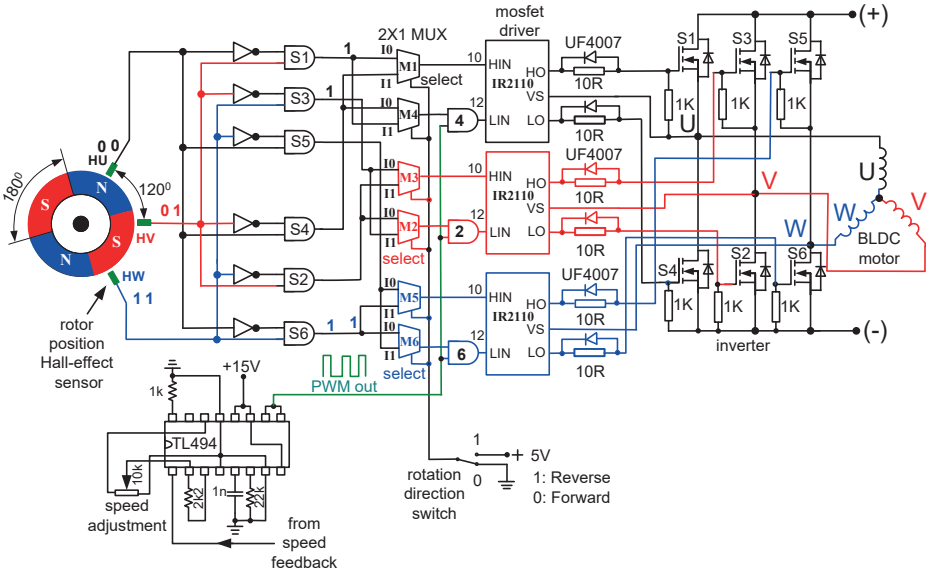

Fig.14. *Complete BLDC motor driver capable of speed and direction control.*

According to this rotor position information, the outputs of the commutation circuit S3 and S6 AND gate become Logic 1 and the other outputs of the commutation circuit become Logic zero. The output of S3 AND gate comes to the I0 input of M3 MUX, and the output of S6 AND gate comes to the I0 input of M6 MUX. Since the selection input of the data selectors is zero, the output of M3 and M6 data selectors becomes Logic 1. The outputs of other data selectors become Logic zero. The output of the M3 data selector comes to the HIN input of the MOSFET driver (red color) and the MOSFET driver turns on the S3 MOSFET. At the same time, the output of the M6 MUX enters the AND gate number 6. The other input of the AND gate number 6 is the PWM signal. The output of the AND gate number 6 is also PWM and enters the LIN (blue color) input of the MOSFET driver. The LO (blue color) output of the MOSFET driver enters the PWM signal to the S6 MOSFET. Thus, the S6 MOSFET is turned on in PWM mode, as it seen Fig. 15 (a), the V phase winding is positively polarized, the W winding is negatively polarized and current passes through the phase windings and the rotor rotates.

As the rotor rotates, this time the rotor position sensors produce the information HU=0, HV=1, HW=1 shown in the second row of table 2.

outputs become logic 1, and the other outputs become logic zero. In this position of the rotor, the S6 MOSFET continues to work in PWM mode and S3 MOSFET is cut off and the current in the V phase winding is cut off. However, the output of S1 AND gate becomes logical 1 and enters the I0 input of M1-MUX. Since the select input of M1-MUX is zero, it selects the logical 1 at the I0 input of M1-MUX and transfers it to its output. The output of MUX M1 (logic 1) is input to the HIN input of the MOSFET driver (black color). The MOSFET driver turns on the S1 MOSFET. Now current starts to flow through the U phase winding as it seen Fig. 15(b). Thus, commutation is realized and commutation will occur every 60 electrical degrees. In the next step, S6 MOSFET will be cut off and the current in the W phase winding will be cut off and S2 MOSFET will be turned on and current will pass in the reverse direction through the V phase winding. As the rotor rotates, commutation occurs every 60 degrees and the currents passing through the phase windings change direction.

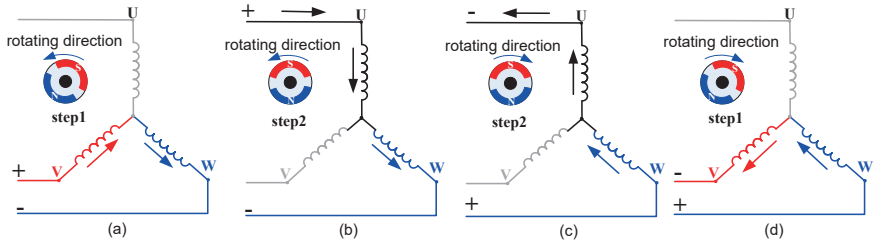

Fig. 15. *Changing the direction of rotation of the BLDC motor.*

In order to change the motor rotation direction, it is necessary to set the rotation direction switch to the Logic 1 position. When the rotor position is in the position in step 2 of Table 2, the rotation switch is set to logic 1 position. Thus, the I1 inputs of all MUXs are selected. In this rotor position, HU=0, HV=1, HW=1, according to this rotor information, the outputs of the S1 and S6 AND gates of the commutation circuit are Logic 1 and the other outputs are Logic zero. The output of the S6 AND gate is connected to input I1 of the M5 MUX, and the output of the S1 AND gate is connected to input I1 of the M4 MUX. Since the I1 input of M4 MUX is selected, its output becomes logic 1. The input of AND gate number 4 becomes logic 1 and its other input is PWM. The PWM signal that enters the LIN input of the MOSFET driver and the output LO of the MOSFET driver (black color)

turns on the S4 MOSFET in PWM mode and the U phase winding becomes negative and the phase current changes its direction as it seen in Fig. 15(c). At the same time, the output of S6 AND gate is connected to the I1 input of M5 MUX. Since the I1 input of M5 MUX is selected by the rotation direction switch, the output of M5 MUX becomes logic 1. The output of M5 MUX is connected to the HIN input of MOSFET driver (blue color). The HO output of MOSFET driver turns on S5 MOSFET. Thus, as seen in Figure 15(c), W phase winding becomes positive and current enters W winding and exits U phase winding, thus W and U phase windings current directions reversed motor rotating direction is also changed.

While the rotor continues to rotate in the reverse direction, after 60 degrees the rotor position sensors produce the position information HU=0, HV=0 and HW=1. In this case, the outputs of S3 and S6 AND gates become logic 1.

While the rotor continues to rotate in the opposite direction, after 60 degrees the rotor position sensors produce the position information HU=0, HV=0 and HW=1. In this case the outputs of the S3 and S6 AND gates become logic 1. The I1 inputs of the M2 and M6 MUXs become logic 1 and by selecting these inputs their outputs also become logic 1. M2 MUX transmits S2 MOSFET in PWM mode with AND gate number 2 and MOSFET driver (red color). V phase winding becomes negative and the current direction changes. M5 MUX continues to turn on S5 MOSFET as seen in Fig. 15(d) and the current enters W phase winding. As the rotor rotates, the rotor position information changes and the phase windings are energized by the inverter according to this information. Thus, both speed control and changing the direction of rotation of the motor are achieved with the driver in Fig. 14.

BLDC motors are widely used and their use is increasing every day. Therefore, companies produce integrated circuits that produce the commutation circuit and PWM generating part of the drives given in Fig. 14. Some companies also produce integrated circuits that include MOSFET/IGBT drivers. There are many integrated circuits on the market. These integrated circuits are called BLDC motor pre-driver integrated

circuits. MC33033 is a complete pre-driver integrated circuit produced by ONSEMI (Onsemi, 2013).

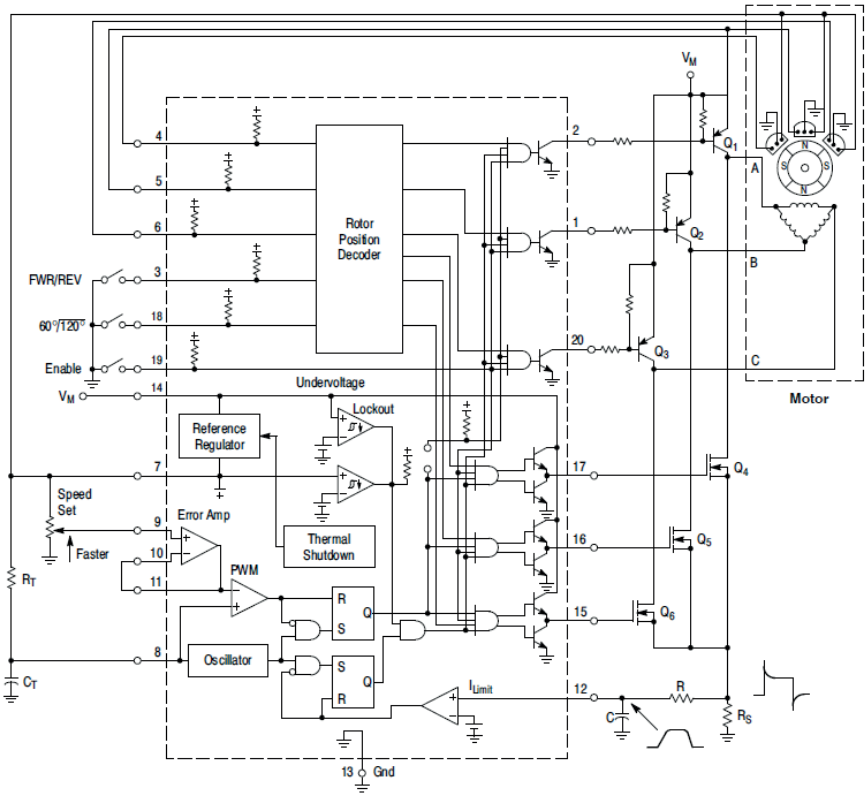

Fig. 16. *BLDC Motor driver with MC33033. (Onsemi.com)*

MC33033 also includes MOSFET/IGBT drivers and requires very few external components. Thus, it is become very easy to realize BLDC motor driver. An example of a pre-BLDC motor driver IC is the FCM8201 IC produced by Fairchild Semiconductor.

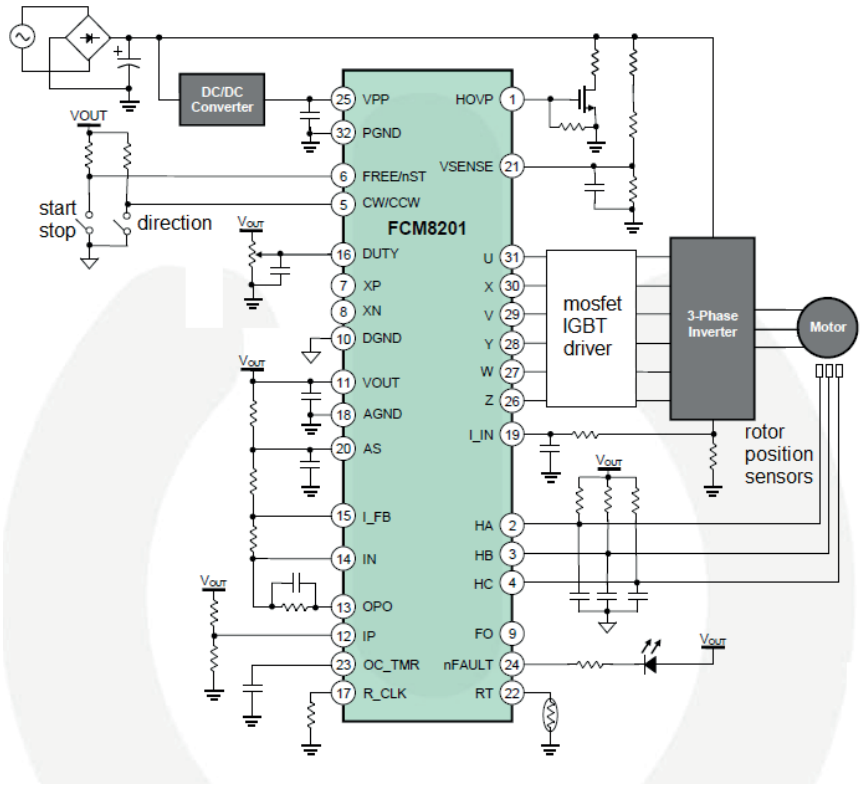

Fig. 17. *BLDC motor driver implemented based on FCM8201 (Fairchild).*

Fig. 17 illustrates the driver implemented with the FCM8201 BLDC motor pre-driver integrated circuit produced by Fairchild Semiconductor. FCM8201 is a multifunctional pre-driver and can also be controlled by a microprocessor (Ozgenel et al., 2016). It should be noted that a MOSFET/IGBT driver IC must be used between the inverter and FCM8201. A wide variety of MOSFET/IGBT driver ICs are readily available on the market. Examples include FAN7388, IR2110, TLP250, FOD3125. The reason for using driver ICs for MOSFET/IGBT is that the connection points of the EMITTER/SOURCE terminals of the transistors on the inverter upper side are in different phases. TLP250 and FOD3125 drivers are optical drivers and these types of optical drivers should be supplied with separate isolated power supply for the transistors on the upper side of the inverter. However, MOSFET/IGBT drivers such as FAN7388 and IR 2110 can be supplied from a single source. It is sufficient to use a single supply voltage for the 3 optical

drivers on the lower side of the inverter. Because the DRAIN/EMITTER of the transistors terminals on the inverter lower side are connected to common ground.

Another option to implement BLDC motor driver is to use a microprocessor. With the program written into the microprocessor, commutation and speed adjustment (PWM) can be easily performed and many control features can be added to the driver. A MOSFET/IGBT driver must be used between the microprocessor and the inverter transistors.

REFERENCES

Bal, Güngör (2004). Özel Elektrik Makinaları, Seçkin Yayıncılık, Ocak 2004, Ankara.

Bodine-Electric(nd). https://www.bodine-electric.com/bldc-gearmotors-and-motors. Retrieved 2024 September 07.

Fairchild Semiconductor Corporation (2013), 3-Phase Sinusoidal Brushless DC Motor Controller, Fairchild Semiconductor, October, 2013.

NEC Electronics Corporation (2006). 3-Phase Brushless DC Motor Control 120-Degree Trapezoidal Drive with Hall Sensors for MC-LVKIT-714 Motor Control Evaluation System, User's Manual, 2006, NEC Electronics Corporation.

Onsemi, (2013) MC33033, NCV33033 Brushless DC Motor Controller, Semiconductor Components Industries, LLC, MC33033/D, February, 2013 – Rev. 11.

Ozgenel Mehmet Cihat (2017). Design, implementation, and application of 150-degree commutation VSI to improve speed range of sensored BLDC motor, Review of Scientific Instruments **88**, 095007 (2017); doi: 10.1063/1.4997613.

Ozgenel Mehmet Cihat (2011). Çözümlü Örneklerle Doğru Akım Elektrik Makinaları, Birsen Yayınevi, 2011, İstanbul.

Özgenel Mehmet Cihat (2020). Design, Producing and Testing of 12-Step Three-Phase Voltage Source Inverter with Flexible Independent PWM Current Control for Brushless Direct Current Motor, Igdir University Journal of the Institute of Science and Technology, 10(2): 956-969, 2020.

Ozgenel Mehmet Cihat, Bal Güngör and Uygun Durmuş, (2017). Design and application of a novel high precision and low cost electronic tachogenerator for sensor-based brushless direct current motor drivers. Review of Scientific Instruments **88**, 035005 (2017); doi: 10.1063/1.4978798.

Ozgenel Mehmet Cihat, Bal Güngör and Uygun Durmuş, (2016). Low-Resolution and Low-Cost Position Sensor Implementation for Permanent Magnet Synchronous Motor Driver, Elektronika Ir Elektrotechnika, Issn 1392-1215, Vol. 22، No. 4، 2016.

CHAPTER 5

MICROWAVE TOMOGRAPHY AND MILLIMETER WAVE IMAGING FOR EARLY BREAST CANCER DETECTION

İremnur Duru[1]

Timuçin Emre Tabaru[2]

1 Res. Asst., Sivas University of Science and Technology, Faculty Of Engineering And Natural Sciences, iremduru@sivas.edu.tr, ORCID ID: 0000-0001-5492-803X

2 Assoc. Prof. Dr., Sivas University of Science and Technology, Faculty Of Engineering And Natural Sciences, etabaru@sivas.edu.tr, ORCID ID: 0000-0002-1373-3620

1.INTRODUCTION

The incidence and mortality rates of cancer have increased rapidly worldwide in recent years. According to the American Cancer Society, approximately 1.9 million new cases and 600,000 deaths are expected in the United States alone. Based on the number of deaths, cancer is the second leading cause of death globally. Among women, breast cancer is one of the most common causes of cancer-related deaths. It is followed by colorectal and lung cancers. (Giaquinto, Miller, et al., 2022; Giaquinto, Sung, et al., 2022; Miller et al., 2022).

When detecting breast cancer, the dielectric properties of breast tissue are a critical topic in the biomedical field. Dielectric properties help understand the electrical behavior and interactions of tissues. These properties measure a material's response to an electric field and provide information about its interactions. Dielectric properties are expressed using the dielectric constant (permittivity) and loss tangent, which define the electrical characteristics of tissues. Electrical conductivity and the propagation of energy within the tissue are measured using these two variables.

Breast tissues have a complex structure composed of various types of tissues, including fat, connective tissues, blood vessels, and mammary glands. Each component has unique dielectric properties. The variability of dielectric properties across tissues significantly alters their electrical characteristics. For instance, fat tissue may have a lower dielectric constant and loss tangent, while tumor tissue is likely to exhibit higher values for both. The dielectric constant is proportional to the energy loss within the tissue.

In microwave imaging, dielectric properties are crucial for tissue characterization. Detecting changes in the dielectric properties of tissues during breast cancer screenings facilitates early diagnosis. Analyzing the electrical properties of tissues can help identify tumors and detect changes in tumors, addressing critical challenges. By employing multifrequency analyses and electromagnetic models, the dielectric properties of breast tissues can be examined in greater detail, providing deeper insights into their characteristics.

Advancements in biomedical and engineering technologies have the potential to resolve significant challenges by enhancing our understanding of the dielectric properties of breast tissue. Early diagnosis of breast cancer allows for the application of personalized treatment plans based on tumor type and size, representing a vital step in improving patient outcomes.

2. Microwave Breast Imaging

Microwave imaging has been introduced as an alternative technology to traditional methods such as mammography, ultrasound, and magnetic resonance imaging due to its advantages. In microwave imaging, the

utilization of the dielectric properties of breast tissues offers a more promising solution for individuals with dense breast tissue compared to mammography. This innovative medical imaging method, which uses electromagnetic radiation, has emerged as a solution for the early detection of breast cancer. Electromagnetic radiation passes through tissues without causing harm and provides information about tissue structure through signals reflected from the tissue. Using dielectric properties for breast cancer detection is crucial for early diagnosis.

The fundamental principle of microwave breast imaging is that different tissue types exhibit varying frequency responses. The dielectric properties of cancerous tissues differ from those of normal tissues, with electrical conductivity properties decreasing in cancerous tissues. By employing microwave frequencies, tumors or abnormal tissues can be identified, and their size, shape, and location can be determined. Compared to other technologies, microwave imaging is more cost-effective, compact, and portable, making it easier to use. Non-invasive microwave imaging allows for more comfortable measurements. Additionally, the ability to capture time-dependent images enables the observation of tissue development over time.

Microwave imaging can provide enhanced results through the integration of machine learning and signal processing applications (Duru et al., 2024). In the future, this method will find applications in other fields for the early detection of breast cancer. As a revolutionary approach in healthcare, microwave imaging will play a critical role as a highly sensitive and alternative method for breast cancer detection. Microwave imaging is categorized into two types: passive microwave imaging and active microwave imaging.

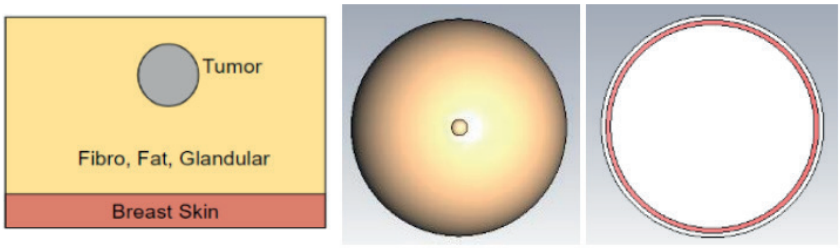

Fig 1. The structure of breast tissue and the front and back view of breast tissue (Duru et al., 2023)

2.1. Passive Microwave Imaging

Passive microwave imaging is a technology that enables imaging without the need for an external energy source, as electromagnetic waves are naturally emitted and reflected by their environment. Using this method, microwave

imaging is achieved by detecting temperature differences and signals emitted from natural sources. Unlike active microwave imaging, passive microwave imaging relies on naturally occurring microwave radiation in the system's surroundings. The fundamental principle of passive microwave imaging is to utilize the reflections and transmissions of microwave radiation from the target object or region, which exhibit different characteristics compared to the environment.

Passive microwave imaging is associated with the detection of thermal radiation and is used to identify surface temperature differences. It is commonly employed in environmental monitoring and military applications, offering the ability to observe without light, regardless of whether it is day or night. This imaging method is widely preferred in defense and security fields, monitoring natural disasters, and observing environmental events. Additionally, it finds applications in agriculture, such as detecting moisture and studying topography, as well as irrigation and water management.

In medical applications, passive microwave imaging is used for detecting tissue temperature, monitoring blood flow, identifying bodily injuries, and early diagnosis of various diseases. Since it utilizes natural microwave radiation from the environment, it minimizes energy consumption, making it a cost-effective and compact technology. However, passive microwave imaging does present some challenges. Compared to active microwave imaging, it has lower resolution and is more susceptible to environmental factors, which can degrade image quality. The dependency on environmental and technical conditions can be considered a disadvantage for certain applications.

Despite these challenges, passive microwave imaging offers the advantage of collecting high-resolution data by leveraging environmental and natural electromagnetic radiation. With its wide range of applications in both military and civilian domains, this technology holds potential for broader adoption in the future, especially due to its low cost, portability, and low energy consumption. However, further advancements in technical capabilities and the development of new algorithms to minimize environmental noise are expected to enhance its efficiency and effectiveness in various fields.

2.2. Active Microwave Imaging

In active microwave imaging, electromagnetic waves are emitted from an active source. Microwave signals are generated at specific frequencies and used to detect signals transmitted from the target object. This method enables the acquisition of high-resolution and comprehensive images, even in low-light conditions or in the absence of a clear surface. Active microwave imaging technology can be combined with radar technology. Measurements are performed by transmitting electromagnetic waves toward the target and analyzing the reflected signals. These received signals contain parameters that

provide information about the size, shape, structure, and components of the target.

Active microwave imaging has a wide range of applications in various fields by utilizing these parameters. It is used in military and defense applications, space observations in aerospace, unmanned aerial vehicles, medical imaging, and structural monitoring. The advantages of the active imaging technique include its effectiveness in low-light conditions, the ability to provide detailed images with high resolution and depth analysis, and its capability to operate effectively over long distances.

However, compared to optical imaging methods, active microwave imaging has lower resolution, which may pose challenges in situations where very fine details are required.

3. Microwave Tomography

Microwave tomography is a three-dimensional imaging technology used to analyze the internal mechanisms and structures of materials using microwaves. It enables the acquisition of 3D images of structures within the body and other materials, as well as the study of microwave propagation and reflection. This imaging technique is highly effective for potential 3D imaging applications in biomedical, environmental, and industrial fields. Microwave tomography examines the interaction of microwave frequencies with different materials. Depending on their dielectric properties, microwave signals can be transmitted, reflected, or absorbed at varying rates.

Microwaves reach the material from a probe tip, and the retrieved signals provide insights into the material's internal structure. The collected data is processed using mathematical modeling and computer algorithms to generate tomographic images. Key advantages of this technology include its non-invasive and safe nature, lack of harm to human health, ability to provide real-time images, capability for in-depth internal structure analysis, and detection of abnormalities within deeper layers.

However, technical limitations such as resolution and data processing challenges currently hinder the broader adoption of this technology. With future advancements, improvements in aspects like resolution and sensitivity are expected to enable broader application areas for microwave tomography.

3. 1. Biomedical Applications

The use of microwave imaging in biomedical fields is quite extensive. Vital signals in the human body must be measured continuously, non-invasively, and with high precision, which can be achieved using electromagnetic signals. Commonly monitored and measured vital signals include pulse rate, respiratory rate, and body temperature. In addition to these, other parameters

such as blood pressure, glucose levels, and oxygen saturation, while medically monitored, do not fall under the category of vital signals.

All these measurements provide critical information about the patient's condition. However, the continuous monitoring of signals such as pulse rate and respiratory rate is essential due to their critical importance. These signals also offer valuable insights into the patient's health status. For example, an elevated pulse rate can indicate infections, fever, cardiovascular diseases, or stress, while a low pulse rate may suggest heart issues, hormonal imbalances, or nerve system damage (Kebe et al., n.d.; Li et al., n.d.). High blood pressure is often associated with hypertension and kidney disease, while low blood pressure may signal blood loss or heart-related issues (Churpek et al., n.d.; Lee et al., n.d.). Therefore, the early detection and prediction of diseases can be achieved through the processing of vital signals. Signal processing refers either to the examination of these signals by healthcare professionals or the application of signal processing methods with the aid of computers. However, in all cases, the methods of obtaining these signals and their accuracy limit the performance of diagnosis and detection.

For instance, while an electrocardiogram (ECG) offers high precision by measuring the electrical activity produced with each heartbeat, it has the disadvantage of requiring the patient to remain continuously connected to the device (Sakamoto et al., n.d.). Another measurement device, the pulse oximeter, detects the substances and movement of blood in the vessels using infrared light. However, this device also requires contact with the skin (Villarroel et al., n.d.). As a result, the currently used measurement methods carry one or more disadvantages, such as low accuracy, lack of non-contact functionality, time delays, sensitivity issues, and so on. At this point, there are studies in the literature focusing on the use of microwave imaging as a non-contact measurement method (Alizadeh et al., n.d.; Villarroel et al., n.d.; D. Wang et al., n.d.). Radar and antennas used for this purpose are generally employed for tasks such as determining the position and movement of objects, measuring speed, and detecting distant objects. Microwave imaging techniques, which possess the characteristics of high accuracy, low power consumption, and the ability to operate under weak signal conditions, are emerging for detecting vital signs (He et al., n.d.; Sacco et al., n.d.; Turppa et al., n.d.; Y. Wang et al., n.d.).

4. Millimeter Wave Imaging

4.1. Millimeter Wave Imaging and Breast Cancer

Millimeter-wave imaging for breast cancer detection has recently become a highly popular topic. Early detection of breast cancer is crucial and life-saving. Millimeter-wave technology offers significant advantages over traditional imaging methods in detecting cancerous cells (Bevacqua

et al., n.d.; Iliopoulos et al., n.d.; Meo et al., 2021; Meo, Matrone, et al., n.d.; Meo, Pasotti, et al., n.d.; Moscato et al., 2013). Millimeter-wave imaging can be used to obtain high-resolution images for detecting the presence of cancerous tumors in breast tissue. This technology utilizes electromagnetic waves with short wavelengths, allowing for in-depth analysis without harming the human body. The interaction of millimeter waves with biological tissues depends on the dielectric properties of the tissues, and these properties create differences between healthy tissue and cancerous tissue. (Bevacqua et al., n.d.; Iliopoulos et al., n.d.). Cancerous tissue differs from healthy tissue in terms of water content, and the interaction of millimeter-wave signals with tissue varies for each type of tissue. Millimeter-wave imaging allows for the detection of tissue differences, helping to identify the presence and spread of breast cancer. Studies have emphasized the importance of using millimeter waves in detecting breast cancer. By interacting with tissue safely, without ionizing radiation, the internal structure of the human body can be examined. In future studies, millimeter-wave imaging for breast cancer will be further enhanced by combining complex signal processing and machine learning algorithms to improve resolution and accuracy.

6. Conclusions

Millimeter-wave and microwave imaging are two distinct electromagnetic wave technologies with significant potential in medical diagnosis, security screenings, industrial applications, and aerospace. Microwave imaging has been actively used for many years, while millimeter-wave imaging offers higher resolution and precision due to its shorter wavelengths. Millimeter waves operate at higher frequency ranges, penetrating deeper into tissues, which is especially important in medical imaging. Microwave imaging, with its longer wavelengths, penetrates more but is particularly effective for scanning larger objects. On the other hand, millimeter-wave frequencies may provide a more effective solution for detecting smaller, newly formed tissues that are difficult to identify.

The use of non-ionizing radiation and the lower cost of millimeter-wave technology make it advantageous. While millimeter-wave imaging has resolved issues related to resolution and depth, clinical applications are still not widespread. In the future, combining millimeter-wave and microwave technologies in hybrid systems could allow for more comprehensive imaging and detailed analyses across different applications. Ultimately, millimeter-wave and microwave imaging technologies complement each other with their respective advantages and limitations. Future research will explore the more effective use of these two technologies, providing new solutions. In the biomedical field, early detection of cancer through advanced applications is expected to be explored further, leading to more in-depth studies and results in the coming years.

REFERENCES

Alizadeh, M., Shaker, G., … J. D. A.-I., & 2019, undefined. (n.d.). Remote monitoring of human vital signs using mm-wave FMCW radar. *Ieeexplore.Ieee.OrgM Alizadeh, G Shaker, JCM De Almeida, PP Morita, S Safavi-NaeiniIEEE Access, 2019•ieeexplore.Ieee.Org*. Retrieved December 26, 2024, from https://ieeexplore.ieee.org/abstract/document/8695699/

Bevacqua, M., Meo, S. Di, … L. C.-I. J. of, & 2021, undefined. (n.d.). Millimeter-waves breast cancer imaging via inverse scattering techniques. *Ieeexplore.Ieee.Org*. Retrieved December 26, 2024, from https://ieeexplore.ieee.org/abstract/document/9325514/

Churpek, M., Adhikari, R., Resuscitation, D. E.-, & 2016, undefined. (n.d.). The value of vital sign trends for detecting clinical deterioration on the wards. *Elsevier*. Retrieved December 26, 2024, from https://www.sciencedirect.com/science/article/pii/S0300957216000770?casa_token=q5HK_zsfgvcAAAAA:aOYcE-6Le0M2pj0UHyyLavwY_arN9PM_4nPr6ksBxEZZpqySvv29TQwGDr0F-BqpxxrxjBtPtfHI6h

Duru, I., Güneş, N., & Tabaru, T. E. (2023). Breast Cancer Diagnosis: Tumor Identification and Localization Based on Millimeter-Wave Spectroscopy with a 33 GHz Patch Antenna. *14th International Conference on Electrical and Electronics Engineering, ELECO 2023 - Proceedings*. https://doi.org/10.1109/ELECO60389.2023.10416034

Duru, I., Güneş, N., & Tabaru, T. E. (2024). Reflection Curves and Machine Learning-Based Tissue Characterization for Early Diagnosis of Breast Cancer with Microwave Imaging. *32nd IEEE Conference on Signal Processing and Communications Applications, SIU 2024 - Proceedings*. https://doi.org/10.1109/SIU61531.2024.10600876

Giaquinto, A. N., Miller, K. D., Tossas, K. Y., Winn, R. A., Jemal, A., & Siegel, R. L. (2022). Cancer statistics for African American/Black People 2022. *CA: A Cancer Journal for Clinicians*, *72*(3), 202–229. https://doi.org/10.3322/CAAC.21718

Giaquinto, A. N., Sung, H., Miller, K. D., Kramer, J. L., Newman, L. A., Minihan, A., Jemal, A., & Siegel, R. L. (2022). Breast Cancer Statistics, 2022. *CA: A Cancer Journal for Clinicians*, *72*(6), 524–541. https://doi.org/10.3322/CAAC.21754

He, M., Nian, Y., Control, Y. G.-B. S. P. and, & 2017, undefined. (n.d.). Novel signal processing method for vital sign monitoring using FMCW radar. *ElsevierM He, Y Nian, Y GongBiomedical Signal Processing and Control, 2017•Elsevier*. Retrieved December 26, 2024, from https://www.sciencedirect.com/science/article/pii/S1746809416302208?casa_token=c--24dAGffkAAAAA:np0PE_GHiVPxLSF-G1HXcwbJom4NMeAS3t9qS4XbTRl5T9UK6hDfbNhIdf2B_rt5sfZ0a8VfqWIpZ

Iliopoulos, I., Meo, S. Di, … M. P.-I. T., & 2020, undefined. (n.d.). Enhancement of penetration of millimeter waves by field focusing applied to breast cancer detection. *Ieeexplore.Ieee.Org*. Retrieved December 26, 2024, from https://ieeexplore.ieee.org/abstract/document/9158380/

Kebe, M., Gadhafi, R., Mohammad, B., Sensors, M. S.-, & 2020, undefined. (n.d.). Human vital signs detection methods and potential using radars: A review. *Mdpi. ComM Kebe, R Gadhafi, B Mohammad, M Sanduleanu, H Saleh, M Al-QutayriSensors, 2020•mdpi.Com*. Retrieved December 26, 2024, from https://www.mdpi.com/1424-8220/20/5/1454

Lee, D., Lee, Y., Chung, W., SENSORS, R. M.-, IEEE, 2006, & 2006, undefined. (n.d.). Vital sign monitoring system with life emergency event detection using wireless sensor network. *Ieeexplore.Ieee.OrgDS Lee, YD Lee, WY Chung, R Myllyla-SENSORS, 2006 IEEE, 2006•ieeexplore.Ieee.Org*. Retrieved December 26, 2024, from https://ieeexplore.ieee.org/abstract/document/4178671/

Li, C., and, J. L.-I. T. on M. T., & 2008, undefined. (n.d.). Random body movement cancellation in Doppler radar vital sign detection. *Ieeexplore.Ieee.OrgC Li, J LinIEEE Transactions on Microwave Theory and Techniques, 2008•ieeexplore.Ieee.Org*. Retrieved December 26, 2024, from https://ieeexplore.ieee.org/abstract/document/4682605/

Meo, S. Di, Matrone, G., Pasian, M., … M. B.-2017 I. M.-S., & 2017, undefined. (n.d.). High-resolution mm-wave imaging techniques and systems for breast cancer detection. *Ieeexplore.Ieee.Org*. Retrieved December 26, 2024, from https://ieeexplore.ieee.org/abstract/document/8247409/

Meo, S. Di, Matrone, G., Sciences, M. P.-A., & 2021, undefined. (2021). Experimental validation on tissue-mimicking phantoms of millimeter-wave imaging for breast cancer detection. *Mdpi.Com*. https://doi.org/10.3390/app

Meo, S. Di, Pasotti, L., … E. L.-2020 42nd A., & 2020, undefined. (n.d.). Combining millimeter-wave imaging, ultrasound and elastography in a new multimodal approach for breast cancer detection: initial experimental results. *Ieeexplore.Ieee.Org*. Retrieved December 26, 2024, from https://ieeexplore.ieee.org/abstract/document/9176088/

Miller, K. D., Nogueira, L., Devasia, T., Mariotto, A. B., Yabroff, K. R., Jemal, A., Kramer, J., & Siegel, R. L. (2022). Cancer treatment and survivorship statistics, 2022. *CA: A Cancer Journal for Clinicians*, *72*(5), 409–436. https://doi.org/10.3322/CAAC.21731

Moscato, S., Matrone, G., Pasian, M., Mazzanti, A., Bozzi, M., Perregrini, L., Svelto, F., Magenes, G., Arcioni, P., & Summers, P. (2013). A mm-wave 2D ultra-wideband imaging radar for breast cancer detection. *Wiley Online Library*, *2013*. https://doi.org/10.1155/2013/475375

Sacco, G., Piuzzi, E., Pittella, E., Sensors, S. P.-, & 2020, undefined. (n.d.). An FMCW radar for localization and vital signs measurement for different chest orientations. *Mdpi.ComG Sacco, E Piuzzi, E Pittella, S PisaSensors, 2020•mdpi.Com*. https://doi.org/10.3390/s20123489

Sakamoto, J., Liu, N., Koh, Z., … D. G.-T. A. J. of, & 2018, undefined. (n.d.). Integrating heart rate variability, vital signs, electrocardiogram. *Elsevier*. Retrieved December 26, 2024, from https://www.sciencedirect.com/science/article/pii/S0735675717305831?casa_token=WrwOmz5652EAAAAA:iDJu-

LEQYckXmwwRVAnj2LKXgWEZx_xHZvCIQNxdvmZ_TCorFCgUvrPYAc_lopuFvHLbvJ05P33Om

Turppa, E., Kortelainen, J., Antropov, O., Sensors, T. K.-, & 2020, undefined. (n.d.). Vital sign monitoring using FMCW radar in various sleeping scenarios. *Mdpi.ComE Turppa, JM Kortelainen, O Antropov, T KiuruSensors, 2020•mdpi.Com*. https://doi.org/10.3390/s20226505

Villarroel, M., Jorge, J., … C. P.-2017 12th I., & 2017, undefined. (n.d.). Non-contact vital sign monitoring in the clinic. *Ieeexplore.Ieee.OrgM Villarroel, J Jorge, C Pugh, L Tarassenko2017 12th IEEE International Conference on Automatic Face, 2017•ieeexplore.Ieee.Org*. Retrieved December 26, 2024, from https://ieeexplore.ieee.org/abstract/document/7961753/

Wang, D., Yoo, S., Sensors, S. C.-, & 2020, undefined. (n.d.). Experimental comparison of IR-UWB radar and FMCW radar for vital signs. *Mdpi.ComD Wang, S Yoo, SH ChoSensors, 2020•mdpi.Com*. https://doi.org/10.3390/s20226695

Wang, Y., Ren, A., Zhou, M., Wang, W., Access, X. Y.-I., & 2020, undefined. (n.d.). A novel detection and recognition method for continuous hand gesture using FMCW radar. *Ieeexplore.Ieee.OrgY Wang, A Ren, M Zhou, W Wang, X YangIEEE Access, 2020•ieeexplore.Ieee.Org*. Retrieved December 26, 2024, from https://ieeexplore.ieee.org/abstract/document/9194242/

CHAPTER 6

EFFECTS OF ELECTROMAGNETIC INTERFERENCE ON AIRCRAFT AND THE IMPORTANCE OF ELECTROMAGNETIC COMPATIBILITY IN AVIATION

Ali Recai ÇELİK[1]

1 Dr., Dicle University, Electrical and Electronics Engineering Department
ORCID ID: 0000-0002-6917-5170

1. INTRODUCTION

Electromagnetic (EM) waves are the rays with electric field and magnetic field components and different energy values according to their frequencies and wavelengths. They can move in various environments like air, water, and solid matter. The EM spectrum is given in Figure 1 (Zhang et al. 2020). The EM field occurs naturally in nature or from man-made sources. All devices powered by electricity can be considered as a source of artificial EM fields. Electronic household appliances such as hair dryers, washing machines, and microwave ovens create EM radiation in their surroundings. However, the main sources are high-frequency systems such as mobile phone transmitters, radio station transmitters, and television antennas used in data transmission (Kodali, 2001).

Electronic systems powered by electricity emit EM energy to the environment. The fact that this emitted energy negatively affects other devices and systems around it and is similarly affected by other devices is called EM interference (EMI). Due to this mutual interference, disruption may occur in the high-performance operation of devices and systems. For this reason, eliminating EMI or reducing its damage has been the primary goal for researchers. In line with the above-mentioned goal, EMI reduction and protection methods used to prevent the performance of the devices using EM energy from deteriorating and not adversely affecting the performance of other devices are called EM Compatibility (EMC).

Aircrafts, where electronic devices and radar systems are used extensively, have systems where EMI and EMC issues must be addressed in detail. In order to effectively realize EMC in aircraft, it is important to choose systems that comply with EMI standards (Stecklein, 2019). Thus, the quality of the vehicle produced increases, and time and costs are saved. Otherwise, in addition to loss of time and cost, fatal accidents may occur.

In this Chapter, firstly, EM waves are defined and the EM spectrum containing waves of different frequencies is shown. The concept of EMI is explained, and its harmful effects on humans, living things, and electronic devices are given. Concerning the subject of interest in the study, the causes and consequences of EMI formation in aircraft are explained. Protection and compatibility methods that can be used to reduce and, if possible, eliminate the negative effects of EMI are mentioned and the importance of EMC is emphasized.

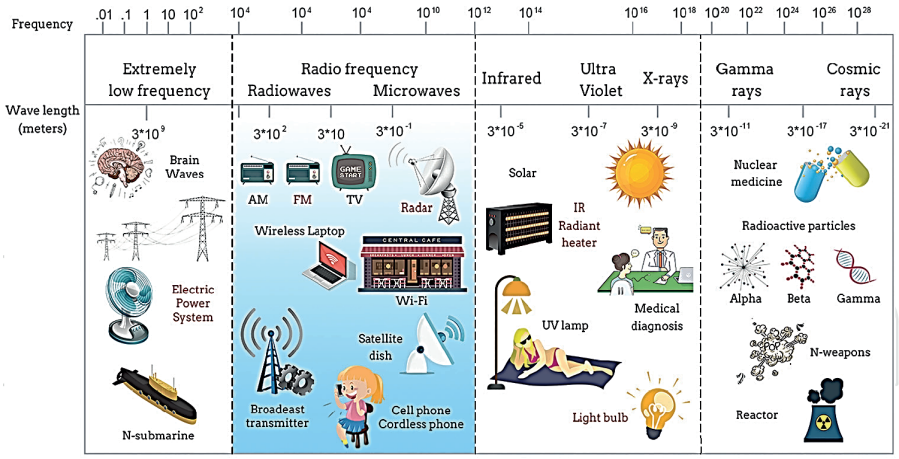

Figure 1. *Electromagnetic radiation spectrum prepared by (Zhang et al. 2020)*

2. ELECTROMAGNETIC INTERFERENCE (EMI)

Systems working together in environments may mutually create unwanted voltages or currents, effects and emissions, that are, noise signals. The fact that this noise disrupts the operation of the systems and reduces their performance is called EMI (Ustuner, 2012). It can be defined as EM energy that affects the operation of an electronic device. As electronic systems continue to develop rapidly and become widespread in society, harmful situations caused by EMI will continue to increase.

EM radiation pollution can directly or indirectly affect humans, other living things, and electronic devices. A device or system can be both a source and a victim of EM pollution in its environment. The source of EM noise, the victim exposed to EM pollution emitted from this source, and the path between the source and the victim are the three main elements of EMI. This path can be formed in two different ways: the path formed by radiation from the air and the path formed by the noise carried over conductive materials. Therefore, the formation of EMI is of two types: by radiation and by conduction (Olcer and Kilic, 2002).

The situation of a mobile phone providing data communication affecting the navigation system of an aircraft in an environment where the EM source is a mobile phone, the coupling path is air, and the affected device is the aircraft system is an example of radiated EMI. In an environment where the EM source is a drill, the coupling path is the energy grid line, and the negatively affected system is the television screen, the television and the drill operating connected to the same transmission line affecting each other can be given as an example of interference caused by conductivity. EMI becomes especially dangerous in

environments where many transceivers work together at the same time and have conductors, such as aircraft and warships.

Lightning is the most dangerous source of naturally occurring EMI. Cosmic cycles and strong natural magnetic fields are other factors that affect electronic communications. All electronic and electromechanical devices designed and produced by human beings are sources that create artificial EMI. All EMI types and sources are summarized in the Table 1 (Montrose and Nakauchi, 2004; Zhai, 2021).

Table 1. *The summary of natural and man-made EMI sources*

Natural Sources		**Man-Made Sources**	
Terrestial	**Celestial**	**Systems**	**Circuits and Components**
Lightning, *Electrostatic Discharge*	*Cosmic Noise* *Solar Noise*	*Avionics Buses,* *Avionics Cables,* *Radar,* *Navigation,* *Communication,* *Power,* *Entertainment,* *Electronic Warfare*	*Motors,* *Switches,* *Oscillators,* *Filters,* *Actuators,* *Heaters,* *Pumbs,* *Digital Circuits*

2.1. Effects of EMI on Aircraft

Aircraft contain many electronic systems, so they have environments where high amounts of EMI can occur. Avionics is a general concept that describes aviation electronics. Some avionic systems are listed below (Committee of the GPS, 1995; Wells and Rodrigues, 2004; Helfrick, 2010):

- Receiving/transmitting antennas located within the system and operating at radio frequencies,
- Systems that enable flight personnel to communicate with tower personnel, among themselves and with passengers,
- Global Positioning System (GPS)
- Navigation systems used to determine the position and direction of the aircraft on the ground,
- Cockpit equipment and computer screens that enable tracking of the aircraft,
- Engine-indicating and crew-alerting system (EICAS)
- Flight data recorders, flight control, and collision avoidance systems,
- Power supplies and power correction units in the system,

- Meteorological systems such as weather radar, lightning detectors, and turbulence detectors.

Aircraft with such various electronic systems will inevitably be affected by radar signals, broadcast transmitters, radio/TV/mobile phone devices, Wi-Fi networks, ignition/trigger systems and lightning strikes, that is, they will be exposed to EMI. EMI can occur both from the aircraft's systems given above and external sources that create high levels of EM fields in the environment. A summary of internal and external EMI sources affecting the aircraft is depicted in Figure 2 (Majid, 2018).

If avionics equipment is not protected from EMI, it will cause damage such as distortion and malfunction in systems. For example, cockpit radios and radar signals may be affected, disrupting communications between the pilot and the control tower. Laptops, mobile phones, and electronic toys may cause the autopilot to be disconnected, the flight display screen to malfunction, and the aircraft to go off course. Protecting avionics equipment from EMI means that it maintains its performance without being affected by the EM energy it is exposed to and that it does not adversely affect the operation of other systems. To achieve this, the design and certification stages of avionics should be carefully considered and EMC methods, which will be explained in the next section, should be applied.

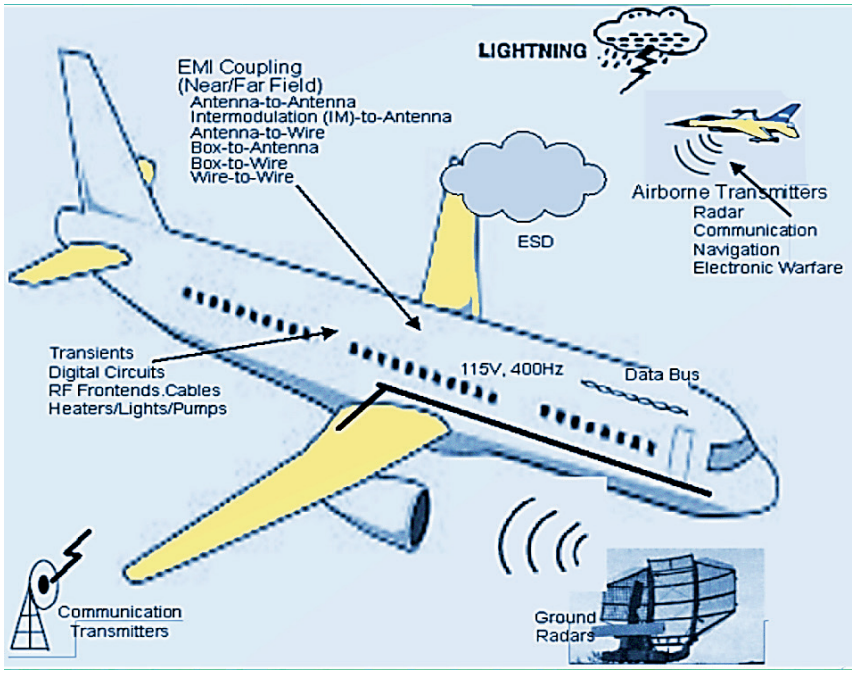

Figure 2. *Some EMI sources affecting the aircraft prepared by (Majid, 2018)*

3. ELECTROMAGNETIC COMPATIBILITY (EMC)

The ability of a device, equipment, or system to be unaffected by interference in the EM environment in which it is located and to operate without disruptions is called EMC (Duff, 1988). Therefore, the EMI threat mentioned in the previous section can be eliminated by the successful implementation of EMC processes.

Today, as technological developments increase day by day, the issue of EMC is gaining more and more importance and national or international EMC standards are determined for equipment such as mobile phones, televisions, computers, kitchen appliances, and systems such as the Internet of Things and 5G. EMC standards have the dual purpose of regulating EM radiation from a device and controlling the immunity of the same device to EMI. In other words, a device is electromagnetically compatible if it does not interfere with other systems, is immune to interference from other systems, and does not cause new interference within itself. With successful EMC, devices perform their functions without being affected by any EMI or affecting the surrounding electronic equipment (Christopoulos, 2022).

In order for EMC to occur, tests are performed to determine the performance disturbances caused by the EM waves emitted by electronic devices and the relationship of the devices to EMI. These tests are generally classified as Emission tests and Immunity tests. Some institutions that determine the rules and standards regarding the tests are International Committee on Non-Ionising Radiation Protection (ICNIRP), International Agency for Research on Cancer (IARC) and World Health Organization (WHO).

If EMI sources are suppressed as much as necessary, coupling paths are reduced, and systems are strengthened, EMC is provided. For example, the harmonious arrangement of EM waves originating from the radar, radio, and microprocessor controlling the systems of an aircraft in the same environment, without damaging each other, is an indication that EMC has occurred. To protect against EMI, thus achieving EMC; methods such as shielding, grounding, bonding, filtering, cabling, and lightning protection etc. are used. These are summarized schematically in Figure 3 (Gurel, 2000; Belous and Saladukha, 2020).

As a result, applying these methods and fulfilling EMC requirements in every environment where electronic devices are located, from military fields to space technologies, from the healthcare sector to industrial applications is mandatory. EMC application in aircraft, which is the subject of this study, is one of the most important procedures in terms of life and property safety, and will be examined in the next section,

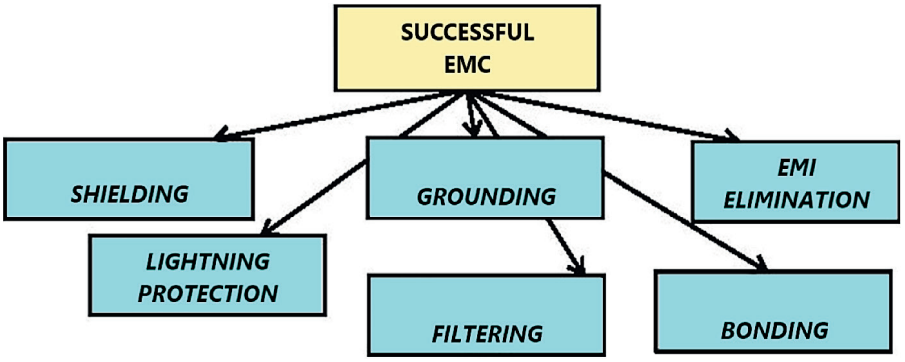

Figure 3. *Some methods of EMC*

3.1. Importance of EMC on Aircrafts

Even small mistakes in defense and aviation can endanger human life and cause high financial losses. For this reason, especially in the civil aviation sector, safety factors should be well inspected, EMC tests should be emphasized, and necessary precautions should be taken. As it is known, the number of electronic equipment and systems in aircraft, and EM field pollution are constantly increasing. For these systems to operate smoothly within themselves, harmoniously integrate with other systems, and provide the desired operating performance without being affected by EMI, it is of great importance to comply with civil aviation standards that meet EMC requirements.

"Environmental Conditions and Test Procedures for Airborne Equipment (RTCA DO-160)" standards are used for this purpose and are accepted worldwide. These rules are published by the Radio Technical Aviation Commission (RTCA), describe the environmental testing of avionic equipment, explain the test setups, and determine the test pass and fail criteria according to the safety level (RTCA, 2010). These standards continue to be updated depending on technology development and the experience gained. EMC applications to eliminate the EMI problem in airplanes, the most commonly used aircraft, started in the 1970s to eliminate the negative effects of navigation systems, and many studies have been conducted on this subject until today (Lee and Marin, 1976; Cooke and Ryan, 1980; Givati and Fourie; 1994; Bai et al., 2011; Miś and Modelski, 2020).

When applying EMC tests, two scenarios should be considered, the avionics system should be considered both as a source and victim of EMI within the aircraft. Firstly, the EM noise emitted by the equipment to the environment is measured and compared with the limit values. Secondly, the equipment is exposed to disturbance signals caused by EMI, and their performance change

is observed. Thus, their immunity and susceptibility are determined. These tests must be carried out in a simulation and laboratory environment before the avionic equipment is placed at real points of use. During tests, antenna types such as monopole, log-periodic, and horn antennas, which have different frequency ranges and high output power, are generally preferred. Various EMC tests are available depending on the size of the aircraft. For example, in Figure 4, EMC testing of two airplanes in the open area and the anechoic chamber are given, respectively (Majid, 2018).

Figure 4. *EMC testing of two airplanes in the open area and anechoic chamber*

Although they do not have a structure as complex as an airplane, helicopters have sensitive equipment that can be easily affected by the EM environment and the EMIs created by other systems. If proper EMC is not performed, they may deviate from their required performance and cause great harm, especially loss of life. EM contamination can often reach helicopter systems through the antenna, coupling, ground line, power line, or equipment chassis.

There are many studies in which EMC analysis of helicopters is carried out both in simulation and experimental environments (Haoyang and Yutang, 2021; Michałowska et al., 2022; Ji et al., 2022). For example, in a study examining the EM radiation to which personnel working in the cabin and surrounding areas were exposed by the newly integrated systems of the helicopter, the results were compared with limit values. For this purpose, a general-purpose helicopter and an attack helicopter were tested. The environmental effects of the EM field resulting from the changing frequency values of the radios were measured. Electric and magnetic field meter and electric field probe were used in the measurements. The image of the S-70A-28D Black Hawk helicopter, one of the helicopters on which the tests were carried out, is given in Figure 5 as an example (Akçam and Şen, 2014). The measured EMC test results were

compared with the MIL-STD-464 standard, which specifies the environmental impacts and required criteria of EM, especially for munitions of air, sea, space, and land systems (MIL-STD-464, 1997).

Today, in addition to airplanes and helicopters, another system whose EMI values need to be examined and EMC is expected to be performed accordingly is the 'Unmanned Aerial Vehicle (UAV)' electronic system. New and updated research continues on UAVs, whose popularity has increased in recent years in parallel with the development of technology (Wu et al., 2020; Hamdalla et al., 2022; Li et al. 2023). In a current study aiming to introduce the strong EMI effect that UAVs may encounter during flight, the data link system, flight control and navigation system, and power system were specifically examined. As a result of the study, the researchers explained that studies aimed at protecting UAVs from EMI are still in the early stages, and they emphasized that relevant research should be updated as the development of UAVs continues (Zhang et al., 2024).

Figure 5. *The image of the S-70A-28D Black Hawk helicopter (Akçam and Şen, 2014)*

4. CONCLUSIONS

There are many electronic systems called avionics in aircraft. These systems and the equipment within them will inevitably interact negatively with each other. In this interaction, each element can be both the source of the problem and the victim. The interaction that occurs in such environments where electric and magnetic fields are high is called EMI. Arrangements that can be made to eliminate or reduce the harms of EMI are called EMC. In this study, which mentions the effects of EMI on aircraft and the importance of EMC in aviation, firstly the EM wave is defined, its theory is explained, its spectrum is shown

and its pollution is mentioned. Then, the avionic systems were introduced and the harmful effects of EMI on these systems were explained. Then, EMC methods were explained by mentioning the criteria and standards required ensure successful compatibility. EMC tests applied in airplanes, helicopters, and UAVs were examined by reviewing studies in the literature. As a result, it was emphasized that if EMC processes are not carried out properly, the quality and performance of the aircraft will decrease, and it was shown with examples that fatal accidents may occur as well as loss of time and cost. The author plans to make both simulation and experimental measurements regarding EMI and EMC in the aircraft theoretically mentioned in this study in future studies.

REFERENCES

Akçam, N., Şen, G. S. (2014). "Hazards of electromagnetic radiation to personnel on air vehicle", *Pamukkale Univ J Eng Sci,* 20(8), pp. 304–309.

Bai, T., Su, D., Liu, Y., & Qiao, Q. (2011). "The method of EMC prediction and analysis for airplane-born communication system", in 4*th IEEE International Symposium on Microwave, Antenna, Propagation and EMC Technologies for Wireless Communications*, pp. 547–550.

Belous, A., Saladukha, V. (2020). "Methods and means of ensuring ınterference resistance of high-speed electronic devices", in: *High-Speed Digital System Design,* Springer, Cham. https://doi.org/10.1007/978-3-030-25409-4_6

Christopoulos, C. (2022). "Principles and techniques of electromagnetic compatibility". *CRC press.*

Committee on the Future of the Global Positioning System. (1995). "The Global Positioning System: A Shared National Asset", *The National Academies Press,* Washington, DC.

Cooke W. ve Ryan C. Jr., (1980). "A GTD computer algorithm for computing the radiation patterns of aircraft-mounted antennas", *Antennas and Propagation Society International Symposium,* Georgia Institute of Technology, Atlanta, 18, 631–634.

Duff W.G., (1988). "Electomagnetic compatibility in telecommunications, ınterference control technologies", *Inc. Gainesville,* Virginia.

Givati O. ve Fourie A.P.C., (1994). "Radiation patterns of antennas mount on a modified mirage aircraft", *AP-S. Digest*, 2, pp. 1158–1161.

Gürel, L. (2000). "Savunma sistemlerinde elektromanyetik uyumluluk (EMC) ve EMC eğitimi", *Savunma Sanayi Sempozyumu,* Ankara, 416–423.

Hamdalla, M. Z., Caruso, A. N., & Hassan, A. M. (2022). Electromagnetic compatibility analysis of quadcopter UAVs using the equivalent circuit approach. IEEE Open Journal of Antennas and Propagation, 3, 1090-1101.

Haoyang, C., Yutang, F. (2021). "Electromagnetic compatibility simulation analysis of helicopter engine irradiated by EMP", *Journal of Physics: Conference Series,* 1871(1), IOP Publishing.

Helfrick, A. (2010). "Principles of avionics", *Avionics Communications,* ISBN: 1885544294

Ji, S., Gou, K., Zhang G. and Zhu, S. (2022). "Evaluation of UHF/VHF communication electromagnetic ınterference in helicopter", *2nd International Conference on Networking, Communications and Information Technology (NetCIT),* Manchester, United Kingdom, pp. 44–46, doi: 10.1109/NetCIT57419.2022.00018.

Kodali, V.P. (2001). "Engineering electromagnetic compatibility: Principles, measurements, technologies, and computer models", *Wiley-IEEE Press,* ISBN: 978-0-780-34743-4

Lee K., Marin L. (1976). "Broadband response of aircraft antennas", *Antennas and Propagation Society International Symposium,* Los Angeles, USA, 14, pp. 78–79.

Li, X., Wang, S., Li, H., Zhou, Y., Guo, H. (2023). "Electromagnetic interference of unmanned aerial vehicle in high voltage environment", *Journal of Physics: Conference Series* 2522(1), p. 012034. IOP Publishing.

Majid, I. (2018). "EMI effects in flight control systems and their mitigations", in *Handbook of Aerospace Electromagnetic Compatibility*, R. Perez (Ed.). https://doi.org/10.1002/9781119082880.ch10

MIL-STD-464. (1997). "Electromagnetic environmental effects requirements for systems", *Department of Denfense*.

Michałowska, J., Puzio, Ł., Tofil, A., & Pytka, J. (2022). "Measuring exposure to high-frequency electromagnetic fields experienced by a helicopter crew during flight", *Transactions on Aerospace Research,* 2022(1), pp. 59–65.

Miś, T. A., & Modelski, J. (2022). "In-Flight electromagnetic compatibility of airborne vertical VLF antennas", *Sensors*, 22(14), 5302.

Montrose, M. I., Nakauchi, E. M. (2004). "Testing for EMC compliance: approaches and techniques", *John Wiley & Sons.*

Ölçer, P., Kılıç, B. (2002). "Temel Bilgiler", Tübitak Ulusal Elektronik ve Kriptoloji Araştırma Enstitüsü, Gebze/Kocaeli, 10, 69.

RTCA DO-160G. (2010). "Environmental conditions and test procedures for airborne equipment", Washington, DC, USA.

Stecklein, J.M. (2019). "Gateway requirements for the control of electromagnetic ınterference characteristics of subsystems and equipment" *(No. DSG-RQMT-007)*

Üstüner, F., (2005). "Elektromanyetik Uyumluluğa Giriş Ve Temel Kavramlar", *Paket Eğitimi,* Tübitak Ulusal Elektronik Ve Kriptoloji Araştırma Enstitüsü, Ankara, Türkiye.

Wells, Alexander T., Rodrigues, Clarence C. (2004). "Commercial aviation safety (4th ed.)", *McGraw-Hill Professional,* p. 245. ISBN: 978-0-07-141742-6.

Wu, Y., Ma, Q., & Xu, P. (2020). "Progress of electromagnetic compatibility design for unmanned aerial vehicles". *MATEC Web of Conferences*, 316, p. 04008, EDP Sciences.

Zhai, L. (2021). "Electromagnetic compatibility foundation of new energy vehicles", in: *Electromagnetic Compatibility of Electric Vehicle, Key Technologies on New Energy Vehicles*. Springer, Singapore. https://doi.org/10.1007/978-981-33-6165-2_2

Zhang, L., Bi, S., Liu, M. (2020). "Lightweight electromagnetic interference shielding materials and their mechanisms", *IntechOpen,* doi: 10.5772/intechopen.82270

Zhang, Z.; Zhou, Y.; Zhang, Y.; Qian, B. (2024). "Strong electromagnetic ınterference and protection in UAVs", *Electronics,* 13, 393. https://doi.org/10.3390/electronics13020393

CHAPTER 7

INTELLIGENT FAULT DIAGNOSIS METHODS IN PV SYSTEMS

Merve Demirci[1]

Rahim Aytug Ozer[2]

1 Assist. Prof. Dr. Merve Demirci, Kafkas University, https://orcid.org/0000-0001-8192-7366, merve.demirci@kafkas.edu.tr

2 Assist. Prof. Dr. Rahim Aytug Ozer, Kafkas University, https://orcid.org/0000-0002-3162-5551, aytug.ozer@kafkas.edu.tr

1. Introduction

The rapid increase in energy consumption is driving the search for new energy sources. Due to their sustainability and security, renewable energy sources are coming into play at this stage, and interest in renewable energy sources (solar, wind, tidal, hydro, geothermal and biomass) is increasing day by day. Solar energy, being one of the most abundant, inexhaustible, and clean options among renewable energy sources, is also widely preferred due to the decreasing installation costs of solar panels over time [1]. Furthermore, the rapid development of solar panel production technology and the continuous improvement of efficiency have made photovoltaic (PV) systems stand out among renewable energy sources [2,3].

According to the 2013-2023 report published by the International Renewable Energy Agency (IRENA) in July 2024, the share of renewable energy in energy capacity has been increasing every year, reaching 43% in 2023. The PV system capacity reached 1,411,139 MW in 2023 [4].

PV systems consist of several components, including PV modules, wiring equipment, converters, protection elements, and inverters. Failures that may occur in these components can negatively impact the system's operation, leading to decreased efficiency. Therefore, diagnosing failures in PV systems becomes crucial, and various diagnostic methods are employed for this purpose.

In this section, the types of failures that occur in PV systems and the smart methods used for diagnosing these failures will be explained in detail, with examples from studies in the literature.

2. PV System Faults

Faults that may occur in PV systems can happen in the PV cells, electrical connections, inverters, MPPT section, or in the cell itself. These faults can be long-lasting or short-term temporary issues. Long-lasting faults may include cable breakages or PV cell fractures, while temporary faults are caused by factors such as shading or soiling [5, 6]. PV system faults can be categorized into three main types. These are environmental faults caused by environmental conditions, electrical faults resulting from faults in electrical components, and physical faults arising from issues such as defects or improper installation of PV panels, as shown in Figure 1.

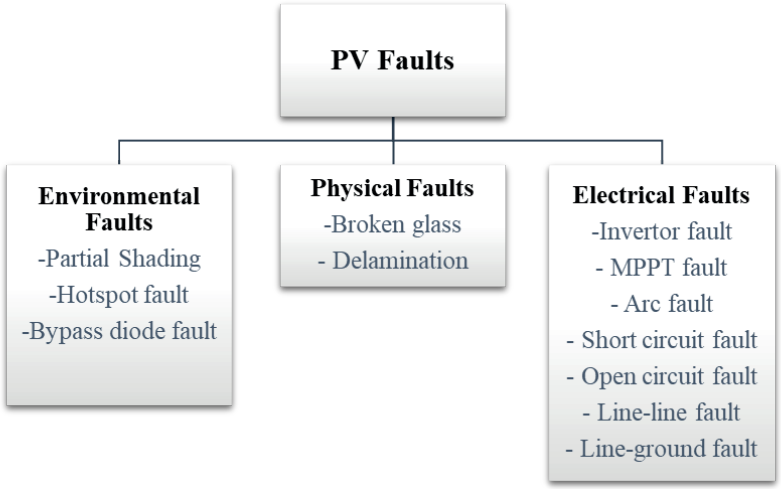

Fig. 1. PV system faults.

2.1. Environmental Faults

One of the faults caused by environmental conditions in PV systems is partial shading faults. Partial shading that occurs during cloud passing over the PV system falls under the category of temporary faults, while partial shading caused by dirt, dust, or bird droppings is considered a permanent fault [7, 8].

Another fault caused by environmental conditions is the hotspot fault. This fault occurs when a specific point on the panel overheats and becomes overloaded. Hotspot faults arise due to poor soldering or panel contamination. Hotspot cells distribute the existing energy, causing an increase in surface temperature. If the hotspot cells become permanent, they can damage the bypass diodes and lead to open circuit failures [9, 10].

Bypass diode faults are caused by incorrect connections, cracks, fractures, hotspots, or loose connections in PV cells. Bypass diodes are located in junction boxes of PV modules to ensure safety. In addition to protecting the module from hotspots, they reduce damage caused by shading and mismatch [11-13]. In the case of a bypass diode fault, efficiency decreases due to power loss.

2.2. Physical Faults

Physical faults are failures caused by microcracks, breaks and deteriorations in PV panels. Even if microcracks that occur in PV panels during transportation, assembly, production or when exposed to any mechanical stress are not noticed during the first operation, the cracks may grow over

time and cause the panel efficiency to decrease. Since it is not possible to repair the cracks, the relevant panel must be replaced [14, 15].

Another physical fault is the internal corrosion that occurs in PV cells. The moisture formed inside the panel causes internal corrosion, which is an undesirable situation. Since the air and water in the environment should not enter the panel, all components must undergo the lamination process with vacuum pressure carefully applied [16].

2.3. Electrical Faults

These are faults that occur in inverters or PV arrays in PV systems [17-18]. Electrical faults occurring in PV strings include line-line faults, open circuit faults, line-ground faults, open short circuit and arc faults [19-21].

Inverter fault: Inverters are one of the most important components in PV systems, converting the DC current produced by the panels into AC current. High levels of mechanical and thermal stress in power switches can lead to faults in the operation of inverters. Additionally, faults that may occur in capacitors and driver circuits can also cause inverter faults [17, 18].

MPPT Fault: MPPT faults are caused by malfunctions in the MPPT charge controller, MPPT sensor, or current-voltage or temperature sensors [17].

Line-Line Fault: These are faults caused by short circuits occurring between PV strings in PV systems. They can be caused by mechanical damage or faults in cable insulation. Effects of such faults include low efficiency, excessive current, or inverter faults [19, 20].

Line-Ground Fault: These are faults caused by short circuits occurring between a conductor and the ground, and they are among the most common faults in PV systems. Line-ground faults, caused by insulation failures in cables, can occur as single-line-to-ground or double-line-to-ground faults. Due to the arcs that form at the fault point, they are serious faults because of the potential fire risk they pose [19, 20].

Open Circuit Fault: The deterioration or aging of connection cables, increased loads, or broken PV modules can cause the electrical connections between them to break, leading to a decrease in current levels. In such cases, the PV panel is unable to continue producing energy [22].

Short Circuit Fault: Short circuit faults can occur in different subsystems of a PV system. A short circuit in a module causes a decrease in the voltage of the string while leading to a slight increase in the current [20].

Arc Fault: An arc fault occurs when the current in a PV system jumps across two unintended dielectric surfaces or creates a brief intense flash of light. These faults are caused by issues in components such as electrical cables

and connectors in PV systems. Arc faults can lead to fires, causing damage to the system [20].

3. Intelligent Faults Diagnosis Methods

Diagnosing faults that may occur during the operation of PV systems is crucial for ensuring their smooth operation, preventing a decrease in efficiency, and extending their lifespan. For this reason, a variety of methods are employed to detect faults. Fault diagnosis methods include those that rely on data based on the electrical properties of the PV system, as well as those that utilize the visual/thermal characteristics of the system.

Fault diagnosis can be performed by using current and voltage values obtained from the I-V curve characterization based on the electrical properties of the PV system, measuring the current and voltage values at the output of the PV modules, calculating power losses, performing statistical fault analysis based on data from various sensors, and utilizing parameters such as resistance, inductance, and capacitance of the PV system [23-25].

Fault diagnosis based on the thermal/visual characteristics of a PV system is performed using various imaging methods (infrared imaging, ultrasonic imaging, electroluminescence imaging, photoluminescence imaging, lock-in thermography) and visual inspection techniques. In the event of a fault in a PV system, a visual inspection is first conducted to determine whether the fault can be identified. If necessary, other imaging techniques are used to identify which component the fault is located in (wiring equipment, junction boxes, diodes, faulty modules, inductors) [26-30].

In recent years, computer-aided intelligent methods have become widely used in fault diagnosis, and successful results are being achieved by utilizing different input data. In PV systems, electrical and thermal/visual characteristics, along with intelligent methods, are also commonly used for fault diagnosis.

Intelligent methods used for fault diagnosis in PV systems include artificial neural networks, fuzzy logic, and machine learning techniques. These methods utilize various data obtained from PV systems to perform fault diagnosis, helping to prevent issues such as reduced efficiency, performance decline, and system outages.

3.1. Artificial Neural Network Methods

This methods are used for various purposes in a wide range of fields such as engineering, medicine, and education. They are widely used in engineering and applied to problems such as classification, regression, and fault diagnosis in different fields.

Artificial neural network-based methods used for PV systems faults diagnosis include Probabilistic Neural Network (PNN), Multi-Layer Perceptron Neural Network (MLPNN), and Radial Basis Function Neural Network (RBFNN).

Probabilistic Neural Network (PNN)

PNN is a supervised classification network model first used by Dr. D.F. Specht in 1989 [31]. It is a feedforward neural network that can perform classification using a probabilistic approach based on Bayes' classification theory. In the classification process, PNN uses Gaussian kernels and creates probability density functions for the classes from the training examples. These probability density functions are then used in Bayes' rule to obtain the classification result [32, 33].

The architecture of the PNN algorithm consists of three layers: the input layer, the hidden layer composed of the pattern and summation layers, and the output layer. Input data is presented to the algorithm, and the first layer performs calculations between the input vectors and the learning vectors, producing a vector. These elements are then sent to the radial basis transfer function, and a probability vector is generated for each input data. In the final step, the maximum of these probability vectors is taken to determine the class label [34].

The PNN algorithm is widely used in classification tasks due to its advantages. Its advantages include: a simple architectural structure, a straightforward learning process, fast learning capability, and good error tolerance. Additionally, its performance improves with an increase in the dataset size [32, 33].

The PNN algorithm is widely used for fault diagnosis in PV systems. In a study conducted by Wang et al. [35], a 4x3 PV system was created, and the Current-Voltage and Power-Voltage curves of the system were obtained. A total of 3985 data points for five different types of faults were collected from these curves and used for fault diagnosis with the PNN algorithm. First, the dataset was normalized, and a 97% diagnostic accuracy was achieved for PNN. In a study conducted by Garoudja et al. [36], the single diode model was first used to obtain the data, and PSIM/MATLAB simulations were used to validate the data. A total of 11,840 input data points were generated for four fault conditions, consisting of four features for both healthy and faulty states. A two-stage PNN was proposed for fault diagnosis: in the first stage, fault detection was performed, and in the second stage, the root cause of the fault was diagnosed. The performance of the proposed PNN algorithm was observed to be higher than that of the ANN, both with normal and noisy datasets. In the study conducted by Zhu et al. [34], seven features were extracted from the I-V and P-V characteristics to diagnose single and multiple fault conditions,

resulting in 826 data points. A three-stage PNN was used: in the first stage, the system's normality was detected, in the second stage, single faults in the system were identified, and in the third stage, multiple faults were detected. The system performance was compared with two different ANN methods.

Multi-layer Perceptron Neural Network (MLPNN)

This algorithm is one of the fundamental artificial intelligence algorithms commonly used in classification, regression, and pattern recognition problems [37]. It consists of three main layers: input layer, hidden layer and output layer. The input data received from the input layer is passed to the hidden layer along with the assigned weights, where it is processed using an activation function. The results are then transmitted to the output layer through connections to obtain the final output [38]. The weights between the layers can be adjusted using optimization and backpropagation algorithms, which can improve the diagnostic performance of the algorithm [37, 39].

Due to its flexible structure and adaptability, MLPNN can produce effective results in complex problems by using hidden layers with different numbers of neurons [37]. In the study conducted by Mouaad et al. [37], 1800 data points were generated from I-V curves in the MATLAB Simulink environment to perform fault diagnosis for normal and short-circuit fault conditions in PV systems. These data were used to train and test the MLPNN algorithm. In the study conducted by Mekki et al. [38], approximately 3000 data points were obtained from a PV system installed on a laboratory roof at the University of Jijel in Algeria, related to partial shading faults. The module's output current and voltage were predicted using the MLPNN model based on solar irradiation and PV cell temperature. Baharath et al. [40] used Wavelet transform to extract features from the electrical characteristics of the simulated PV system in their study, then applied Principal Component Analysis (PCA) for feature reduction. They obtained approximately 98% diagnostic performance by performing fault diagnosis with the MLPNN algorithm for 4 different conditions (normal condition, inverter fault, converter fault and modulated fault) with a data set consisting of 656 data. They showed that the performance of the proposed method is superior to the Radial Basis Function Extreme Learning Machine algorithm in the literature. In their study, Haque et al. [41] conducted experiments in a laboratory in India, involving the normal operation, dusty operation, and hot spot conditions of a PV system. They obtained images corresponding to these operating modes using an infrared camera. From these images, six different features were extracted using Discrete Wavelet Transform, creating a dataset of approximately 2000 data points. During the training process with the MLPNN algorithm, they achieved 100% success, and during testing, 99% accuracy. Additionally, they measured the fault detection time of the model during alarm conditions as 9 seconds.

Radial Basis Function Neural Network (RBFNN)

This method consists of three layers: input layer, hidden layer and output layer. The input data received from the input layer is transferred to the hidden layer for processing. The activation functions used here are radial basis functions. The data processed in the hidden layer is then transmitted to the output layer, and the results are obtained. RBFNN, a supervised learning algorithm, passes all the data in the dataset through the network and classifies the test data based on the similarity to the data in the input. In this process, the information of the training data is stored through the operations in the hidden layer, and based on this, the classification of new data is performed [42-44].

Pederson et al. [42], in their study, created 6000 data consisting of nine features by simulating the normal, shading, dirty/deteriorated conditions of PV systems. They proposed the RBFNN model for fault diagnosis and achieved 98.9% success. In their study, Kurukuru et al. [44] modeled the PV system in MATLAB/Simulink and obtained 7182 data points for 14 different fault conditions, including eight different features. They tested the RBFNN model proposed for fault diagnosis with different kernel functions, and during the test phase, the highest diagnostic accuracy was achieved with dynamic fusion, while the lowest diagnostic accuracy was obtained with Gaussian Euclidean. The performance of the proposed method was tested at different noise levels (20 to 50 dB signal-to-noise ratio (SNR)) and a success rate of 97.52% was achieved even at a 52 dB noise level.

3.2. Fuzzy Logic Methods

Fuzzy logic (FL) is a logic system that, unlike classical logic systems, focuses on modeling uncertainty and vagueness rather than making strictly true or false decisions. FL allows for a more flexible solution to real-world problems because, in many cases, data is not completely clear and precise. It was developed to better model human decision-making processes and is applied in various fields [45, 46].

Fuzzy Logic methods prefer to use interval values instead of exact values. This allows for more flexible and realistic results when making decisions. By using different membership functions, it establishes connections between different categories and aims to achieve the most accurate result. Additionally, Fuzzy Logic has a rule-based approach in the form of "if... then." These rules determine the outputs for the input data through mathematical operations. To generate outputs for the input data, the steps of fuzzification, fuzzy inference, and defuzzification are applied. First, in the fuzzification step, the data is expressed as fuzzy values. Then, in the fuzzy inference step, outputs are derived from fuzzy rules based on the information. Finally, in the defuzzification step, the fuzzy results are processed and converted into concrete/numerical values [47, 48].

The greatest advantage of fuzzy logic methods is their ability to be used in situations with uncertain, ambiguous, or incomplete data. They are commonly used in fault diagnosis, decision-making processes, and control systems in various fields.

In PV systems, when using fuzzy methods for fault diagnosis, the first step is to obtain parameters from thermal images, sensors, or electrical characteristics in the PV system in order to create fuzzy rules. A database containing corresponding faults is then created. Next, membership functions are generated using traditional methods. To determine the fuzzy diagnostic results, the three stages of fuzzy logic-based evaluation (fuzzification, fuzzy inference, and defuzzification) are completed. Finally, the fault diagnosis is performed.

Diminish et al. [49] diagnosed faults related to shading fault in PV systems using fuzzy logic, based on voltage and power ratio information in their study. They used LabVIEW software for data logging and monitoring the PV system, achieving a minimum fault diagnosis success rate of 98.8%. Belaout et al. [50] collected 2730 data from a PV system using an emulator in their study and employed Adaptive Neuro Fuzzy Inference System (ANFIS) method to classify the system's status into five different states. They compared the performance of ANFIS with that of an Artificial Neural Network (ANN). Spatura et al. [51] obtained data from I-V characteristics for increased series resistance losses condition, partial shading and potential-induced degradation conditions, and performed fault diagnosis using the fuzzy logic method. Zhao et al. [52] modeled a 3x13 PV array in MATLAB Simulink, and then experimentally collected 200 data points. They used the Fuzzy C-Means Clustering Method for the diagnosis of partial shading and short circuit faults, achieving a 96% diagnostic performance.

3.3. Machine Learning Methods

This methods are algorithms that enable computers to behave and think like humans with the help of algorithms. Initially, they allow computer software to learn from existing data and experiences in similar situations. Later, the computer system that has learned from these experiences draws conclusions about new situations [53]. Machine learning methods have become one of the most widely used techniques due to their computational capability and the continuous improvement of this capability.

Machine learning methods, widely used in various fields, are also commonly applied in fault diagnosis, following a series of steps. In fault diagnosis using ML methods, the first step is to select and prepare the dataset to be used. Next, the appropriate algorithm is chosen and trained with the dataset. To improve the algorithm's performance, the results are evaluated and then implemented. The model is tested with test data, and prediction results are obtained.

Machine learning methods are also widely used in fault diagnosis in PV systems. These methods are frequently employed for early fault detection, improving system efficiency, and reducing maintenance costs. Commonly used ML algorithms for fault diagnosis in PV systems include Support Vector Machine (SVM), K-Nearest Neighbors (kNN), Random Forest (RF), and Decision Tree (DT).

Support Vector Machine (SVM)

This algorithm is one of the machine learning methods introduced by Vapnik in 1979, which is widely used in regression and classification problems [54]. It is frequently preferred because it produces effective results in both linear and nonlinear classification problems. In the classification process, it works based on the principle of determining the optimal separating hyperplane by maximizing the margin (the distance between the data points) between the data points [55, 56].

SVM aims to achieve results by using different kernel functions in nonlinear classification problems. Kernel functions increase the diagnostic accuracy in the classification process by mapping the data to a higher dimensional space. Kernel functions are highly effective when working with complex data. Commonly used kernel functions include: polynomial kernel, Linear kernel, radial basis kernel and sigmoid kernel [55].

The SVM algorithm is frequently preferred due to its strong generalization ability in problems with large amounts of data, its capability to minimize structural risks, its ability to produce high-accuracy results, and its effectiveness in handling complex situations. However, the performance of SVM is negatively affected when the dataset is small or the data quality is low [57].

The SVM algorithm is commonly used for fault diagnosis in PV systems. Wang et al. [57] applied the SVM algorithm to diagnose short circuit, open circuit, and irradiation deficiency faults. They used information such as maximum power current, maximum power voltage, short-circuit current and open-circuit voltage from the I-V curves as input data. During the preprocessing step, k-means clustering and the hot-decking methods were applied to a dataset consisting of 697 collected data points. For optimization of the SVM parameters, grid search and k-fold cross-validation were used. They achieved an accuracy of 98.72% during the training phase and 97% during the testing phase. Yi et al. [58] used current and voltage information instead of sensor data to detect line-line faults in PV systems, and they extracted features using multiresolution signal decomposition. Then, fault diagnosis was performed using the SVM algorithm with a dataset of 177 data. Chen et al. [59] worked on fault diagnosis in PV systems for short circuit faults, open circuit faults, normal conditions, and partial shading conditions. They

prepared the PV system both in simulation and experimentally, obtaining two different datasets. To determine the most effective features in the obtained datasets, they used Principal Component Analysis and performed fault diagnosis with the SVM algorithm. Winston et al. [60] performed fault diagnosis in PV systems affected by hotspots and microcracks using open-circuit voltage, solar irradiance, short-circuit current, internal impedance, panel temperature, and power loss percentage as input data. They applied SVM and artificial intelligence methods for fault diagnosis. Using 1505 data, they achieved an accuracy of 99% with the SVM.

K Nearest Neighbors Algorithm (KNN)

This) algorithm is one of the supervised machine learning methods commonly used in classification and regression problems, which makes predictions by considering the similarities between data points. The KNN algorithm makes decisions by looking at the classes of a data point and its nearest neighbors. Therefore, in the KNN algorithm, the number of K-neighbors and the distance measurement method are important parameters. The number of K-neighbors indicates how many neighbors' labels will be considered, while the distance measurement method refers to the techniques used to measure the distance between the unlabeled data and its neighbors [61, 62].

The KNN algorithm is preferred due to its simple structure, ease of understanding, good performance, and ability to work with high-dimensional data. Challenges encountered with the KNN algorithm include an imbalanced dataset, improper selection of the number of neighbors, differences in scaling between features, and the computational cost that arises with large datasets [61].

The KNN algorithm is commonly used in fault diagnosis of PV systems, and successful results can be achieved through proper parameter selection and optimization, especially in the case of large datasets. Harrou et al. [61] proposed a Shewart-based KNN algorithm for detecting faults on the DC side of PV systems but observed that the proposed method could not detect partial shading. Maouleloued et al. [62] proposed a modified KNN algorithm for detecting faults caused by short circuits and disconnections between strings in PV systems. The input dataset was composed of cell temperature, irradiance, and the current and voltage values observed at the maximum power point. To convert multi-class classification to binary classification operation, they combined the KNN algorithm with the Giza Pyramid Construction Algorithm, achieving better performance compared to SVM, DT, and RF algorithms. Patil et al. [63] used the Multi-Resolution Signal Decomposition (MSD) technique along with fuzzy logic and KNN for detecting line-line and line-ground faults.

Decision Tree (DT)

The DT algorithm, which is commonly used in classification, estimation and regression problems, is one of the supervised machine learning algorithms. The DT algorithm analyzes patterns and relationships within the data, thereby creating a tree-like structure for decision-making. The DT structure primarily consists of root, branch, and leaf nodes. The roots represent the dataset, while the branches include decision stages that allow the data to be split according to specific rules and lead to the final outcome. The leaves are the sections where the outputs are obtained [64].

The DT algorithm, with its simple and easily understandable structure, fast prediction capability, and high performance, offers several advantages. However, its disadvantages include performance issues with large datasets, the need for preprocessing in datasets, and its tendency to overfitting [65].

The DT algorithm is widely used in fault diagnosis of PV systems due to its advantages. In their study, Zhao et al. [65] set up a small grid-connected PV system to simulate faults under real operating conditions. They applied data cleaning to the collected data for detecting line-line faults, shading and open circuit faults, and added different attributes to improve the performance of the DT algorithm. In the classification process performed in WEKA, they used 764,529 examples and achieved near 100% accuracy. Benkercha et al. [66] applied a two-stage diagnostic model using ambient temperature, power ratio, and irradiance features in the DT algorithm. In the first stage, they classified the PV system as faulty or healthy, and in the second stage, they classified the faulty PV system into four different conditions.

Random Forest (RF)

It is one of the supervised machine learning algorithms used in classification and regression tasks. It is an ensemble learning algorithm, which emerged to address the disadvantages of decision tree (DT) algorithms and consists of a combination of multiple tree structures. Subsets created from the dataset are used to obtain prediction results with different trees. The final result is obtained by applying majority voting to the outcomes of all decision trees [67, 68].

n the RF algorithm, multiple DT algorithms are used to reduce the risk of overfitting and make it easier to handle noisy data. It has advantages such as handling high-dimensional data, high accuracy, and ease of implementation. Its disadvantages include computational cost, performance degradation in imbalanced data situations, and reduced interpretability compared to DT [67].

Due to its advantages, the RF algorithm is used in fault diagnosis in PV systems. Yang et al. [67] proposed the RF algorithm for fault diagnosis in PV systems in their study. They used the Synthetic Minority Oversampling

Technique (SMOTE) and random undersampling methods for imbalanced datasets. By performing feature reduction using the Modified Independent Component Analysis technique, they enhanced the RF performance and achieved an accuracy of approximately 100%. Amiri et al. [68] proposed a two-stage RF for fault detection and diagnosis. By using the Modified Grey Wolf Optimization method to obtain the parameters, they achieved a performance of 99.4% for fault detection and diagnosis. In their study, Chen et al. [69] used simulation and experimental data for fault diagnosis of line-line faults and mismatch faults in PV systems with the RF algorithm. To achieve high performance with low computational load in the RF algorithm, they performed parameter optimization using the grid search algorithm.

4. Conclusion

This chapter covers the environmental, electrical, and physical faults that occur in PV systems. These faults and their effects are explained in detail. The smart methods commonly used in the literature for fault diagnosis in PV systems have been examined under three headings: artificial neural network methods, fuzzy methods, and machine learning methods. Their advantages and disadvantages are discussed. Examples of studies conducted in the literature are provided.

References

1. H. Li *et al*., "Applications of vacuum vapor deposition for perovskite solar cells: A progress review," in *iEnergy*, vol. 1, no. 4, pp. 434-452, December 2022, doi: 10.23919/IEN.2022.0053.
2. Liu, B., Sun, K., Wang, X., Zhao, J., & Hou, X. (2024). Fault diagnosis of photovoltaic strings by using machine learning-based stacking classifier. *IET Renewable Power Generation*, *18*(3), 384-397.
3. Khoshnami, A., Sadeghkhani, I.: Sample entropy-based fault detectionfor photovoltaic arrays. IET Renewable Power Gener. 12(16), 1966–1976(2018)
4. Renewable energy statistics- 2024, International Renewable Energy Agency (IRENA), https://www.irena.org/Publications/2024/Jul/Renewable-energy-statistics-2024.
5. Solórzano, J., & Egido, M. A. (2013). Automatic fault diagnosis in PV systems with distributed MPPT. *Energy conversion and management*, *76*, 925-934.
6. Deshkar, S. N., Dhale, S. B., Mukherjee, J. S., Babu, T. S., & Rajasekar, N. (2015). Solar PV array reconfiguration under partial shading conditions for maximum power extraction using genetic algorithm. *Renewable and Sustainable Energy Reviews*, *43*, 102-110.
7. Chepp, E. D., & Krenzinger, A. (2021). A methodology for prediction and assessment of shading on PV systems. *Solar Energy*, *216*, 537-550.
8. Bayrak, F., Ertürk, G., & Oztop, H. F. (2017). Effects of partial shading on energy and exergy efficiencies for photovoltaic panels. *Journal of cleaner production*, *164*, 58-69.
9. Ma, M., Liu, H., Zhang, Z., Yun, P., & Liu, F. (2019). Rapid diagnosis of hot spot failure of crystalline silicon PV module based on IV curve. *Microelectronics Reliability*, *100*, 113402.
10. Flicker, J., & Johnson, J. (2013, June). Electrical simulations of series and parallel PV arc-faults. In *2013 IEEE 39th Photovoltaic Specialists Conference (PVSC)* (pp. 3165-3172). IEEE.
11. Vieira, R. G., de Araújo, F. M., Dhimish, M., & Guerra, M. I. (2020). A comprehensive review on bypass diode application on photovoltaic modules. *Energies*, *13*(10), 2472.
12. Ramaprabha, R., & Mathur, B. L. (2012). A comprehensive review and analysis of solar photovoltaic array configurations under partial shaded conditions. *International Journal of Photoenergy*, *2012*(1), 120214.
13. W. Chine, A. Mellit, A. M. Pavan and V. Lughi, "Fault diagnosis in photovoltaic arrays," *2015 International Conference on Clean Electrical Power (ICCEP)*, Taormina, Italy, 2015, pp. 67-72, doi: 10.1109/ICCEP.2015.7177602.

14. Cheng, T., Al-Soeidat, M., Lu, D. D. C., & Agelidis, V. G. (2019). Experimental study of PV strings affected by cracks. *The Journal of Engineering*, *2019*(18), 5124-5128.

15. C. M. Whitaker, B. G. Pierce, A. M. Karimi, R. H. French and J. L. Braid, "PV Cell Cracks and Impacts on Electrical Performance," *2020 47th IEEE Photovoltaic Specialists Conference (PVSC)*, Calgary, AB, Canada, 2020, pp. 1417-1422, doi: 10.1109/PVSC45281.2020.9300374.

16. Meena, R., Pareek, A., & Gupta, R. (2024). A comprehensive Review on interfacial delamination in photovoltaic modules. *Renewable and Sustainable Energy Reviews*, *189*, 113944.

17. Jiang, L. L., & Maskell, D. L. (2015, July). Automatic fault detection and diagnosis for photovoltaic systems using combined artificial neural network and analytical based methods. In *2015 International Joint Conference on Neural Networks (IJCNN)* (pp. 1-8). IEEE.

18. Chan, F., & Calleja, H. (2006, October). Reliability: A new approach in design of inverters for PV systems. In *2006 IEEE International Power Electronics Congress* (pp. 1-6). IEEE.

19. Zhao Ye, Yang Ling, Lehman Brad, de Palma JJF, Lyons R. Decision Tree-Based Fault Detection and Classification in Solar Photovoltaic Arrays, in Proceedings of the 27th Annual IEEE Applied Power Electronics Conference and Exposition; 2012.

20. Alam, M. K., Khan, F., Johnson, J., & Flicker, J. (2015). A comprehensive review of catastrophic faults in PV arrays: types, detection, and mitigation techniques. *IEEE Journal of Photovoltaics*, *5*(3), 982-997.

21. S. E. Forman, "Performance of Experimental Terrestrial Photovoltaic Modules," Reliability, IEEE Transactions on, vol. R-31, pp. 235-245, 1982.

22. Abdulmawjood, K., Refaat, S. S., & Morsi, W. G. (2018, April). Detection and prediction of faults in photovoltaic arrays: A review. In *2018 IEEE 12th International Conference on Compatibility, Power Electronics and Power Engineering (CPE-POWERENG 2018)* (pp. 1-8). IEEE.

23. Chen, Y. H., Liang, R., Tian, Y., & Wang, F. (2016, August). A novel fault diagnosis method of PV based-on power loss and IV characteristics. In *IOP Conference Series: Earth and Environmental Science* (Vol. 40, No. 1, p. 012022). IOP Publishing.

24. Takashima, T., Yamaguchi, J., Otani, K., Oozeki, T., Kato, K., & Ishida, M. (2009). Experimental studies of fault location in PV module strings. *Solar Energy Materials and Solar Cells*, *93*(6-7), 1079-1082.

25. Chouder, A., & Silvestre, S. (2010). Automatic supervision and fault detection of PV systems based on power losses analysis. *Energy conversion and Management*, *51*(10), 1929-1937.

26. Vergura, S., Acciani, G., & Falcone, O. (2011). A finite-element approach to analyze the thermal effect of defects on silicon-based PV cells. *IEEE Transactions on*

Industrial Electronics, *59*(10), 3860-3867.

27. Koch, S., Weber, T., Sobottka, C., Fladung, A., Clemens, P., & Berghold, J. (2016, June). Outdoor electroluminescence imaging of crystalline photovoltaic modules: Comparative study between manual ground-level inspections and drone-based aerial surveys. In *32nd European Photovoltaic Solar Energy Conference and Exhibition* (pp. 1736-1740).

28. Breitenstein, O., Bauer, J., Trupke, T., & Bardos, R. A. (2008). On the detection of shunts in silicon solar cells by photo-and electroluminescence imaging. *Progress in Photovoltaics: research and Applications*, *16*(4), 325-330.

29. Breitenstein, O., & Sturm, S. (2019). Lock-in thermography for analyzing solar cells and failure analysis in other electronic components. *Quantitative InfraRed Thermography Journal*, *16*(3-4), 203-217.

30. Akram, M. W., Li, G., Jin, Y., & Chen, X. (2022). Failures of Photovoltaic modules and their Detection: A Review. *Applied Energy*, *313*, 118822.

31. Specht. (1988, July). Probabilistic neural networks for classification, mapping, or associative memory. In *IEEE 1988 international conference on neural networks* (pp. 525-532). IEEE.

32. Mohanty, S. R., Ray, P. K., Kishor, N., & Panigrahi, B. K. (2013). Classification of disturbances in hybrid DG system using modular PNN and SVM. *International Journal of Electrical Power & Energy Systems*, *44*(1), 764-777.

33. Ouhibi, R., Bouslama, S., & Laabidi, K. (2016, December). Faults classification of asynchronous machine based on the probabilistic neural network (PNN). In *2016 4th International Conference on Control Engineering & Information Technology (CEIT)* (pp. 1-7). IEEE.

34. Zhu, H., Ahmed, S. A. Z., Alfakih, M. A., Abdelbaky, M. A., Sayed, A. R., & Saif, M. A. A. (2020). Photovoltaic failure diagnosis using sequential probabilistic neural network model. *IEEE Access*, *8*, 220507-220522.

35. xiao Wang, X., Dong, L., yang Liu, S., Hao, Y., & Wang, B. (2019, June). A fault classification method of photovoltaic array based on probabilistic neural network. In *2019 Chinese Control And Decision Conference (CCDC)* (pp. 5260-5265). IEEE.

36. Garoudja, E., Chouder, A., Kara, K., & Silvestre, S. (2017). An enhanced machine learning based approach for failures detection and diagnosis of PV systems. *Energy conversion and management*, *151*, 496-513.

37. Mouaad, B. O. U. G. O. F. F. A., Samir, B. E. N. M. O. U. S. S. A., & Mohand, D. J. E. Z. I. R. I. (2024, January). Dynamic Modeling for Fault Diagnosis in PV Systems Utilizing AI Techniques Based on Multilayer Perceptron (MLP). In *2024 ASU International Conference in Emerging Technologies for Sustainability and Intelligent Systems (ICETSIS)* (pp. 1032-1036). IEEE.

38. Mekki, H., Mellit, A., & Salhi, H. (2016). Artificial neural network-based modelling and fault detection of partial shaded photovoltaic modules. *Simulation Modelling Practice and Theory*, *67*, 1-13.

39. Maharjan, K., Maharjan, A., & Motra, L. (2023). Machine Learning Approach for Fault Detection and Diagnosis of PV Modules.

40. Bharath, K. V. S., Haque, A., & Khan, M. A. (2018, October). Condition monitoring of photovoltaic systems using machine leaming techniques. In *2018 2nd IEEE International Conference on Power Electronics, Intelligent Control and Energy Systems (ICPEICES)* (pp. 870-875). IEEE.

41. Haque, A., Bharath, K. V. S., Khan, M. A., Khan, I., & Jaffery, Z. A. (2019). Fault diagnosis of photovoltaic modules. *Energy Science & Engineering*, *7*(3), 622-644.

42. Pedersen, E., Rao, S., Katoch, S., Jaskie, K., Spanias, A., Tepedelenlioglu, C., & Kyriakides, E. (2019, July). PV array fault detection using radial basis networks. In *2019 10th International Conference on Information, Intelligence, Systems and Applications (IISA)* (pp. 1-4). IEEE.

43. Manjunath, T. G., & Kusagur, A. (2016, December). Multilevel inverter fault diagnosis using optimised radial basis neural network—A novel performance enhancement. In *2016 International Conference on Electrical, Electronics, Communication, Computer and Optimization Techniques (ICEECCOT)* (pp. 102-105). IEEE.

44. Kurukuru, V. S. B., Blaabjerg, F., Khan, M. A., & Haque, A. (2020). A novel fault classification approach for photovoltaic systems. *Energies*, *13*(2), 308.

45. Su, Q., Mi, C., Lai, L. L., & Austin, P. (2000). A fuzzy dissolved gas analysis method for the diagnosis of multiple incipient faults in a transformer. *IEEE Transactions on Power Systems*, *15*(2), 593-598.

46. Khan, S. A., Equbal, M. D., & Islam, T. (2015). A comprehensive comparative study of DGA based transformer fault diagnosis using fuzzy logic and ANFIS models. *IEEE Transactions on Dielectrics and Electrical Insulation*, *22*(1), 590-596.

47. Yan, H., Xu, Y., Cai, F., Zhang, H., Zhao, W., & Gerada, C. (2018). PWM-VSI fault diagnosis for a PMSM drive based on the fuzzy logic approach. *IEEE Transactions on Power Electronics*, *34*(1), 759-768.

48. Gmati, B., Jlassi, I., Khojet El Khil, S., & Marques Cardoso, A. J. (2021). Open-switch fault diagnosis in voltage source inverters of PMSM drives using predictive current errors and fuzzy logic approach. *IET Power Electronics*, *14*(6), 1059-1072.

49. Dhimish, M., Holmes, V., Mehrdadi, B., & Dales, M. (2017). Diagnostic method for photovoltaic systems based on six layer detection algorithm. *Electric Power Systems Research*, *151*, 26-39.

50. Belaout, A., Krim, F., Mellit, A., Talbi, B., & Arabi, A. (2018). Multiclass adaptive neuro-fuzzy classifier and feature selection techniques for photovoltaic array fault detection and classification. *Renewable energy*, *127*, 548-558.

51. Spataru, S., Sera, D., Kerekes, T., & Teodorescu, R. (2015). Diagnostic method for photovoltaic systems based on light I–V measurements. *Solar Energy*, *119*, 29-44.

52. Zhao, Q., Shao, S., Lu, L., Liu, X., & Zhu, H. (2018). A new PV array fault diagnosis method using fuzzy C-mean clustering and fuzzy membership algorithm. *Energies*, *11*(1), 238.

53. Bulbul, H. I., & Unsal, Ö. (2011, December). Comparison of classification techniques used in machine learning as applied on vocational guidance data. In *2011 10th International Conference on Machine Learning and Applications and Workshops* (Vol. 2, pp. 298-301). IEEE.

54. Cortes, C. (1995). Support-Vector Networks. *Machine Learning*, 273-297.

55. Et-taleby, A., Chaibi, Y., Allouhi, A., Boussetta, M., & Benslimane, M. (2022). A combined convolutional neural network model and support vector machine technique for fault detection and classification based on electroluminescence images of photovoltaic modules. *Sustainable Energy, Grids and Networks*, *32*, 100946.

56. Yi, Z., & Etemadi, A. H. (2017). Line-to-line fault detection for photovoltaic arrays based on multiresolution signal decomposition and two-stage support vector machine. *IEEE Transactions on Industrial Electronics*, *64*(11), 8546-8556.

57. Wang, J., Gao, D., Zhu, S., Wang, S., & Liu, H. (2023). Fault diagnosis method of photovoltaic array based on support vector machine. *Energy sources, part a: recovery, utilization, and environmental effects*, *45*(2), 5380-5395.

58. Yi, Z., & Etemadi, A. H. (2017). Line-to-line fault detection for photovoltaic arrays based on multiresolution signal decomposition and two-stage support vector machine. *IEEE Transactions on Industrial Electronics*, *64*(11), 8546-8556.

59. Chen, L. C., Lin, P. J., Zhang, J., Chen, Z. C., Lin, Y. H., Wu, L. J., & Cheng, S. Y. (2018, October). Fault diagnosis and classification for photovoltaic arrays based on principal component analysis and support vector machine. In *IOP Conference series: Earth and Environmental science* (Vol. 188, No. 1, p. 012089). IOP Publishing.

60. Winston, D. P., Murugan, M. S., Elavarasan, R. M., Pugazhendhi, R., Singh, O. J., Murugesan, P., ... & Hossain, E. (2021). Solar PV's micro crack and hotspots detection technique using NN and SVM. *IEEE Access*, *9*, 127259-127269.

61. Harrou, F., Taghezouit, B., & Sun, Y. (2019). Improved $ k $ NN-based monitoring schemes for detecting faults in PV systems. *IEEE Journal of Photovoltaics*, *9*(3), 811-821.

62. Mouleloued, Y., Kara, K., & Chouder, A. (2023). A Developed Algorithm Inspired from the Classical KNN for Fault Detection and Diagnosis PV Systems. *Journal of Control, Automation and Electrical Systems*, *34*(5), 1013-1027.

63. Patil, M., & Hinge, T. (2019, March). Improved fault detection and location scheme for photovoltaic system. In *2019 Innovations in Power and Advanced Computing Technologies (i-PACT)* (Vol. 1, pp. 1-6). IEEE.

64. Pahwa, K., Sharma, M., Saggu, M. S., & Mandpura, A. K. (2020, February). Performance evaluation of machine learning techniques for fault detection and classification in PV array systems. In *2020 7th International Conference on Signal Processing and Integrated Networks (SPIN)* (pp. 791-796). IEEE.

65. Zhao, Y., Yang, L., Lehman, B., de Palma, J. F., Mosesian, J., & Lyons, R. (2012, February). Decision tree-based fault detection and classification in solar photo-

voltaic arrays. In *2012 Twenty-Seventh Annual IEEE Applied Power Electronics Conference and Exposition (APEC)* (pp. 93-99). IEEE.

66. Benkercha, R., & Moulahoum, S. (2018). Fault detection and diagnosis based on C4. 5 decision tree algorithm for grid connected PV system. *Solar Energy*, *173*, 610-634.

67. Yang, N. C., & Ismail, H. (2022). Robust intelligent learning algorithm using random forest and modified-independent component analysis for PV fault detection: In case of imbalanced data. *IEEE Access*, *10*, 41119-41130.

68. Amiri, A. F., Oudira, H., Chouder, A., & Kichou, S. (2024). Faults detection and diagnosis of PV systems based on machine learning approach using random forest classifier. *Energy Conversion and Management*, *301*, 118076.

69. Chen, Z., Han, F., Wu, L., Yu, J., Cheng, S., Lin, P., & Chen, H. (2018). Random forest based intelligent fault diagnosis for PV arrays using array voltage and string currents. *Energy conversion and management*, *178*, 250-264.

CHAPTER 8

A SWIN TRANSFORMER BASED EXPERT SYSTEM FOR THE DETECTION OF GASTROINTESTINAL DISEASES

Andaç İMAK[1]

1 Dr., Department of Electrical and Electronic Engineering, Faculty of Engineering, Munzur University, Tunceli, Turkey, ORCID: 0000-0002-3654-040X

1. Introduction

Gastrointestinal (GI) disorders are common in humans. When statistics are examined worldwide, more than 700,000 people die each year from stomach cancer, which is among these diseases (1). When these figures are considered, it emerges as an important element that endangers public health. Among digestive system diseases, esophageal cancer and colorectal cancers pose a threat to large populations worldwide (2-3). The frequency of these types of cancer in countries is directly proportional to nutritional habits and environmental factors.

Polyps in the intestine pose a great risk for stomach cancer, which endangers public health. Early detection and follow-up of these are of great importance (4). Endoscopic examinations are critical for the prevention of GI diseases by experienced doctors to diagnose changes in the digestive mucosa (5). Endoscopy is a type of examination in which the internal organs of a person, such as the intestines, esophagus and stomach, are viewed through a device called an endoscope. The endoscope transmits the image obtained by the camera and light on it to the monitor. The specialist doctor analyzes these images and detects tumors or other abnormalities in the GI tract and makes a diagnosis. In the next stage, appropriate treatment methods are determined according to this diagnosis. Thanks to the imaging system, it reduces the need for invasive surgical interventions and facilitates health services for detection and treatment.

The classification of symptoms diagnosed in endoscopic images may vary according to the experience of the specialists. In addition, it may occur in situations that are overlooked during the day due to motivation and fatigue. Today, along with developing imaging devices, artificial intelligence (AI)-based diagnostic systems and automatic detection systems in the health system help specialists. Thanks to these systems, the error rate in diagnosis is minimized and prognosis is improved (6). Artificial intelligence-based systems that will help specialists in the early diagnosis of common GI diseases continue to develop.

Recently, advances have been made in AI with good performance in deep learning-based classification and segmentation tasks (7-10). Machine learning-based studies are also available in the literature in the field of gastroenterology. Srivastava et al. proposed a deep learning architecture called FocalConvNet for the classification of luminal findings in the small intestine. They achieved 63.73% accuracy with this lightweight deep learning architecture (11). Agrawal et al. studied the classification performance of GI symptoms using transfer learning approach of convolution neural network (CNN). They developed a new metric for combining knowledge-driven features of CNN based transfer learning approach. As a result, they achieved a performance of 83.8%

(12). KahsayGebreslassie et al. conducted a study on a dataset containing gastrointestinal endoscopic images of eight different classes. They fine-tuned popular deep learning models such as DenseNet121 and ResNet50. They achieved 86.9% and 87.8% accuracy on the proposed models, respectively (13). Yoshiok et al. examined how well the deep learning architectures GoogleNet, ResNet-50, and MobileNet V3 performed on the endoscopic image dataset Kvasir. As a result of their applications, they achieved a performance of 84.6%, 84.2%, 83.3% and 83% for GoogLeNet, MobileNet V3, ResNet-50 and MobileNet V2, respectively (14). Fonollá et al. proposed a model that includes CNN and a global pooling layer. Considering an imbalanced class distribution, they achieved 90.2% success in classifying polyps in this study where data imputation methods were also used in the proposed method (15).

This study examined the diagnosis of GI illnesses using the Kvasir dataset, which contains polyps with specific characteristics. The DenseNet121 deep learning architecture, which has become well-known for its performance because to its dense layered and skip connections, served as the backbone network in the recommended method. In the second stage, the Swin Transformer design was used to capture long-range components and acquire more powerful characteristics. The performance of the proposed concept was assessed through extensive research on the Kvasir dataset.

The structure of this study is designed as given below. Section 2 will cover materials and methods, Section 3 will cover the experiments results. Section 4 will include the conclusion.

2. Materials and Methods

2.1. Proposed Method

As can be seen in Figure 1, in the proposed model, we have a classification network consisting of the DenseNet121 backbone network and the Swin transformer for polyp classification. First, the DenseNet121 network used is a successful deep learning model that provides information flow in the formation of features by providing dense skip connections. Strong features were obtained with the DenseNet121 architecture used for polyp classification. The $7^{\times}7^{\times}1024$ dimensional feature map obtained in the last layer is subjected to a 256-filter process to reduce the processing cost in the second step. Then, these feature maps are reshaped and converted to a 2-dimensional tensor.

In the second part proposed in the model, the feature map is transferred to the Swin transformer block with self-attention mechanism. Here, it becomes a powerful model where more detailed information is obtained thanks to the long-range context. The number of neurons in the dense layer of the MLP, the number of multi-heads, the window size, and the sliding window step size are the parameters of the Swin Transformer in the suggested model, which are

128, 4, 4, and 4, respectively. The swin transformer block has a 49×128 output. The classification procedure is carried out in the last step using the softmax, dense (8), and flatten (6272) layers.

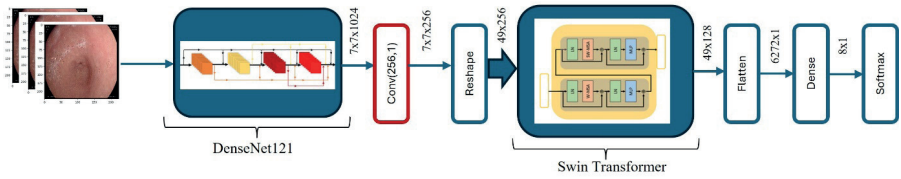

Figure 1. *Proposed hybrid model*

2.2. Swin Transformer

Transformer is a neural network architecture based on the self-attention mechanism, which is known for its superior performance in natural language processing (16). In later stages, it attracted the attention of researchers in the field of computer vision with its strong modeling performance.

Swin Transformer is a model that Liu et al. devised and refined for image processing (17). In the CNN design, they suggested optimizing the convolution layer's global context constraint. Processing the full input as a whole yields strong global long-range contextual information. Swin Transformer facilitates efficient learning of local contexts using window-based multi-head self-attention (W-MSA) and shifted window multi-head self-attention (SW-MSA) techniques, in contrast to conventional multi-head self-attention (MSA).

The basic Swin Transformer block is shown in Figure 2. The self-attention calculated by Swin Transformer blocks can be formulated as in Equation (1):

$$\text{Attention}(Q,K,V) = \text{Softmax}\left(\frac{QK^T}{\sqrt{d}}\right)V \quad (1)$$

Here Q(query), K(key), V are the value matrix and d is the query/key size (18).

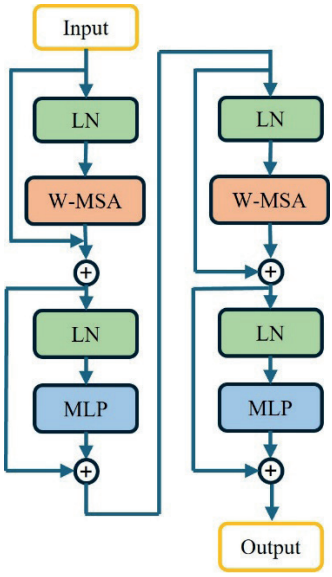

Figure 2. *Swin transformer*

2.3. Dataset

Endoscopy pictures from Norwegian hospitals connected to the Vestre Viken Health Foundation make up the Kvasir dataset. In order to identify precancerous lesions or tumors as soon as feasible, the dataset's data classes comprise a variety of images. There are 8,000 photos of different diseases and lesions in the publicly available Kvasir collection. The Pogorelov et al. study contains the annotations for the class labels. It is divided into eight classes, as shown in Figure 3: Ulcerative colitis, Normal (cecum, pylorus, z line), Esophagitis, Dyed lifted polyps, and Dyed resection margins (19).

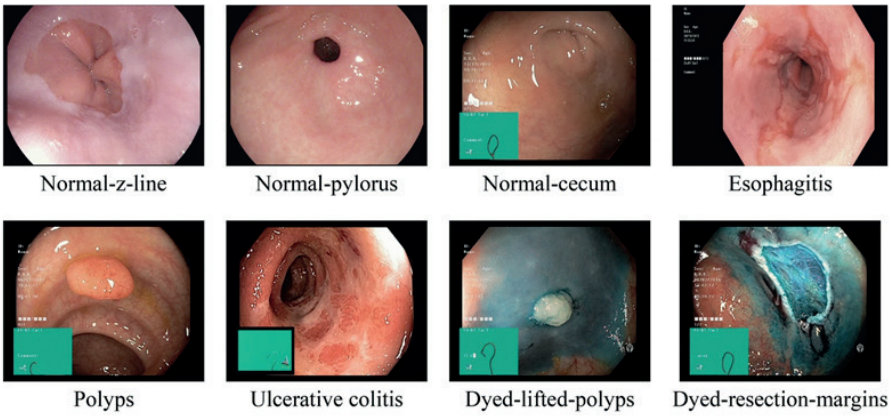

Figure 3. *An example image for 8 classes in the Kvasir dataset (20)*

3. Experimental Results

In this section, experimental studies are carried out with a specific hyperparameter to train the proposed architecture with the Kvasir dataset using the TensorFlow library in Google Colab. Accuracy, recall, F1-score and precision metrics are used to evaluate the efficiency of the proposed Swin transformer in the testing phase. These metrics provide quantitative metrics that highlight the potential of the model. The explanation of the performance metrics is given in the equations below.

$$\begin{aligned} \text{Accuracy} &= \frac{TN + TP}{TN + FN + TP + FP} \\ \text{Recall} &= \frac{TP}{TP + FN} \\ \text{Precision} &= \frac{TP}{TP + FN} \\ \text{F1} - \text{score} &= 2x\frac{\text{Precision x Recall}}{\text{Precision} + \text{Recall}} \end{aligned} \tag{2}$$

True negative and true positive are denoted by TN and TP, respectively, in Equation (2). False positive and false negative are denoted by the letters FN and FP.

The Kvasir dataset is split into three sections at random in the first step of the suggested model: 70% for training, 15% for testing, and 15% for validation. The pixel size of the image is 224 × 224. We trained using 32 batch size and 32 epoch size for 25 epochs, setting the learning rate (lr) to 0.0001 and the weight decay to 0.00001. First, the ImageDataGenerator using the Keras tensorflow library was used to do the picture data augmentation process for the train dataset. The following techniques were used: rotation rate, shear range, zoom range, width shift range, height shift range, and horizontal and vertical flip methods. The loss procedures were minimized using the Adam optimization technique. Figure 4 displays the training curves for the suggested Swin Transformer model.

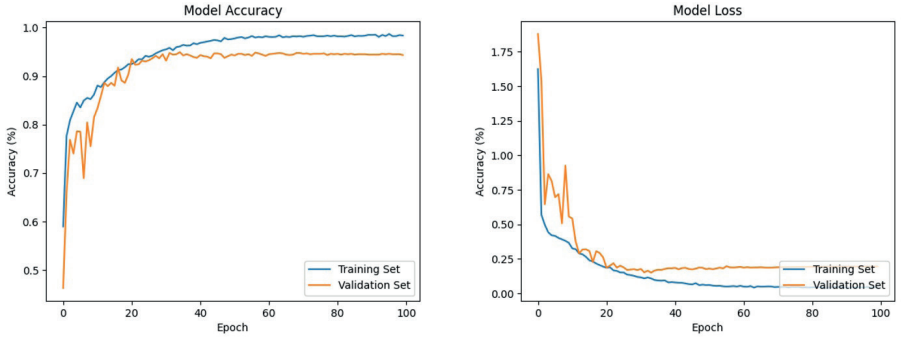

Figure 4. *Proposed Swin Transformer accuracy and loss curve*

Examining Figure 4, the model's accuracy curve during training demonstrated a performance of roughly 20 epochs and above 90% thereafter. In the designated period parts, the loss curve also showed a good decline. Figure 5 shows the confusion matrix that was produced using the trained model's 8-class test data.

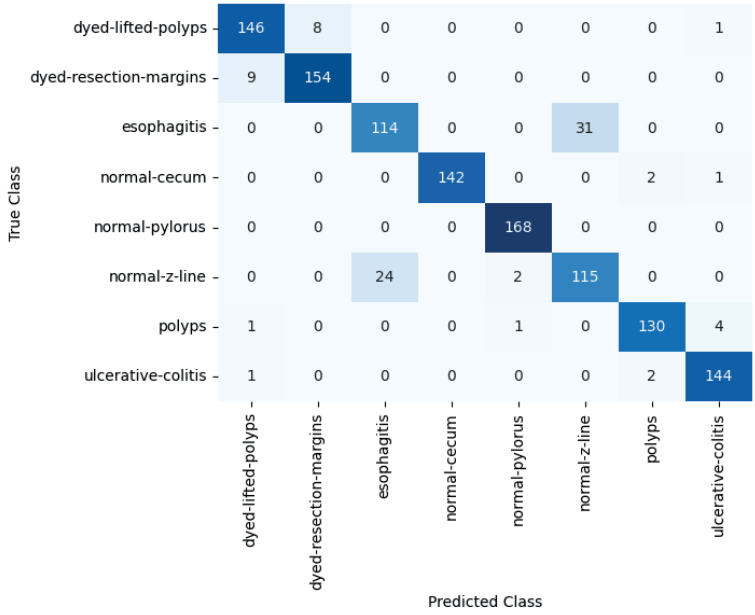

Figure 5. *Confusion matrix of the proposed model*

When the confusion matrix is examined in Figure 5, it correctly predicted 146 of 155 Dyed lifted polyps images, 154 of 162 Dyed resection margins images, 114 of 138 Esophagitis images, 142 of 142 Normal cecum images, 168 of 171 Normal pylorus images, 115 of 146 Normal z-line images, 130 of 134 Polyps images and finally 144 of 150 Ulcerative colit images. In addition, the 8-class test results of the proposed Swin transformer model according to the confusion matrix with the performance metrics mentioned above for each class are given in Table 1.

Table 1. *Class-based classification report for the proposed models*

Classes	Precision	Recall	F1-score	Support
dyed-lifted-polyps	0,93	0,94	0,94	155
dyed-resection-margins	0,95	0,94	0,95	163
esophagitis	0,83	0,79	0,81	145
normal-cecum	1,00	0,98	0,99	145
normal-pylorus	0,98	1,00	0,99	168

normal-z-line	0,79	0,82	0,80	141
polyps	0,97	0,96	0,96	136
ulcerative-colitis	0,96	0,98	0,97	147
accuracy			0.93	1200
macro avg	0,93	0,93	0,93	1200
weighted avg	0,93	0,93	0,93	1200

The comparison of their accuracies with the studies carried out with the publicly available Kvasir data set is presented in Table 2.

Table 2. *Comparison results with studies using the Kvasir dataset in the literature*

Author	Dataset	Accuracy (%)
Srivastava et al. [11]	Kvasir	63.73
Agrawal et al. [12]	Kvasir	83.8
KahsayGebreslassie et al. [13]	Kvasir	87,8
Yoshiok et al. [14]	Kvasir	84.6
Fonollá et al. [15]	Kvasir	90.2
Proposed	***Kvasir***	***93***

Using Kvasir data, Srivastava et al. [11] achieved 63.73%, Agrawal et al. [12] 83.8%, KahsayGebreslassie et al. [13] 87.8%, Yoshiok et al. [14] 84.6%, Fonollá et al. [15] 90.2% success. When the performance results were compared with the model, it produced a difference between the Swin Transformer model and the existing methods with 93% success. This comparison table supports the performance of the model.

4. Conclusion

In this study, open access kvasir dataset was used for early detection of GI diseases and designing a system that helps experts. The main purpose of the model is to automatically classify GI diseases with a deep learning-based model. With this dataset, which includes 8000 images with 8 classes including normal tissues, researchers continue their work to develop deep learning-based systems.

The proposed model highlights a hybrid approach with Swin transformer of features obtained from DenseNet121. Thanks to this hybrid model, it has increased its effectiveness with dense semantic features. The model showed good performance with 93% success. With the obtained results, it is planned to develop the hybrid model with new optimizations or systems in which new deep learning models are integrated for future studies.

References

1. Hong JH, Rho SY, Hong YS. Trends in the aggressiveness of end-of-life care for advanced stomach cancer patients. Cancer Res Treat. 2013;45(4):270-275.
2. Sung H, Ferlay J, Siegel RL, Laversanne M, Soerjomataram I, Jemal A, Bray F. Global cancer statistics 2020: GLOBOCAN estimates of incidence and mortality worldwide for 36 cancers in 185 countries. CA Cancer J Clin. 2021;71:209-249.
3. Pogorelov K, Randel KR, Griwodz C, Eskeland SL, De Lange T, Johansen D, Spampinato C, Dang-Nguyen DT, Lux M, Schmidt PT, et al. Kvasir: A multi-class image dataset for computer aided gastrointestinal disease detection. In: Proceedings of the 8th ACM Multimedia Systems Conference, MMSys 2017; Taipei, Taiwan; 2017:164-169.
4. Pozdeev AA, Obukhova NA, Motyko AA. Automatic analysis of endoscopic images for polyps detection and segmentation. In: 2019 IEEE Conference of Russian Young Researchers in Electrical and Electronic Engineering (EIConRus); 2019:1216-1220. IEEE.
5. Muto M, Yao K, Kaise M, Kato M, Uedo N, Yagi K, Tajiri H. Magnifying endoscopy simple diagnostic algorithm for early gastric cancer (MESDA-G). Dig Endosc. 2016;28(4):379-393.
6. Lonseko ZM, Adjei PE, Du W, Luo C, Hu D, Zhu L, Rao N. Gastrointestinal disease classification in endoscopic images using attention-guided convolutional neural networks. Appl Sci. 2021;11(23):11136.
7. İşgüzar S, Türkoğlu M, Ateşşahin T, Dürrani Ö. FishAgePredictioNet: A multi-stage fish age prediction framework based on segmentation, deep convolution network, and Gaussian process regression with otolith images. Fish Res. 2024;271:106916.
8. Zhang Y, Shen Z, Jiao R. Segment anything model for medical image segmentation: Current applications and future directions. Comput Biol Med. 2024;108238.
9. Xu Y, Quan R, Xu W, Huang Y, Chen X, Liu F. Advances in medical image segmentation: A comprehensive review of traditional, deep learning and hybrid approaches. Bioengineering. 2024;11(10):1034.
10. Aslan M. CoviDetNet: A new COVID-19 diagnostic system based on deep features of chest x-ray. Int J Imaging Syst Technol. 2022;32(5):1447-1463.
11. Srivastava A, Tomar NK, Bagci U, Jha D. Video capsule endoscopy classification using focal modulation guided convolutional neural network. In: 2022 IEEE 35th International Symposium on Computer-Based Medical Systems (CBMS); 2022:323-328. IEEE.
12. Agrawal T, Gupta R, Narayanan S. On evaluating CNN representations for low resource medical image classification. In: ICASSP 2019-2019 IEEE Inter-

national Conference on Acoustics, Speech and Signal Processing (ICASSP); 2019:1363-1367. IEEE.

13. KahsayGebreslassie A, Hagos MT. Automated gastrointestinal disease recognition for endoscopic images. In: 2019 International Conference on Computing, Communication, and Intelligent Systems (ICCCIS); 2019:312-316. IEEE.

14. Yoshiok K, Tanioka K, Hiwa S, Hiroyasu T. Deep-learning models in medical image analysis: Detection of esophagitis from the Kvasir dataset. 2023. Available at: http://arxiv.org/abs/2301.02390.

15. Fonolla R, van der Sommen F, Schreuder RM, Schoon EJ, de With PH. Multi-modal classification of polyp malignancy using CNN features with balanced class augmentation. In: 2019 IEEE 16th International Symposium on Biomedical Imaging (ISBI 2019); 2019:74-78. IEEE.

16. Zu B, Cao T, Li Y, Li J, Ju F, Wang H. SwinT-SRNet: Swin transformer with image super-resolution reconstruction network for pollen images classification. Eng Appl Artif Intell. 2024;133:108041.

17. Liu Z, Lin Y, Cao Y, Hu H, Wei Y, Zhang Z, Guo B. Swin transformer: Hierarchical vision transformer using shifted windows. In: Proceedings of the IEEE/CVF International Conference on Computer Vision; 2021:10012-10022.

18. Yao D, Shao Y. A data efficient transformer based on Swin Transformer. Vis Comput. 2024;40(4):2589-2598.

19. Pogorelov K, Randel KR, Griwodz C, Eskeland SL, de Lange T, Johansen D, Halvorsen P. Kvasir: A multi-class image dataset for computer aided gastrointestinal disease detection. In: Proceedings of the 8th ACM on Multimedia Systems Conference; 2017:164-169.

20. Demirbaş AA, Üzen H, Fırat H. Spatial-attention ConvMixer architecture for classification and detection of gastrointestinal diseases using the Kvasir dataset. Health Inf Sci Syst. 2024;12(1):32.

CHAPTER 9

A REVIEW FOR BLDC MOTOR DRIVER AND PWM SIGNALS CONTROL WITH DEEP LEARNING MODELS

M. Murat TEZCAN[1]

Elif Sinem AKTAŞ[2]

1 (Ph.D), Kütahya Dumlupınar University Faculty of Engineering, Dept. of Electrical Electronics Engineering, ORCID ID: 0000-0002-5390-4527, murat.tezcan@dpu.edu.tr

2 (Bs.C.), ORCID ID: 0009-0001-8619-3282, elif.aktas3@dpu.edu.tr

1) MOTIVATION

The study addresses the integration of deep learning and artificial intelligence in motor driver control and PWM (Pulse Width Modulation) signal generation, combining machine learning with power electronics principles for advanced research and analysis. This approach aims to optimize motor driver performance. Motor drivers regulate the speed and torque of motors by adjusting operating parameters (such as current, voltage, etc.) over time. PWM signals, a technique used in speed and torque control, serve to regulate the power delivered to devices by managing motor energy through switching pulses. This, in turn, ensures effective speed and torque control, preventing potential damage to devices and improving motor performance. The key focus of this study is to advance PWM signal output control through artificial intelligence, moving beyond traditional methods. By examining the limitations of conventional control methods in motor drivers, the research explores how deep learning-based approaches can introduce flexibility, adaptability, and significant advantages to such systems. The use of deep learning-based control in power converters and motor drivers offers numerous benefits, particularly in reducing control errors, enhancing energy efficiency, and optimizing performance.

The importance of electric motor drivers in today's industrial sector is significant due to their role in optimizing production processes, improving energy efficiency, and enhancing the precision of machinery. To begin by detailing the importance and types of electric motors in industrial applications today: Electric motors are devices that use electrical energy to produce mechanical energy and are widely used across various industries. Adjustable Speed Drives

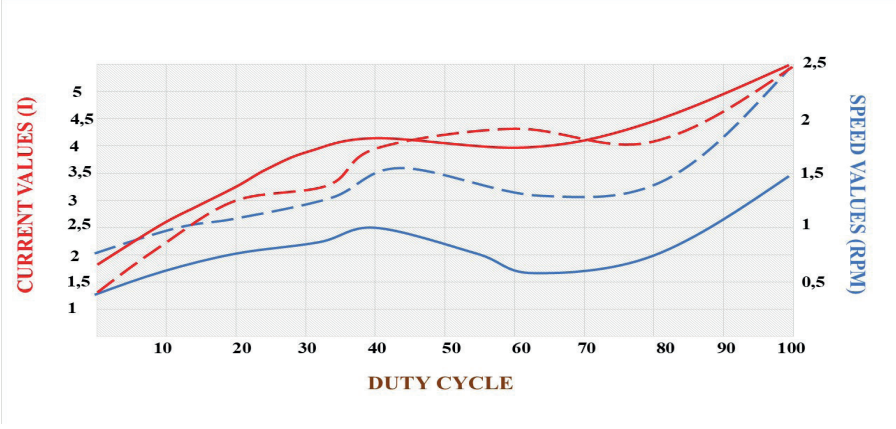

Figure 1. *Variation of Current and Speed of a BLDC Motor According to PWM Duty Cycle*

(ASDs) adapt to various production processes by controlling the speed and torque of the motor. These systems not only improve motor performance but also optimize energy consumption. Modern motor drivers have significantly enhanced the performance of electric motors through precise control mechanisms. In this context, Pulse Width Modulation (PWM) is a critical technique that increases the effectiveness of motor driver systems. PWM optimizes motor speed, torque, and energy consumption by controlling the voltage and current levels in motor drivers. When examining PWM's contributions to motor performance, it allows for energy efficiency by enabling the motor to conserve energy at variable speeds, providing precise control over speed and torque, and ensuring an efficient optimization environment.

According to the values presented in Figure 1, the PWM duty cycle is represented along the X-axis, while the motor speed ( ) and current ( ) parameters are shown along the Y-axis. Observing the blue line, we can see that as the PWM duty cycle increases, the motor speed increases linearly. In contrast, the red line illustrates that the current drawn by the motor is directly proportional to the PWM duty cycle. This graph clearly demonstrates how PWM signals are utilized in motor speed and torque control and the effects of the duty cycle on motor performance. It can be observed that at higher duty cycles, the motor consumes more power and accelerates, whereas at lower duty cycles, it consumes less energy and experiences a decrease in speed.**[1].**

2. MOTOR OPERATING SYSTEMS AND DATA CONTROL

The plan analysis conducted using the sensors shown in Figure 2 provides a technical review of sensorless methods for controlling Brushless Direct Current (BLDC) motor drivers, including limitations and developments. Figure 2 specifically illustrates graphs displaying various measurements such as temperature, voltage, and current, or a diagram explaining how sensors' feedback is utilized in motor control systems. It also briefly analyzes the most relevant techniques based on predictions and models, such as Artificial Neural Networks. The control of BLDC motors can be performed in either sensor-based or sensorless mode. However, to reduce the overall cost of drive devices, sensorless control techniques are typically used. The advantage of sensorless BLDC motor control is that it eliminates the sensing part, significantly reducing overall costs. [2].

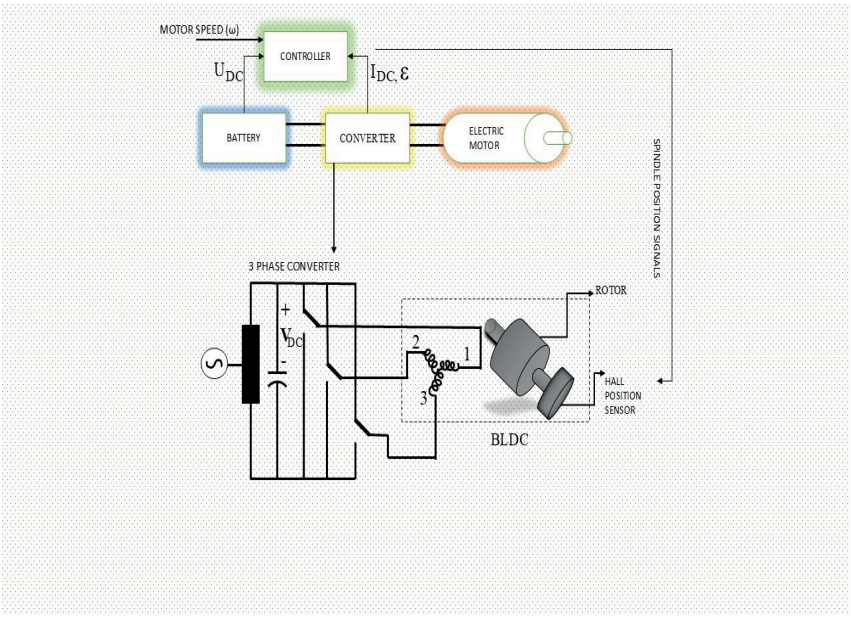

Figure 2. *Motor Operating System and PWM Relationship*

The disadvantages of sensorless control include increased requirements for control algorithms and more complex electronics. In contrast, sensor-based control facilitates real-time data acquisition with greater accuracy and speed. An example illustrating the operation of a BLDC motor using a Hall sensor is provided. [3].

BLDC motors are typically powered by a series of currents that have a trapezoidal waveform for operation. To rotate these motors, the stator windings must be energized in a specific sequence. Knowing the rotor position is crucial for determining this energization sequence. The rotor position is detected by

Hall effect sensors located within the motor. These sensors detect changes in the magnetic field to determine the rotor's position. Hall sensors are used to control the motor's speed, direction, and torque, producing output signals based on magnetic field intensity. These signals are sent to the motor driver control system, allowing for continuous monitoring of the rotor position. PWM signals are generated using this information to precisely adjust the motor's speed and torque. Furthermore, the data collected from the data acquisition systems are processed in a digital environment, and this information is analyzed through microcontrollers to provide feedback to the control system. This process helps optimize motor performance, ensuring that the rotor position is continuously monitored and that PWM signals can accurately adjust the motor's speed and torque. Hall sensors are commonly used, especially in brushless DC motors. **[4].** The data collected from the example data acquisition systems (DAQ) processes the information in a digital environment. The processed data is analyzed using microcontrollers, providing feedback within the control system.

PWM Analysis Stages with Microcontroller:

1. **Data Acquisition:** Microcontrollers receive data obtained from PWM through sensors. Data is transmitted to the microcontroller using speed, torque, and current sensors, thus enabling data flow.

2. **Signal Processing:** The collected data is analyzed in real-time and accurately to generate PWM signals aimed at enhancing motor performance. The motor's performance is measured through the pulse width of the signals based on speed and torque information. The processing of the measured data directly affects the voltage and current of the motor.

3. **Control Algorithms:** The microcontroller optimizes the motor speed and torque by continuously updating the PWM signals. Especially under varying load conditions, the pulse width of the signals keeps the motor's performance under control.

2.1. Data Analysis and Control Algorithms Using Microcontrollers

PWM controls the motor speed and torque by regulating the voltage and current through changes in the pulse width of the signal. Microcontrollers generate these PWM signals and play a role in data flow for analysis. Sensors facilitate the collection of data on speed, torque, current, and voltage, enabling the transmission of this information to the microcontrollers. By processing the transmitted information and data, appropriate PWM signals for motor operation are generated.

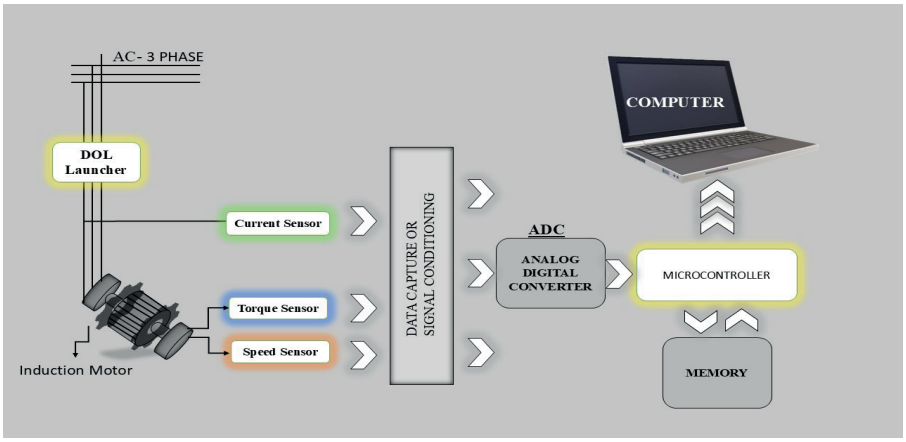

Figure 3. *Relationship Diagram of Motor Driver Data with Sensors and Microcontrollers*

The diagram depicted in Figure 3 illustrates how critical data, including speed, torque, current, and voltage, is collected through sensors from electric motor drivers and transmitted to the microcontroller. The microcontroller processes this data to facilitate real-time control of the motor driver. Furthermore, the analysis of this data is employed for various applications, including optimizing motor performance, enhancing energy efficiency, enabling fault diagnostics, and controlling PWM signals in real time via motor drivers, thus ensuring effective data management through microcontrollers. [5].

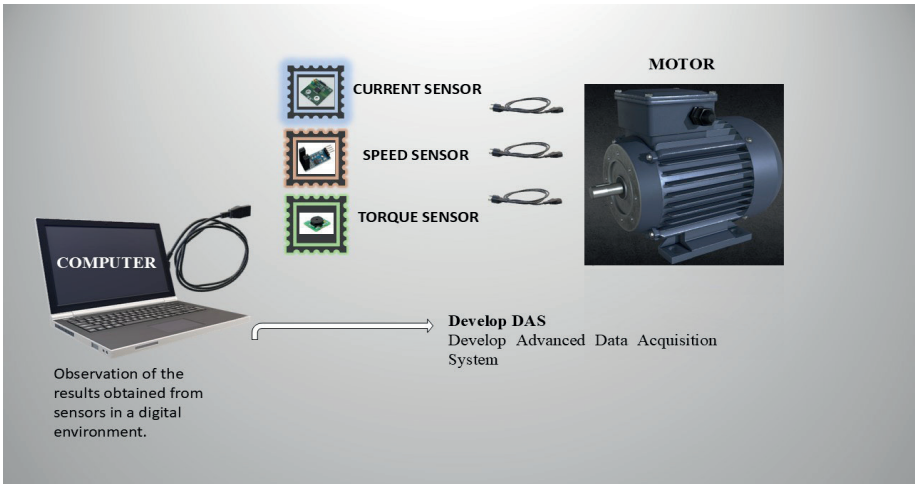

Figure 4. *The Data Acquisition System and the Collaboration of Microcontrollers with Sensors*

In **Figure 4**, a system is presented where torque, speed, and current sensors are controlled through an advanced data acquisition system and microcontrollers. In this system, microcontrollers are seen to work together with the Develop Data Acquisition System (DAS). The advanced data acquisition system (Develop DAS) enables the collection, processing, and analysis of data obtained from various sensors. The analyzed data can be used, for example, to monitor the performance of electric motors. These systems enable the continuous monitoring of critical parameters such as the motor's speed, torque, and current by obtaining real-time data.

2.2. Real-Time Model Training and Artificial Neural Networks

2.2.1 Artifical Neurals Networks (ANN)

Machine learning, particularly artificial neural networks (ANN), is widely used to solve complex problems that are difficult to approach or cannot be solved by traditional computational methods. Artificial neural networks are commonly employed in image processing and engineering applications due to their ability to model complex and nonlinear relationships, as well as their low error tolerance. Various libraries and tools for artificial neural networks have been developed in numerous programming languages. Some of the most commonly used and widely accepted ones are listed below.: **[6].**

- The Stuttgart Neural Network Simulator (SNNS) is a simulator developed by the Institute of Parallel and Distributed Systems (IPVR) at the University of Stuttgart specifically for artificial neural networks. It is designed to provide an efficient and flexible simulation environment for neural network applications and research.

- FANN (Fast Artificial Neural Network Library) is a library written in the C programming language that facilitates the implementation of multilayer perceptrons in artificial neural networks.

- JOONE (Java Object-Oriented Neural Engine) is a library for artificial neural networks developed in a Java environment.

- The MATLAB Neural Network Toolbox is a MATLAB-based tool that enables the design, implementation, visualization, and simulation of artificial neural networks.

Artifical Neurals Networks (ANN) Models

Single-Layer Perceptrons: This is a simple artificial neural network model that consists of an input layer and a single output layer. Each input is multiplied by a weight, summed, and then passed through an activation function. It is capable of performing only linear classification.	**Perceptron Model**: This is an algorithm that multiplies input values by weights, sums them up, and classifies the resulting value based on a threshold. It is capable of distinguishing only between two classes. Doesn't exis to complex layer.
Adaline Model (Adaptive Linear Neuron): This model utilizes error feedback to adjust the weights of the inputs. The output is determined through a linear combination based on the weighted sum of the inputs. The least squares method is employed for error minimization.	**Multi-Layer Perceptrons (MLP):** This architecture includes one or more hidden layers. Each layer receives outputs from the previous layer. MLPs can model complex relationships using non-linear functions and are trained using the backpropagation algorithm.

Among the artificial neural network models mentioned above, Multi-Layer Perceptrons (MLP) are the most suitable for controlling PWM signals due to their ability to learn complex relationships [6].

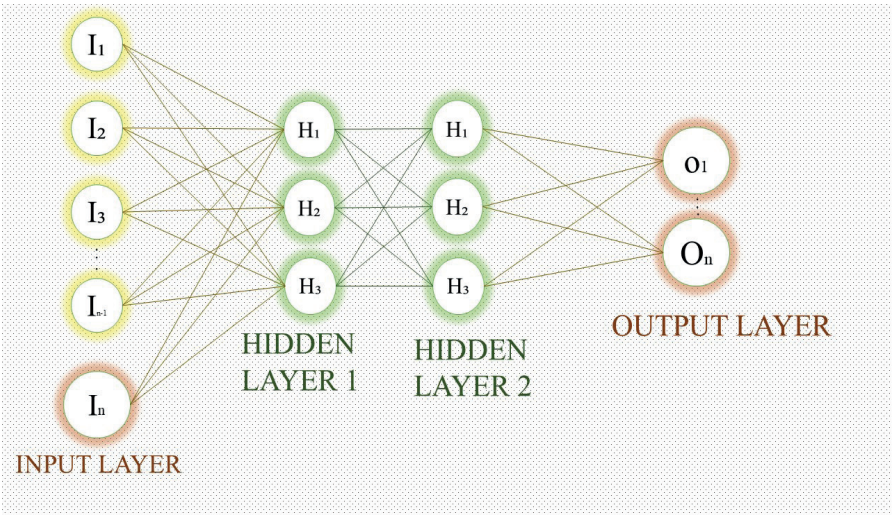

Figure 5. *Basic Logical Structure of Multi-Layer Perceptrons with Neural Network Architecture*

As illustrated in the logical structure of multilayer perceptrons in Figure 5, multilayer perceptrons (MLPs) comprise an input layer for data entry, one or more hidden layers, and an output layer. Within MLPs, there exist

forward and backward transitions, commonly referred to as feedforward and backpropagation. In the feedforward phase, the network's output and the error value are computed. Subsequently, in the backpropagation phase, the connection weights between the layers are adjusted to minimize the computed error value. This architecture effectively provides a solution for optimizing PWM signals by accepting sensor data such as speed, torque, and current as input, thereby facilitating a multi-layered information system. Examples of such complex structures include the Stuttgart Neural Network Simulator (SNNS), FANN, MATLAB, and JOONE [8]. YOLOv8 offers significant advancements over its predecessors, exhibiting enhanced speed and reduced latency, making it particularly suitable for real-time applications. This model achieves a higher accuracy rate, resulting in superior performance in object detection tasks. Consequently, YOLOv8 is frequently employed in image processing and model training endeavors, demonstrating its effectiveness and reliability in various computational vision applications.

Considering real-time trained models and libraries, YOLO versions can be utilized during the model training phase. YOLOv8 is a robust computer vision algorithm capable of quickly and efficiently detecting various objects, as it is trained on a large dataset. [7]. In addition, deep learning models such as **YOLOv5 and YOLOv8** are commonly integrated with popular libraries like **PyTorch and TensorFlow**. Consequently, establishing direct integration with artificial neural network libraries such as the Stuttgart Neural Network Simulator (SNNS), FANN, or JOONE may pose certain challenges. However, the **MATLAB Neural Network Toolbox** serves as an effective platform for training and deploying these models. MATLAB offers a comprehensive suite of tools tailored for the development of deep learning architectures and facilitates seamless integration with YOLO. Throughout this research, both the integration process and practical applications will be conducted using **MATLAB**, ensuring a robust framework for model implementation and evaluation.

2.2.2. Integration of PWM Signal and Deep Learning Model with MATLAB

The steps for integrating the PWM signal into a deep learning model using MATLAB are outlined below:

a) Model Training

- **Data Collection**: Microcontrollers receive data obtained from PWM through sensors. Data is transmitted to the microcontroller using speed, torque, and current sensors, thereby facilitating a data flow in conjunction with PWM. [page. 7]

- **Feature Selection**: Input and output data are determined; for example,

speed and torque can be used as inputs, while PWM can be utilized as outputs. The feedback of the identified data is facilitated through microcontrollers. In summary, it can be observed that the collected data is related to PWM in conjunction with microcontrollers. [page. 8]

- **Network Design**: The appropriate network architecture is determined based on the model to be trained. If the model includes complex structures, multilayer perceptrons are selected; otherwise, single-layer or less complex perceptrons are chosen. An artificial neural network model algorithm is developed that aligns with the selected network structure. The chosen structures consist of a multilayer neural network implemented using the Neural Network Toolbox in MATLAB, and a system is created that is compatible with this network architecture. [page. 10]

b) Training Process and FNN Structure

- **Model Training**: The necessary input and output data for the PWM signal are collected. The input data typically includes information such as the motor's speed, torque, current, and voltage conditions, which are provided through sensors. The input data contains sensor data. The output data consists of the values of the PWM signal over a specific time interval. Using the collected data, the artificial neural network is defined, and an appropriate algorithm for its fundamental logic structure is created and trained. The trained neural network is constructed using the MLP model in MATLAB. Software functions, such as (train), are utilized to enable the network to learn and recognize the data. The model is integrated to produce PWM signal output. Data is extracted through the integrated model, and the network structure is established. PWM (Pulse Width Modulation) signals are frequently used in motor driver control systems. In this study, to provide PWM signal output, we will examine the design and implementation phases of a Fuzzy Neural Network (FNN) in conjunction with the MATLAB Neural Network Toolbox; FNN is a type of artificial neural network that combines the ability to process uncertain information with learning capability. These structures are used, particularly to achieve better control performance in complex systems.

Utilization of FNN in PWM Control:

- Input Data: Parameters such as speed and torque required for generating the PWM signal serve as input data.

Design of a Fuzzy Neural Network (FNN) with MATLAB Neural Network Toolbox:

- The implementation process involves defining the network architecture and training the FNN to accurately predict PWM signals based on the provided input parameters..

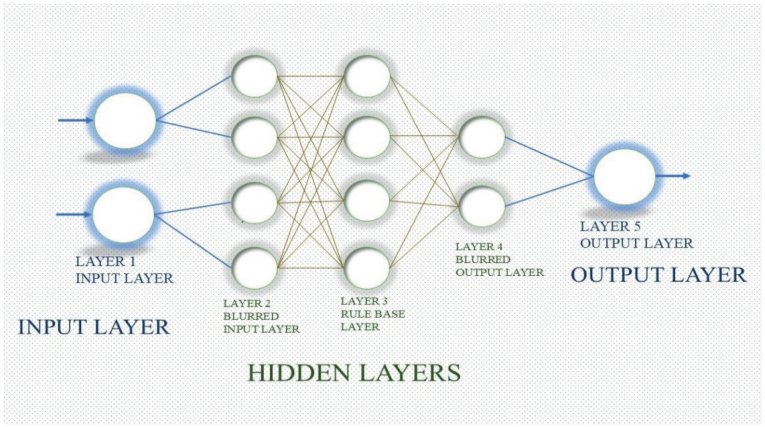

Figure 6. *Basic Logic Diagram of the FNN Structure*

The layers of the diagram shown in **Figure 6** are listed as follows:

Input Layer: In this layer, the error (e) and delta error (Δe) are processed.

Membership-Fuzzy Input Layer: This layer is responsible for processing fuzzy (if-then) logic rules. Membership functions corresponding to each input are defined at this stage.

Rule Layer: Fuzzy (if-then) rules based on the input parameters are executed within this layer. For example, straightforward rules such as "if the error is significant, then the PWM output signal should also be substantial" are applied.

Output Layer: The PWM signal generated in this layer is subsequently transmitted to the motor driver.

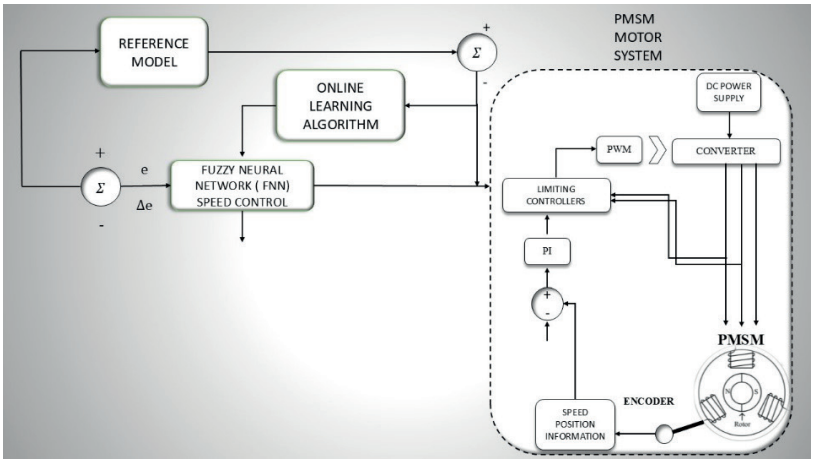

Figure 7. *Signal Diagram Controlling the PWM Signal Output of the PMSM Motor in Conjunction with a Neural Network*

[9]. **Figure 7** depicts a diagram illustrating the generation of control signals for the PWM signal output of a Permanent Magnet Synchronous Motor (PMSM) utilizing a Fuzzy Neural Network (FNN) structure. In this FNN control system, the input layer consists of critical parameters, namely the error signal (e) and the change in error (Δe). These parameters are calculated based on the difference between the motor's target speed and its actual speed. The primary objective of the system is to accurately adjust the PWM signals to minimize these errors, thereby maintaining the motor's speed and torque at a constant level. The neural network provides the necessary inputs to generate the PWM signal. The PWM output is represented as a control signal denoted by qi, which can be expressed through the following formulas:[9].

Error signal: $\mathbf{e(t)=\omega r(t)-\omega m(t)}$ (ωr(t): actual rotor speed , ωm(t): Desired rotor speed)

Delta Error: $\mathbf{\Delta e(t)=e(t)-e(t-1)}$

These data are fed into the neural network, and the Fuzzy Neural Network (FNN) generates an output PWM signal based on these errors.

FNN Training Process

The training of the FNN is conducted using supervised and continuous learning. The neural network is trained on datasets and the arguments derived from these datasets, and the system performs the learning process in a way that minimizes errors. In particular, the digital learning capability provides continuous adaptation against parameter uncertainties and changes in motor control. The training of the FNN is typically achieved using a supervised backpropagation algorithm.

Advantages of FNN- Based Contol [10].

- **Adaptability**: The Fuzzy Neural Network (FNN) can adapt to changing system conditions and uncertainties.
- **Accuracy**: It controls the PWM signal precisely based on error and delta error information. Continuous monitoring ensures data accuracy
- **Rapid Response**: Thanks to its precise and continuous control structure, the FNN can quickly adjust the PWM signal in response to external influences, providing a high level of accuracy.

Briefly, generating PWM signals in a PMSM motor driver using an FNN-based control system enhances both the accuracy and speed of the system while improving its stability. This approach not only reduces errors arising from external influences and enables rapid adaptation to changing conditions but also optimizes motor performance. The learning capability of the FNN continuously optimizes PWM signals based on errors, thereby ensuring effective control of the motor's speed and torque, which ultimately leads to an

improvement in motor performance.

3. INTEGRATION OF MOTOR DRIVERS AND DEEP LEARNING ALGORITHMS

In recent years, the utilization of artificial intelligence and deep learning algorithms in industrial automation and robotic systems has been increasing. Deep learning-based image processing algorithms, such as YOLOv8, not only excel in object detection but also provide valuable inputs in areas like motor driver control. Parameters such as speed and torque control in motor drivers can be optimized through accurate signal processing, leading to enhanced performance. Artificial intelligence positively influences the accuracy and speed metrics of the system through autonomous intervention.

Motor Drivers and PWM Signals:

PWM (Pulse Width Modulation) signals in motor drivers are fundamental parameters that control the speed and torque of the motor. **[1].** In traditional control systems, PWM signals are optimized using information obtained from sensor data, whereas deep learning algorithms enhance this process, making it more precise and predictive.

Advanced Control with Deep Learning and YOLOv8:

YOLOv8 is a model that provides fast and accurate object detection. **[8].** Object data obtained through image processing can be critical in motor control. For instance, the distance of a robotic arm from an object can influence the PWM signals. These signals are processed by a Fuzzy Neural Network (FNN) based on the analysis of data received from YOLOv8, thereby optimizing driver control.**[10].**

3.1. Real-Time Control Integration with Artificial Intelligence

The motor control is achieved by utilizing a model trained to detect and recognize objects using the YOLOv8 model. The model processes input images to identify the location and class of specific objects. For real-time data streaming in MATLAB, the YOLOv8 model is executed through Python, utilizing the integration features between Python and MATLAB. Invocations are made through Python.In example, By invoking the Python detect() function, operations are performed on the detected objects and their positions. To facilitate data sharing between MATLAB and Python, the matlab.engine is used. This tool allows you to execute MATLAB commands within Python code, enabling data transfer between Python-based projects and MATLAB, and allowing direct invocation of MATLAB functions from Python.

3.2 Integration of YOLOv8 in MATLAB and PWM Signal Generation

The position or status of the detected objects can provide parameters (error, delta error) that will be used in PWM signal generation. For instance,

deviations in an object's position or instantaneous parameter changes, such as excessive current values, can be utilized to adjust the PWM signal accordingly.

3.3. Integration with FNN

Model Integration: The trained model is integrated into the PWM control circuit. Outputs from the model that generates the PWM signal are utilized to connect to the motor driver. In summary, an integrated system is established through the FNN neural network by calculating error and feedback parameters for controlling the PWM signal based on image data processed by the YOLOv8 model. This integration is achieved through MATLAB-Python integration and data sharing.

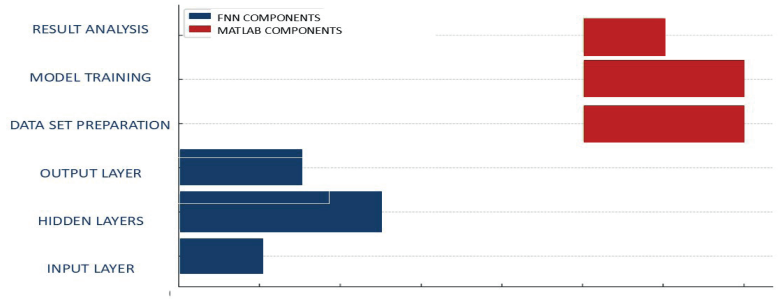

Figure 8. *Components of Fuzzy Neural Network (FNN) and MATLAB Integration*

In **Figure 8**, a diagram illustrating the integration of the Fuzzy Neural Network (FNN) and MATLAB is presented. The details are outlined as follows:

Input Data: At the top of the diagram, there is a block labeled "Input Data," representing the raw data necessary for the system's operation. This data includes PWM control data from sensors or other sources, as well as motor speed, position information, or object recognition results obtained from a model such as YOLOv8.

FNN Structure: Following the preprocessing of the input data, there is a block representing the FNN structure. This section contains a network model created by combining fuzzy (if-then)logic and artificial neural networks. This model is designed to control the PWM signal output using predefined fuzzy rules and neural network learning algorithms. The output of the FNN block is a signal that represents the PWM signal, which will function as the PWM signal used to control the motor drivers. The PWM signal is a critical component for controlling the motor's speed and torque, and the FNN can enhance the motor's performance by optimizing this signal.

Output Signal: The output of the FNN block produces a signal that represents the PWM output. This signal will serve as the PWM signal utilized for controlling the motor drivers.

Feedback Loop: Following the output signal, a feedback loop is illustrated. This loop is utilized to assess the system's performance and make necessary adjustments. Feedback is crucial for the stabilization and accuracy of the system.

MATLAB Integration: All these components are integrated within the MATLAB environment to form a control system. MATLAB serves as the platform for the training, simulation, and integration of the FNN. Utilizing the tools available in MATLAB, data analysis and system optimization can be effectively performed. **[11].**

4. CONCLUSIONS

The study addresses the integration of deep learning and artificial intelligence in motor driver control and PWM (Pulse Width Modulation) signal generation, combining machine learning with power electronics principles for advanced research and analysis. This approach aims to optimize motor driver performance. Motor drivers regulate the speed and torque of motors by adjusting operating parameters (such as current, voltage, etc.) over time. PWM signals, a technique used in speed and torque control, serve to regulate the power delivered to devices by managing motor energy through switching pulses. This, in turn, ensures effective speed and torque control, preventing potential damage to devices and improving motor performance. The key focus of this study is to advance PWM signal output control through artificial intelligence, moving beyond traditional methods. By examining the limitations of conventional control methods in motor drivers, the research explores how deep learning-based approaches can introduce flexibility, adaptability, and significant advantages to such systems. The use of deep learning-based control in power converters and motor drivers offers numerous benefits, particularly in reducing control errors, enhancing energy efficiency, and optimizing performance.

A brief summary of the stages of the study is as follows:

1. **Data Acquisition During Motor Operation:** Speed, torque, current, and voltage feedbacks are collected using sensors (speed sensors, torque sensors, current sensors). These data from the sensors are typically transmitted in digital form to microcontrollers or data acquisition systems, allowing the initial states and effects of PWM signals to be observed.

2. **Real-Time Model Training:** Based on the collected data, the deep learning model is trained to understand how the motor responds under various operating conditions. The model can be trained using several deep learning

applications such as Python, OpenCV, Keras, YOLOv5, and YOLOv8. Thus, the feedback data can be analyzed in real-time by the deep learning model or stored for later processing. This approach provides flexibility and control in terms of PWM signal adaptation. The model determines the PWM signals to ensure the motor operates at its optimal performance, dynamically adjusting the signal based on varying speed and load conditions.

3. Collaboration Between Motor Driver and Deep Learning Algorithm: The motor driver uses PWM signals generated by the deep learning algorithm to power the motor. These PWM signals regulate the motor's current and voltage, thereby controlling its speed and torque. Since the pulse width of the PWM signals determines the motor's supply voltage, the quality of these signals directly impacts motor performance. Through deep learning, these signals are optimized in real-time and continuously, enhancing the motor's efficiency.

5. REFERENCES

[1]. Heggo, M. et al., 2019. "Operation of aerial inspections vehicles in HVDC environments Part B: Evaluation and mitigation of magnetic field impact." , Journal of physics. https://doi.org/10.1088/1742-6596/1356/1/012010.

[2]. Becerra, RC; Ehsani, "M. Fırçasız Kalıcı Mıknatıs Motorlarının Yüksek Hızlı Tork Kontrolü." IEEE Trans. Ind. Electronics 1988 , 35 , 402–406.

[3]. AN10661 Brushless DC motor control using the LPC2141 - NXP Semiconductors ; AN10661, NXP Semiconductors: Eindhoven, Hollanda; Ekim; 2007.

[4]. Fault tolerant BLDC motor control for hall sensors failure . 2015 21st International Conference on Automation and Computing (ICAC)

[5]. T.Ugale, R. et al., 2012. "A low cost fast data acquisition system for capturing electric motor starting and dynamic load transients." 2012 IEEE International Conference on Power Electronics, Drives and Energy Systems (PEDES)

[6]. A. C. Kınacı, "Görsel yazilim geliştirme ortamı ile beraber bir yapay sinir aği kütüphanesi tasarımı ve gerçekleştirimi," Ege Üniversitesi, 2006.

[7]. NurOrtataş, F. & Kaya, M., 2023. "Performance Evaluation of YOLOv5 YOLOv7 and YOLOv8 Models in Traffic Sign Detection." 2023 8th International Conference on Computer Science and Engineering (UBMK). http://dx.doi.org/10.1109/ubmk59864.2023.10286611.

[8]. https://docs.ultralytics.com/tr/models/

[9]. Lin, C.-H. & Lin, C.-P., 2009. "Fuzzy neural network control for a permanent magnet synchronous motor drive system" 2009 4th IEEE Conference on Industrial Electronics and Applications. Available at: http://dx.doi.org/10.1109/iciea.2009.5138697

[10]. Feedforward neural network - Wikipedia İleri beslemeli sinir ağı (FNN)

[11]. Arafat, Yunus Bakhtiar, and H. U. Weiwei. "The Development of a Matlab-Based Fuzzy PID Controller and The Simulation." *International Journal of Engineering Continuity* 2.1 (2023): 14-26.